ISSN 0236-2945

LIGHT & ENGINEERING

Volume 23, Number 4, 2015

LLC “Editorial of Journal “Light Technik”, Moscow

Dear Colleagues,
Authors and Co-authors!
Dear Friends!

Wishing you multiple successes and happiness in a fulfilling and creative new year for 2016!

The past year has been filled with many important milestones and passed remarkably quickly.

We hope that 2015 will be a year of success for "Light & Engineering", for you and your loved ones, filled with positive experiences and only manageable obstacles.
The close and productive relationship between the editorial office and board is a pillar of the journal's success!
We always look forward to your papers, feedback and suggestions.

With best wishes and warm regards,
Your Editorial office

LIGHT & ENGINEERING
(Svetotekhnika)

СВЕТО ТЕХНИКА

Moscow, 2015

Editorial Office:
VNISI, Rooms 327 and 334
106 Prospekt Mira,
Moscow 129626, Russia
Tel: +7.495.682.26.54
Tel./Fax: +7.495.682.58.46
E-mail: lights-nr@inbox.ru
http://www.sveto-tekhnika.ru

Scientific Editors
Sergey G. Ashurkov
Raisa I. Stolyarevskaya

Style Editor
Marsha Vinogradova

Art and CAD Editor
Andrey M. Bogdanov

CONTENTS

VOLUME 23 **NUMBER 4** **2015**

LIGHT & ENGINEERING
(SVETOTEKHNIKA)

Light & Engineering
Vol. 23, No. 4, pp. 4-5, 2015

Svetotekhnika
No. 6, 2015, pp. 39-40

CIE Statement on Non-Visual Effects of Light
RECOMMENDING PROPER LIGHT AT THE PROPER TIME

BACKGROUND

The definition of light identifies it as the electromagnetic radiation that stimulates vision. However, we now know conclusively that photoreception in the eye leads not only to vision but also to effects on human physiology, mood and behavior, often summarized as non-visual effects of light. Research on such effects intensified at the beginning of this millennium. It was fueled by the revolutionary detection of a new class of photoreceptors in the human eye that detect optical radiation but do not contribute to image formation. These photoreceptors were first identified in connection with their role in circadian regulation, particularly of the hormone melatonin, and for this reason one reads of circadian or melanopic effects. We are learning now that these photoreceptors influence many other processes as well. In recent years the catchphrase "Human-Centric Lighting" (HCL) has come to describe lighting that is intended to address all of these effects.

The basic evidence for the new photoreceptors, called melanopsin-containing or intrinsic photosensitive retinal ganglion cells (ipRGC), and the first identified implications for lighting have been summarized in CIE158:2004 (which was revised to become 158:2009, including Erratum 1). CIE continued to explore this topic with two expert symposia in 2004 and 2006, with workshops at its Session meetings in 2007 and 2011, and by initiating several technical committees. Other societies also responded with events, debates, and discussion concerning how best to incorporate this knowledge into lighting practice.

Scientists, the lighting industry, lighting designers and other stakeholders in the lighting community have continued to identify options and to design products and solutions that make use of non-visual lighting effects in a beneficial way, despite the fact that the established knowledge in this field is still premature. Among the few points of general agreement is that the non-visual effects of light exposure depend on the spectrum, intensity, duration, timing and temporal pattern (light history) of the light exposure.

In order to give further guidance to all interested parties on the future use of non-visual effects of light for human health and performance, while at the same time avoiding possible risks, CIE will be presenting two new publications on the state of science in this exciting research field:

1. How to measure light with respect to non-visual effects: Technical Note of CIE DR6–42 (TN003)

One of the greatest limitations to making concrete recommendations for healthy non-visual light exposures has been the difficulty in characterizing the impact of ipRGC exposures. In 2013, an independent workshop of leading scientist in the field of quantifying light for non-visual effects took place in Manchester, with support from a moderator and a reporter from CIE. This workshop resulted in a scientific consensus and agreement concerning the action spectrum of the ipRGC photoreceptor and a strategy for quantifying the stimulus for non-visual input into the human photoreception system, recognizing the interaction between all of the photoreceptors (Lucas et al. 2014). CIE TN003 gives comprehensive information on the workshop and its outcome. This technical note will be freely available from the CIE web site, together with a calculation toolbox to facilitate consistent stimulus calculation and intercomparison of results.

2. Identifying the Proper Light: Technical Report of CIE TC3–46

The Manchester workshop concluded that non-visual responses are subject to complex signal processing in the central nervous system and influenced by as-yet-unresolved interactions of photoreceptive units. The missing understanding of the input-output char-

acteristics between light stimulus and the resulting non-visual response seems to make tailored light application for a desired lighting effect impossible. On the other hand, observations in laboratory and application studies show beneficial effects on human health and performance, using lighting systems developed on the basis of very general ideas concerning how to translate basic scientific findings into lighting design specifications. The main principles for these observations have been to increase the light levels and/or change spectral composition during daytime in order to increase the input into the ipRGCs and to do the opposite in the recovery phases of evening and night, by reducing light input to these cells. Thus there may be "low hanging fruits" in terms of application opportunities in this field, but this still needs clarification.

Even prior to the confirmation that ipRGCs constitute a separate retinal photoreceptor class to the rods and cones, there was a fundamental difference of opinion between those who would see this new information incorporated into lighting practice immediately, and those who argued for a more cautious approach with stronger evidence both for beneficial effects and to eliminate unintended adverse consequences. CIE TC3–46 WD "Research Roadmap for Healthful Interior Lighting Applications" focuses on identifying the gaps in current knowledge for a safe and beneficial future use of light including non-visual responses. The report also delivers a research roadmap and tools for a systematic and sound understanding of the biological system to enable predictions with respect to biological outcome on the basis of the input characteristics. The purpose of this report is to focus research attention on the knowledge gaps that most impede the development of recommendations for interior lighting.

FURTHER CIE STRATEGY

CIE is setting up a new Joint Technical Committee between the relevant Divisions[1] to follow up on the results of the Manchester workshop and translate the scientific consensus into a first international standard on quantifying irradiance with respect to stimulation of all ocular photoreceptors. To address the issues of safe and healthy applications, CIE will coordinate with ISO/TC274 and other interested stakeholders on guidance for those who are beginning to apply lighting in new ways, to intentionally include non-visual effects, with a particular emphasis on achieving integrated recommendations for high-quality lighting. This dual approach shall lead to an improved and comprehensive understanding of the lighting effects on humans and to more healthful interior lighting in the future.

[1] D1 „Vision and Colour", D2 „Physical Measurement of Light and Radiation", D3 „Interior Environment and Lighting Design", D6 „Photobiology and Photochemistry"

REFERENCES

1. CIE158:2009 Ocular Lighting Effects on Human Physiology and Behaviour.
2. CIE x027:2004 Proceedings of the CIE Symposium 2004 on Light and Health: Non-Visual Effects, 30 Sep. – 2 Oct. 2004, Vienna, Austria.
3. CIE x031:2006 Proceedings of the 2nd CIE Expert Symposium "Lighting and Health", 7–8 September 2006, Ottawa, Ontario, Canada.
4. CIE TN003:2015 Report on the First International Workshop on Circadian and Neurophysiological Photometry, 2013 (in press)
5. Lucas, R.J., Peirson, S.N. et al. (2014). Measuring and using light in the melanopsin age. Trends Neurosci 37(1): 1–9.

ABOUT CIE

The International Commission on Illumination – also known as the CIE from its French title, the Commission Internationale de l´Eclairage – is devoted to worldwide cooperation and the exchange of information on all matters relating to the science and art of light and lighting, colour and vision, photobiology and image technology.

With strong technical, scientific and cultural foundations, the CIE is an independent, non-profit organization that serves member countries on a voluntary basis. Since its inception in 1913, has been accepted as representing the best authority on the subject and as such is recognized by ISO as an international standardization body.

For any further information please contact

CIE Central Bureau
Dr. Peter Zwick email: peter.zwick@cie.co.at Babenbergerstraße 9/9A, A-1010 Vienna, Austria T: +43 1 714 31 87
ZVR: 640982399
Website: http:/www.cie.co.at

Light & Engineering
Vol. 23, No. 4, pp. 6-14, 2015

Svetotekhnika
No. 5, 2015, pp. 12-18

VISION EXPERIMENT ON CHROMA SATURATION FOR COLOUR QUALITY PREFERENCE*

Yoshi Ohno[1], Mira Fein[2], and Cameron Miller[1]

[1] National Institute of Standards and Technology, Gaithersburg, MD USA,
[2] Psychology Department, Oberlin College, Oberlin, Ohio, USA
E-mail: ohno@nist.gov

ABSTRACT

Colour Rendering Index (CRI) often does not correlate well with visual evaluation of colour rendering of light sources at real illuminated scenes. The main reason is that CRI measures colour fidelity, while general users judge colour rendering based on their preference of object colour appearance, thus there is a need for a colour- preference based metric. Colour preference is mainly affected by saturation of object chroma. To obtain data for such colour preference evaluation, a series of vision experiments have been conducted using the NIST Spectrally Tunable Lighting Facility simulating an interior room, where 20 subjects viewed various fruits, vegetables, and their skin tones, under illumination of varied saturation levels at correlated colour temperatures (CCT) of 2700 K, 3500 K, and 5000 K. The results of the experiment show that subjects' preference is consistently peaked at saturation level of $\Delta C^*_{ab} \approx 5$ at all CCT conditions and for all target objects. The results may be useful to develop a colour preference metric.

Keywords*:* colour rendering, colour preference, chroma saturation, perception, vision experiment

1. INTRODUCTION

Colour Rendering Index (CRI) often does not correlate well with perceived colour rendering of illuminated scenes, especially with light-emitting diode (LED) sources, as summarized in reference [1]. There have been several proposals for alternative metrics [2, 3, 4, 5] but none of them has been

* On basis of report published in Proceedings of the 28th CIE Session, 2015, Manchester

Fig. 1. View of the two cubicles of NIST Spectrally Tunable Lighting Facility

adopted as a standard. The Colour Quality Scale (CQS) developed by NIST [4] has not been accepted as a standard mainly due to a difficulty defining a metric that evaluates combined effects of colour fidelity and colour preference. International Commission on Illumination (CIE) has now two separate TCs, one developing a new colour fidelity metric (TC1–90) and another writing a report on existing metrics for colour quality other than fidelity (TC1–91). It is considered that an improved colour fidelity metric alone will not solve the problem of correlation with perception, and there is a need for a preference-based metric to evaluate the colour quality of light sources in real applications as perceived by general users.

To develop such a preference-based metric, visual evaluation data are needed. The main reason for the discrepancy between the CRI score and the perception is that the CRI measures colour fidelity, only one aspect of colour quality, while general user judge colour rendering based on their preference of object colour appearance. The discrepancy mainly occurs when the chroma of objects is enhanced by lighting, e.g., by narrowband white LED sources or hybrid sources (combination of broadband and narrow- band red). It is experienced that chroma-enhanced sources are generally preferred, but if the chroma saturation is excessive, the objects appear unnatural and the preference will decrease. Such quantitative evaluation data on the preferred level of chroma saturation have not been available. To obtain such data, a series of vision experiments have been conducted using the NIST Spectrally Tunable Lighting Facility (STLF) [6] simulating an interior room, where 20 subjects evaluated colour appearance of variety of fruits, vegetables, and their skin tones, under lights with varied chroma saturation levels. The results of the experiment are presented and a way toward developing a colour preference metric based on these results is discussed.

2. EXPERIMENTAL SETTINGS WITH NIST STLF

The NIST STLF, as shown in Fig. 1, was used, which has 25 channels of LED spectra (from 405 nm to 650 nm peak) and can control spectral distribution, correlated colour temperature (CCT), Duv[1], and illuminance, independently, illuminating real-room size cubicles (each 2.5 m x 2.5 m x 2.4 m). There are two cubicles side by side, independently controlled, and the walls of different colours and surface textures can be replaced easily. For this experiment, only one cubicle with off-white (achromatic) walls was used (the right side in Fig. 1). The facility can produce up to about 300 lx to 800 lx of white light illumination on the table, depending on the spectrum of light.

The light source unit of the STLF has very large heat sinks, which are cooled by forced air, and the temperature of the heat sink is only about 27 °C when these spectra at ~300 lx are produced, while the room temperature is kept at 25 °C ±1 °C. The STLF needs only about 15 minutes to stabilize, after which the chromaticity is stable to within ± 0.0005 in (*u', v'*) for four hours, and reproduces the set chromaticity to within ± 0.001 in (*u', v'*) over one month. The STLF can change the light spectrum in-

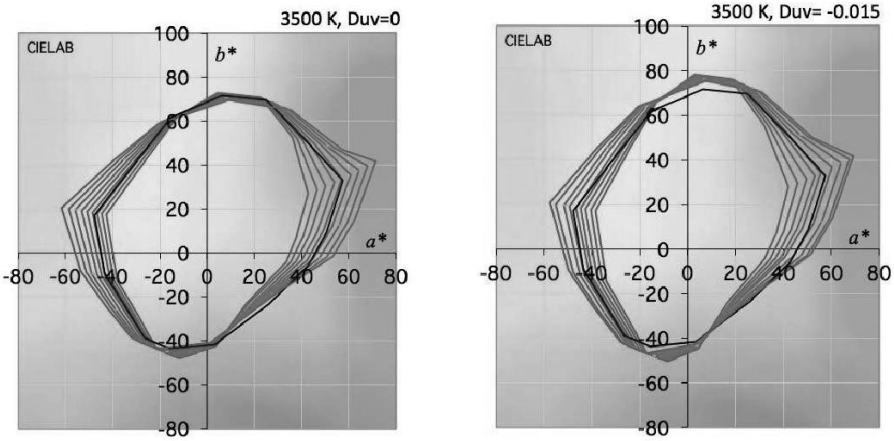

Fig. 2. The CIELAB (a*, b*) plots of the 15 CQS samples for the nine different saturation levels used for the experiment for 3500 K, Duv=0 (left) and Duv= –0.015 (right). The black line is for the reference illuminant in CRI (Planckian radiation at the same CCT)

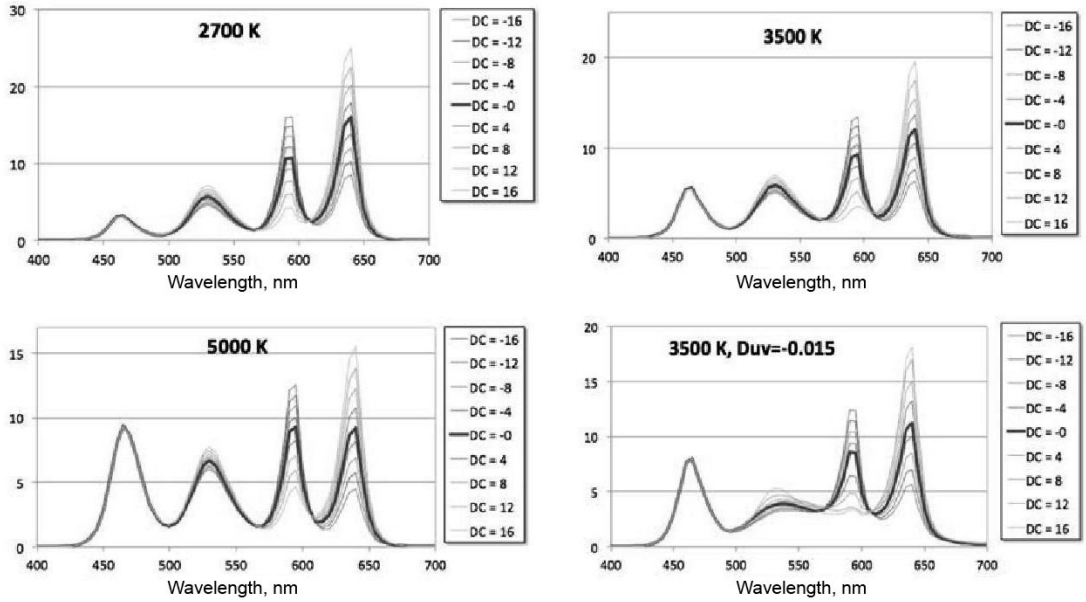

Fig. 3. The spectral distributions set at NIST STLF for the four CCT/Duv conditions for the experiment. "DC" in the figures represents ΔC*ab

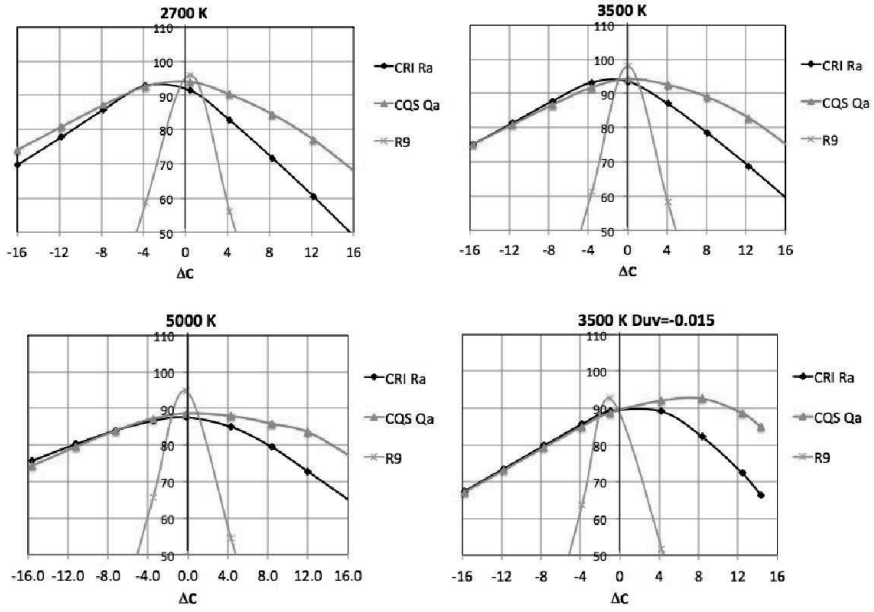

Fig. 4. The CRI Ra, R9 values and CQS Qa values of the spectra at the four CCT/Duv conditions used in the experiment

stantly so that there was no switching time between two lights presented sequentially and stable immediately, which allows easy comparison of a pair of lights presented sequentially.

For the experiment, the STLF was set for RGBA spectra with peaks around 460 nm, 530 nm, 590 nm, and 635 nm. Such a combination of narrowband peaks was needed to create increased chroma saturation. (Smooth broadband spectra cannot achieve it). The chroma saturation was varied by changing the red/amber ratio. Nine different levels of chroma saturation as shown in Fig. 2 (left) were prepared at each of 3 different CCTs; 2700 K, 3500 K, and 5000 K. The chroma was set to CIELAB chroma differences, $\Delta C^*_{ab} = -16$ to +16 from the neutral condition (the chroma of the reference illuminant of CRI) at intervals of 4 ΔC^*_{ab} units, measured on the red CQS sample [4]. The chroma for the green CQS sample had slightly smaller changes of chroma than the red sample, while there were very small changes in chroma in yellow and blue regions with changes of the amber/red ratio. So the overall gamut area also increased or decreased as the chroma saturation was changed.

Fig. 5. The set-up of the STLF cubicle with objects on the table used in the experiments

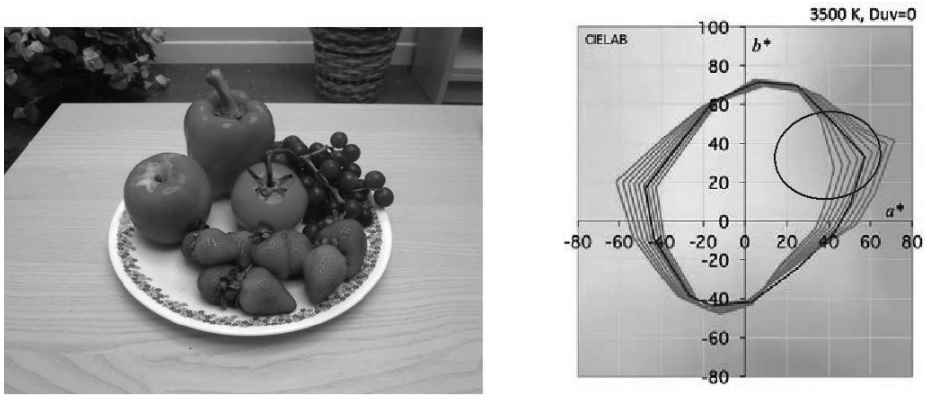

Fig. 6. Photo of the red samples only and the CIELAB plots of the chroma saturation setting of lights at STLF

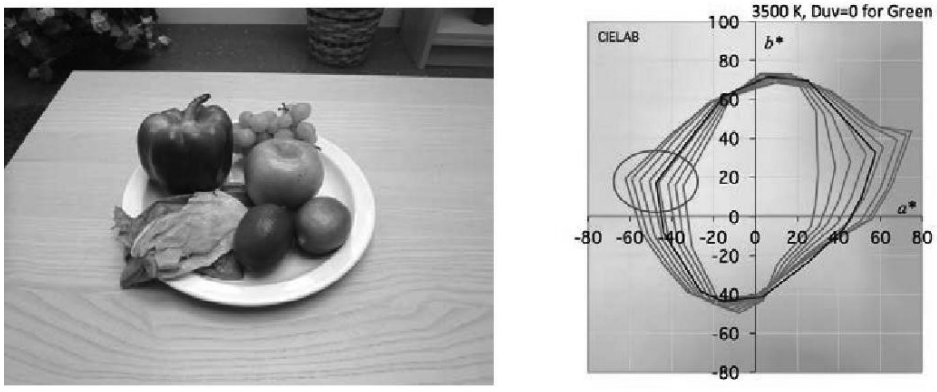

Fig. 7. The photo of the green samples only and the CIELAB plots of the chroma saturation setting of lights at STLF

In addition, another condition was set for a negative Duv[2] [7], Duv = –0.015, at 3500 K as shown in Fig. 2 (right). All other conditions were at Duv=0.000. This condition was added, considering that the Duv level might affect the preference for chroma saturation,

At each of the four CCT/Duv conditions, the chromaticity on the STLF was kept constant, to within ± 0.0003 in (u', v'), while the chroma saturation was varied at 9 different levels; thus, there was no issue of chromatic adaptation for observations within each CCT/Duv condition. Chromatic adaptation period was needed only when the CCT/Duv condition was changed.

The measured spectra for these four CCT/Duv conditions are shown in Fig. 3. The spectral distributions of the lights were measured on the center of

[2] The signed distance from the Planck locus on CIE u', 2/3 v' coordinates [10] based on the results of the previous experiment on Duv preference [8], in which the Duv level of –0.015 on the average was found most preferred.

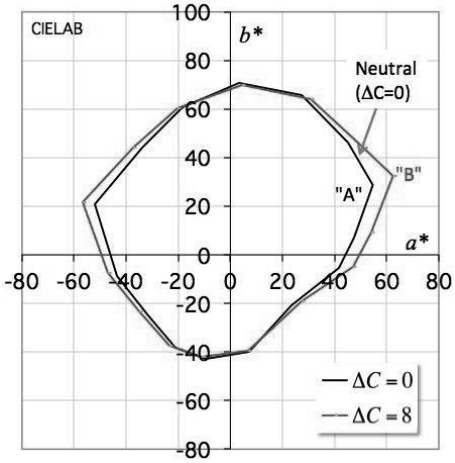

Fig. 8. An example of a pair of lights in the experiment

the table in the cubicle, using an array type spectroradiometer with a small integrating sphere input for cosine response, calibrated with a standard lamp traceable to NIST spectral irradiance scale [9].

The spectroradiometer measured spectra and illuminance on the coffee table (see Fig. 5) from the 2π solid angle from the entire room including reflections from the walls and other objects as well as from the light source itself. The estimated expanded uncertainties (k=2) of measurements varied depending on spectra, but in all cases, they were within 0.0012 in *u'* and v', 0.0009 in Duv, 24 K in CCT at 2700 K and 92 K at 6500 K. The repeatability of the spectroradiometer was 0.0002 in u' and v'.

Fig. 4 shows the plots of the CRI *R*a and *R*9 values as well as the CQS *Q* a values, calculated from the spectral distribution data in Fig. 3, as a function of chroma saturation ΔC^*_{ab}, for all the four (CCT, Duv) conditions.

The STLF cubicle for the experiment was prepared as an interior room as shown in Fig. 5, with a coach (not shown in the photo), a coffee table, a bookshelf with books, some artificial flowers, paintings on the walls. A mirror was also placed on the wall against the coach, to allow evaluation of skin tone of the face of the subject. On the table there were two plates of real fruits and vegetables; apples, oranges, bananas, strawberries, peppers, lettuce, tomatoes, red cabbage, and grapes. These fruits and vegetables were replaced every few days to keep them fresh during a few weeks of the experiment period. Pictures of these fruits and vegetables were taken, and when these were replaced, those having as similar colours and sizes as possible were purchased and used throughout the experiments.

In addition to these settings, the experiments were also done for red samples only and for green samples only. For the green samples, the chroma saturation levels were set for steps of 4 ΔC^*_{ab} units for the CQS green sample. Fig. 6 shows the photo of the

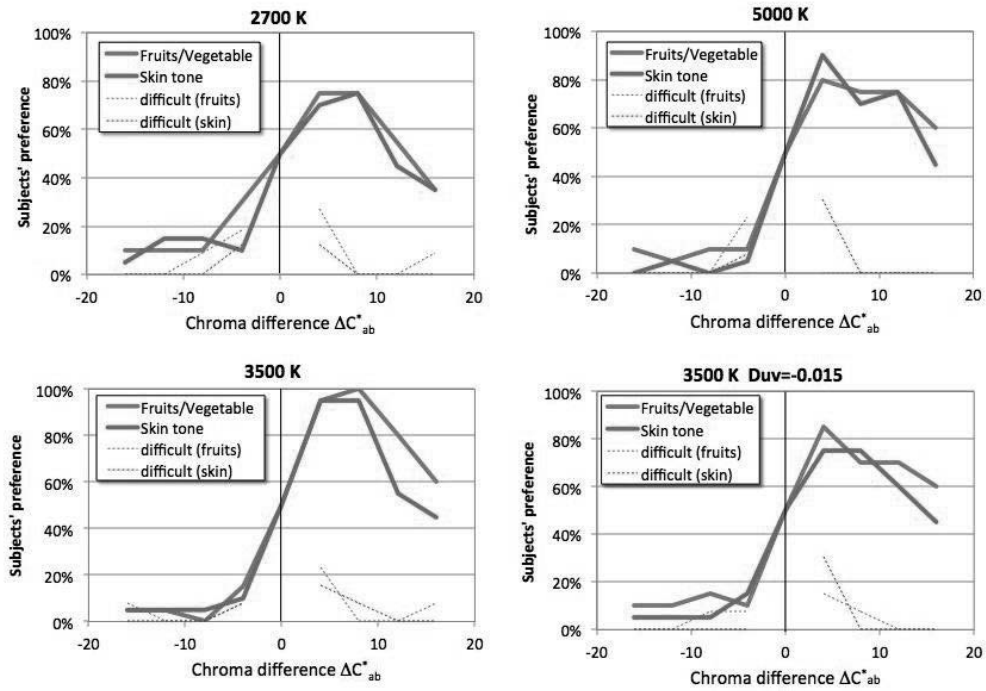

Fig. 9. Average results of all subjects for mixed fruits/vegetables and skin tone, shown in percentage of subjects' preference over the neutral

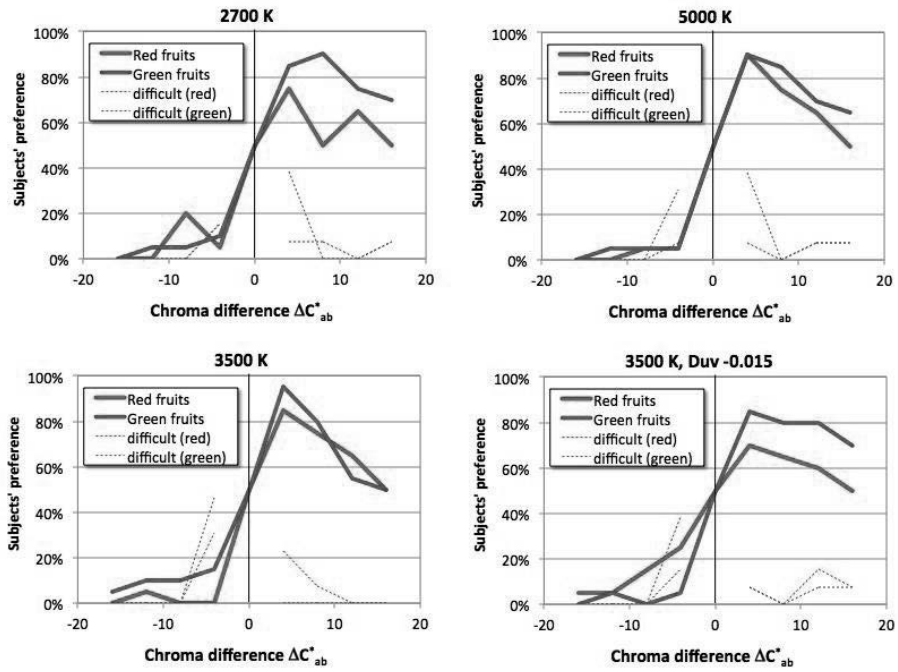

Fig. 10. The average results of all subjects for red and green fruits/vegetables only, shown in percentage of subjects' preference over the neutral

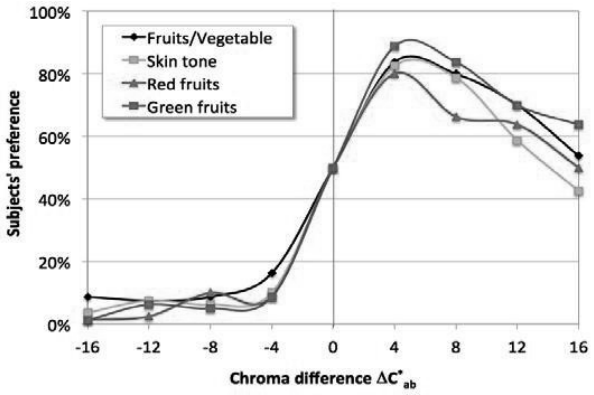

Fig. 11. The average results of all CCT/Duv conditions for the different viewing targets

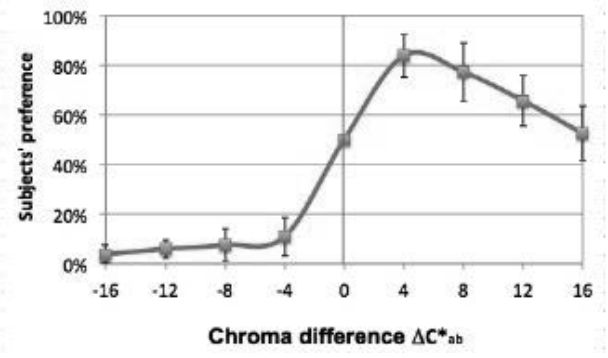

Fig. 12. Average results for all CCT/Duv conditions and all viewing targets

red samples only and the CIELAB (a*, b*) plots of the lights prepared, and Fig. 7 shows those for the green samples only.

3. EXPERIMENTAL PROCEDURES

Total 20 subjects having normal colour vision were recruited for the experiments. They were 10 males and 10 females with their ages from 20 to 59, consisting of 7 Caucasians, 5 Hispanics, 4 Asians, and 4 dark- skin persons (African or Indian origin). The subjects were volunteers working at NIST, who are not experts on colour, including eight summer students. Each subject was first tested for normal colour vision using Ishihara Test, and instructions were given for the experiment including a trial comparison of light pairs.

Experiments were conducted for the four CCT/Duv conditions described in Section 2. The subject was adapted to the first CCT/Duv condition for at least ten minutes before the experiment started (this was achieved when instructions were given), and at for least three minutes when CCT or Duv was changed. The experiments were repeated for 3500 K condition only (due to limited time available) for all viewing conditions and for each subject, to evaluate reproducibility of results.

For each CCT/Duv condition, experiments were conducted on four viewing targets: 1) the mixed fruits/vegetables on the table and the entire room,

Table 1. Conditions for the 16 experiment-runs for each subject

Session	Run	CCT [K]	Duv	Viewing target
1	1	3500	0	Mixed fruits and vegetables
	2	3500	0	Skin tone
	3	2700	0	Mixed fruits and vegetables
	4	2700	0	Skin tone
	5	5000	0	Mixed fruits and vegetables
	6	5000	0	Skin tone
	7	3500	-0.015	Mixed fruits and vegetables
	8	3500	-0.015	Skin tone
2	9	3500	0	Red fruits and vegetables only
	10	3500	0	Green fruits and vegetables only
	11	2700	0	Red fruits and vegetables only
	12	2700	0	Green fruits and vegetables only
	13	5000	0	Red fruits and vegetables only
	14	5000	0	Green fruits and vegetables only
	15	3500	-0.015	Red fruits and vegetables only
	16	3500	-0.015	Green fruits and vegetables only
3	17	3500	0	Mixed fruits and vegetables
	18	3500	0	Skin tone
	19	3500	0	Red fruits and vegetables only
	20	3500	0	Green fruits and vegetables only

2) their skin tone (face in a mirror and hands), 3) red fruits/vegetables only, and 4) green fruits/vegetables only, as shown in Figs. 5, 6 and 7.

For the above CCT/Duv conditions and viewing targets, the experiments were grouped into three sessions, and conducted for 20 experiment-runs for each subject as listed in Table 1, and conducted in this order.

In each experiment-run, 8 pairs of lights were prepared from the 9 different saturation levels as shown in Fig. 2, with one light of each pair being always the reference light (neutral saturation). Each pair of light was presented sequentially. Fig. 8 shows an example of such a pair. In this example, light "A" is the reference ($\Delta C^*_{ab}=0$), and light "B" is at $\Delta C^*_{ab}=8$. When each light was presented, the operator said "A" or "B" and asked "which light looks better, A or B?," and the pair was repeated two or more times as necessary, till subject answered. Each light was presented for about three seconds before switching to next light. The order of the reference light, coming first or second, was changed for different pairs and the subject did not know about the existence of reference light and when it was presented.

The subject's answer was a forced choice, but in addition, the subject was also instructed to report if the choice was difficult, and such information was recorded together with the answers A or B. The order of pairs of light for different saturation levels were set in a random manner as shown in Table 2.

Each experiment-run took about five minutes on the average, and all sessions took about two and half hours on the average for each subject. The three sessions for each subject were scheduled in one or two days depending on their schedules. Experiments were done for one or two subjects a day. All experi-

ments for 20 subjects were carried out over a period of three weeks.

4. RESULTS

The subjects' response data were first analysed as shown in Table 3. In that table, 0 as the subject response means that the subject chose the reference light as better, and 1 means that the subject chose the light with the ΔC^*_{ab} value of the column as better. For example, subject 1 responded that the reference was better than all de-saturated lights, and the saturated lights ΔC^*_{ab} =4, 8, 12, were better than the reference, but the saturated lights ΔC^*_{ab} =16 was not as good as the reference. The last two rows show the average values of all subjects at each ΔC^*_{ab} level for this CCT/Duv condition and the percentages that subjects chose the light with each ΔC^*_{ab} level better than the reference (neutral). The percentage value 50% is given for ΔC^*_{ab} =0 (comparing the same light, which was not included in the experiment), as it is supposed to be even.

The analysis shown in Table 3 was done for all CCT/Duv conditions and for all viewing targets. Fig. 9 shows all the results for mixed fruits/vegetables and skin tone. The solid lines show the percentage values as in the bottom of Table 3, which show subjects' preference of each ΔC^*_{ab} light over the neutral, and the thin dashed lines are the percentages that subjects answered as "difficult to choose". Figure 10 shows all the results for red fruits/vegetables only and green fruits/vegetables only.

Examining Figs. 9 and 10, all curves are surprisingly similar for all different CCT/Duv conditions and viewing targets. Subjects' preference consistently peaked (80 to 90%) at a saturation level of $\Delta C^*_{ab} \approx 5$ and decreases slowly as light becomes more saturated (≈ 50% at ΔC^*_{ab}=16), while the percentages at all levels of de-saturation are very low (less than 20%).

Table 2. Light pairs for the eight comparisons in an experiment-run

Pair	ΔC^*_{ab} of 1st light "A"	ΔC^*_{ab} of 2nd light "B"
1	-8	0
2	8	0
3	0	16
4	-12	0
5	-4	0
6	4	0
7	0	12
8	0	-16

Fig. 11 shows the averages of all CCT/Duv conditions for the four viewing targets, and Fig. 12 shows the grand average of all results. The error bars are the standard deviations of four points at each ΔC^*_{ab} in Fig. 11.

5. DISCUSSIONS AND CONCLUSIONS

The results of the experiments indicate that lights having chroma saturation around $\Delta C^*_{ab} \approx 5$ from the neutral are most preferred and the preference slowly decreases when chroma saturates further, when viewing fruits/vegetables and skin tone. Based on the results, a colour preference metric may be devel-

Table 3. Example of raw data for Run 1 (3500 K, mixed fruits and vegetables)

		Chroma saturation ΔC^*_{ab} and subject response							
Subject	-16	-12	-6	-4	0	4	8	12	16
1	0	0	0	0		1	1	1	0
2	0	0	0	0		1	1	1	0
3	0	0	0	0		1	1	1	1
4	0	0	0	1		1	1	1	1
…	…	…	…	…		…	…	…	…
20	0	0	0	0		1	1	1	1
Average	0.05	0.05	0	0.15		0.95	1	0.8	0.6
Percentage	5%	5%	0%	15%	50%	95	100%	80	60

oped by using a reference illuminant that has chroma saturation of $\Delta C^*_{ab} \approx 5$ so that the metric would yield the highest score for such lights and score decreases when ΔC^*_{ab} deviates in either direction. In this experiment, however, the chroma was changed mostly in the red and green region. It is not clear whether the preference effects in yellow and blue regions (or other colours) are the same. It was difficult to produce such experimental lights for yellow and blue this time. It is hoped that such preference experiments can be conducted for yellow, blue, or even other colours in the future. Also, further studies are desired to verify applicability of these results in various real application conditions.

ACKNOWLEDGEMENT

This research was conducted when Mira Fein stayed as a guest researcher at NIST under NIST-NSF Summer Undergraduate Research Fellowship Program.

REFERENCES:

1. CIE2007. CIE177: 2007 Colour rendering of white LED light sources.

2. Hashimoto, K., Yano, T., Shimizu, M. and Nayatani, Y. 2007. New method for specifying colour-rendering properties of light sources based on feeling of contrast," Colour Res. Appl. 32, pp. 361–371.

3. Rea, M., Freyssinier, J.P. 2008. Colour rendering: a tale of two metrics. Colour Res. Appl. 33.

4. Davis, W. and Ohno, Y. 2010. "Colour Quality Scale," *Optical Engineering*, 033602–1 March 2010/ Vol. 49_3.

5. Smet, K., Ryckaert, W., Pointer, M., Deconinck, G., Hanselaer, P. 2010. Memory colours and colour quality evaluation of conventional and solid-state lamps. Opt. Expr. 18.

6. C Miller, Y. Ohno, W. Davis, Yu. Zong, K. Dowling. 2009. Nist Spectrally Tunable Lighting Facility for Colour Rendering and Lighting Experiments. Light & Engineering Journal, V.17,#4, pp.57–61.

7. Ohno, Y. 2013, Practical Use and Calculation of CCT and Duv" *LEUKOS*, 10:1, 47–55, DOI: 10.1080/15502724.2014.839020.

8. Ohno, Y. and Fein, M. 2014. Vision Experiment on Acceptable and Preferred White Light Chromaticity for Lighting, CIE x039:2014, pp. 192–199.

9. Yoon, H. W. and Gibson, C. E. 2011. NIST Special Publication 250–89 Spectral Irradiance Calibration.

10. ANSI 2011, ANSI_NEMA_ANSLG, C78.377–2011 Specifications for the Chromaticity of Solid State Lighting Products.

Yoshi Ohno
obtained Ph.D. in engineering from Kyoto University, Japan. He started his career at Panasonic then joined NIST in 1992. He was the Group Leader for Optical Sensor Group and later Lighting and Colour Group from 2003 to 2012. He is appointed as NIST Fellow since 2010. He is active in international standardization. He currently serves as the President of International Commission on Illumination (CIE). He played leadership roles in developing several important standards for solid state lighting, including IES LM-79, ANSI C78.377, and CIE S025

Cameron Miller
obtained his Ph.D. in Physical Chemistry from Cornell University (1994). He joined the National Institute of Standards and Technology in 1996 and in 2013 was appointed the group leader for the Optical Radiation Group. His research areas include all aspects of Photometry, Measurement Uncertainty and Vision Science applied to lighting. Cameron is active in standards organization and professional societies, such as IES – Testing Procedure Committee (Chairman), CIE, CIEUSA (Technical VP), and ISCC. He is also an NVLAP assessor for the Energy Efficient Lighting Program and the Calibration Program

Mira Fein
earned a bachelor's degree in Psychology from Oberlin College (2015). She worked as an undergraduate research assistant in the Physical Measurements Laboratory at the National Institute of Standards and Technology in the summers of 2012 through 2014. She participated in research in the areas of Vision Science and current lighting technology and standards. Mira is currently working on earning her master's in Speech Language and Hearing Sciences at the University of Arizona

Light & Engineering
Vol. 23, No. 4, pp. 15-21, 2015

Svetotekhnika
No. 4, 2015, pp. 29-33

EXPERIMENTAL RESEARCH OF EVALUATION METHODS FOR COLOUR RENDITION QUALITY

Dmitry V. Skums and Lyubov D. Chaikova

The Belarus State Institute of Metrology Republic Unitary Enterprise,
Minsk, Republic of Belarus
E-mails: dmitri_scums@mail.ru, optic@belgim.by

ABSTRACT

The principles of evaluation of colour rendition quality for energy saving light sources are considered. Disadvantages of the existing method of colour rendition evaluation are presented, and alternative measuring methods are described. Results of visual experiments of colour rendition quality evaluation of light-emitting diode light sources are given, and their comparison with theoretical predictions is presented. Possible directions for the modernisation of the *CQS* method of colour rendition evaluation are shown.

Keywords: light-emitting diode light sources, colour rendition index, CIE, *CQS*

INTRODUCTION

Up to 20% of electric energy consumed in the Republic of Belarus is used for illumination of streets and rooms [1, 2]. In recent years, compact fluorescent lamps (CFL) have become widespread. However, their use entails a number of challenges. In particular, they contain mercury, and require special recycling methods. This certainly reduces the economic benefit of introducing these lamps, and mercury pollutants into the environment. Light-emitting diode light sources (LEDLS) don't have such disadvantages, and have a number of well documented benefits [3, 4]. An analysis of effective technical standard legal acts (TSLA) has shown that light sources colour rendition index (CRI) value is a feature of a number of requirements, and poor performance against prescribed values can prevent the application of such sources. At the same time, there are no TSLAs normalising CRI measurement methods for modern energy saving light sources. The only TSLA normalising measurement methods of chromatic characteristics of light sources is the out-of-date GOST 23198–94 [5]. It is based on the CIE publication of 1974 "Measurement methods and specifications of properties of light source colour rendition", in which the current method is the 1994 version. For similar reasons, the US Department of Energy has recommended not to use CRI as an indicator of LEDLS quality. However, this approach is unacceptable in the Republic of Belarus as some TSLAs regulating CRI values [5, 6] are still in effect now.

THEORETICAL BASES OF COLOUR RENDITION QUALITY EVALUATION

The CRI characterises a similarity or difference of chromatic stimulus, when an observer perceives an object illuminated by investigated and reference light sources [6]. When determining CRI, eight reference samples from the Munsell's Atlas are used as test objects.

The general CRI R_a recommended by CIE is determined as follows:

$$R_a = \sum_{i=1}^{8} R_i,$$

$$R_i = 100 – 4.6\Delta E_a,$$

where R_i is special colour rendition index calculated for one reference sample, ΔE_a is the chromatic dif-

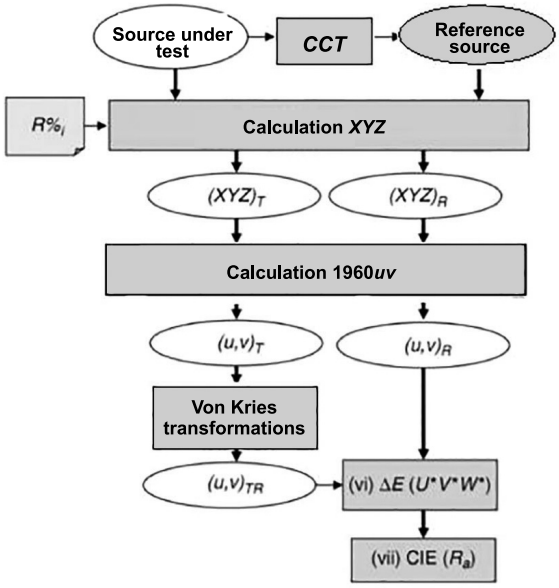

Fig. 1. Flow chart of CRI calculation recommended by CIE, R_a

ference between the investigated and reference light sources calculated in colorimetric system $W^*U^*V^*$ [7] (Fig. 1). Coefficient 4.6 was chosen so that R_a of fluorescent lamps with halo-phosphate phosphor amounted to 50.

R_a has a number of essential disadvantages, whilst being the basis of the method. The CIE does not recommend any more chromatic space be applied when calculating chromatic differences, because it has a big heterogeneity in the red area. A big source of measurement result errors is also the fact that it is recommended to use as the reference light source a light source, which correlated chromatic temperature (CCT) is the same or maximally close to the sources under test. A source with CCT lower than 5000 K, is an absolute black body, and with CCT higher than 5000 K, type *D* radiation takes place (different phases of daylight). The calculations show that a source with a CCT of 4999 K and R_a = 100 obtains a considerably smaller CRI, if its CCT rises by 2 K only [8]. A big disadvantage of R_a is that it is calculated as an arithmetic average of eight special CRIs. Thus a light source with a very low colour rendition in any part of the spectrum, obtains a high CRI due to the averaging. In this case, the consumer cannot comprehensively estimate quality of the light source. This problem is revealed especially clearly when calculating CRI of modern energy saving light sources, such as CFLs and LEDLSs. The radiation spectrum of the latter is essentially different from absolute black bodies and from the CIE standard light sources. This problem is vividly shown in publication [9]. As samples under test, LED clusters based on LEDs of blue (460 nm), green (540 nm) and of orange (605 nm) phosphorescence were used with a CCT of 3300 K and R_a = 81. After this, a mathematical model of a similar radiator was developed with radiation peaks at wavelengths of 455, 534 and 616 nm and with R_a = 67. This means that such light sources are unacceptable for use in premises. However, research of special CRI R_i have showed that the mentioned LED clusters reproduce most colours much better, except for moderately blue area, which causes an essential decrease of CRI. Consumers consequently prefer precisely these light sources. Besides, in the chromatic shift calculation process, out dated transformations of von Kries are applied. At present, CIE recommends to use two models of chromatic transformation: *Colour Measurement Committee's Chromatic Adaptation Transform of 2000* (*CMCCAT2000*) and *CIE's Chromatic Adaptation Transform* (*CIE CAT02*).

Based on the all arguments set forth above, the CIE published technical report 177:2007 "Measurement of colour rendition of white light emitting diodes". The results section states that CRI CIE R_a should not be applied to evaluate colour rendition of light sources based on white LEDs (or having them in their composition). CIE recommends developing a new CRI or another measurement method of evaluation of colour rendition quality. The new additional CRI (or a set of CRI) should be applicable to all types of light sources, and not just to white LEDLSs [10].

ALTERNATIVE METRICS OF EVALUATING COLOUR RENDITION QUALITY

It follows from the reference analysis that instead of effective CRI R_a, the following metrics are proposed:

• ***Rank-order based colour rendering index (RCRI)*** [11]. This is an update of the effective method with 17 test samples. Samples 1–12 are from the *Colour checker* set of *GretaghMacbeth* Company and samples 13–17 are of the *Colour Set NIST* set. To calculate chromatic differences, the *CAM02UCS* model of chromatic perception is applied. Reference light sources are similar to the sources for the effective CIE method. After the calculation of chromat-

ic differences is made using a special formula, they are transferred to a rank scale from 1 to 6, where 1 means good colour rendition, and 5 is very bad and absolutely unacceptable.

• ***Feel of contrast index (FCI)*** [12]. This CRI expresses numerically a contrast sensation of light transition of test samples by a reference source to the sample under test. As a test samples, red, yellow, green and blue samples from Mansell's Atlas are used. As a reference light source, a source of D_{65} type is used. The calculation is performed using the formula:

$$FCI=(G(T, E_t=1000\ lx)/\ G(D65, E_t=1000\ lx),$$

where $G(T, E_t=1000\ lx)$ is the total area of a figure formed in the *LAB* chromatic space by a contact of the points with chromaticity coordinates of test samples when illuminating them using the test source, illuminance value is 1000 lx; $G(D65, E_t = 1000\ lx)$ is the total area of a figure formed in the *LAB* chromatic space by a contact of the points with chromaticity coordinates of test samples when illuminating them using D_{65} radiation.

• ***CRI–CAM02UCS*** [13]. This is a modification of the CIE CRI R_a. The calculation procedure of this CRI is the same as in R_a calculation except that the von Cries transformations are replaced with the *CIE CAT02*, and the *CAM02UCS* model of chromatic perception is applied. The general CRI *CRI–CAM02UCS* is calculated as

$$CRI–CAMO2UCS =$$

$$=\frac{1}{8}\sum_{1}^{8}(100-8\Delta E_{i\text{CRI-CAM02UCS}}),$$

where $\Delta E_{i\text{CRI-CAM02UCS}}$ is a chromatic difference of test samples when transiting from the reference source light to the one under test, which is computed according to model *CAM02UCS; i* is a number of the standard sample.

Colour quality scale (CQS) [14]. This metrics is conceptually close to the R_a calculation method. However, unlike its fundamental principle, it takes into consideration different aspects of colour quality, such as colour rendition, chromatic discrimination and observer preferences. The scale is based on 15 Munsell's samples with a more saturated colour than in the R_a calculation method. The von Kries's transformations are replaced with the *CMCCAT2000*.

Fig. 2. Appearance of the colour rendition visual evaluation chamber prepared for the experiment. The right half of the camera is illuminated with a reference source, and the *left – with light-emitting diode light source "3"*

Calculations of chromatic differences are performed within the *LAB* colour space. The general CRI Q_a is calculated according to the formula

$$Q_{\text{a}} = M_{CCT}\cdot 10\ln(\exp((100-3{,}1\cdot\Delta E_{\text{RMS}})/10)+1),$$

where ΔE_{RMS} is the mean-square deviation of chromatic differences of test samples when transiting from the reference source light to the one under test, M_{CCT} is the correction coefficient penalising sources with extremely low CCTs. This is introduced to ensure that sources with low CCTs and with spectral distribution close to Planck's do not obtain a high final CRI due to the features of the calculation method. It is calculated using the formula:

$$M_{\text{CCT}} = T^3(9{,}2672\cdot 10^{-11}) - T^2(8{,}3959\cdot 10^{-7}) +$$
$$+T(0{,}00255) - 1{,}612\ (\text{при}\ \ T<3500\ \text{K}),$$
$$M_{\text{CCT}} = 1\ \ (\text{при}\ T\geq 3500\ \text{K}).$$

• ***Harmony rendering index (HRI)*** [14]. This CRI is determined as a difference of chromatic harmony of test samples when illuminated by reference and by test light sources.

• ***Categorical colour rendering index (CCRI)*** [15]. The method is based on a visual evaluation by observers of a considerable sample number when illuminating them with reference and test light sources (in the experiments cited, 295 samples were used).

Appendix

Questionnaire of a participant of the experiment on the visual evaluation of colour rendition

Your age_____

Your sex: male ○ female ○

Do you have visual deficiencies, if the answer is yes, which ones?_____

Specify your visual acuity, you can do it approximately

_____

By a scale from one to ten estimate your psychological state where 1 is absolutely quiet, 10 is very annoyed

_____

By a scale from one to ten estimate your physical state, where 1 is fresh and vigorous, 10 is extremely tired and feel very badly_____

Write what figure you see on the picture

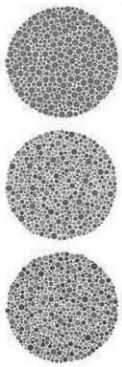

Source 1 :
Do you see you any difference between the right and the left chromatic samples:
yes ○ no ○
If yes, estimate a similarity of the left sample colour in comparison with the right by a ten-point scale, where 0 is completely not similar, 10 is absolutely identical
Source 2:
Do you see you any difference between the right and the left chromatic samples:
yes ○ no ○
If yes, estimate a similarity of the left sample colour in comparison with the right by a ten-point scale, where 0 is completely not similar, 10 is absolutely identical
Source 3 :
Do you see you any difference between the right and the left chromatic samples:
yes ○ no ○
If yes, estimate a similarity of the left sample colour in comparison with the right by a ten-point scale, where 0 is completely not similar, 10 is absolutely identical
Source 3 +:
Do you see you any difference between the right and the left chromatic samples:
yes ○ no ○
If yes, estimate a similarity of the left sample colour in comparison with the right by a ten-point scale, where 0 is completely not similar, 10 is absolutely identical
Source 123
Do you see you any difference between the right and the left chromatic samples:
yes ○ no ○
If yes, estimate a similarity of the left sample colour in comparison with the right by a ten-point scale, where 0 is completely not similar, 10 is absolutely identical

Fig. 3. The questionnaire for observers

• ***Memory CRI (MCRI)*** [16]. The method is based on the colour memory effect. Real objects (fruits, etc.) are used as test samples.

It should be noted that each of these methods, even if it corrects some CIE CRI R_a disadvantages, does not solve completely the problems set out in the report [10]. Therefore, we have conducted a number of experiments with the participation of observers in order to reveal the most promising method of colour rendition quality evaluation.

EXPERIMENTAL RESEARCH

Choosing a method of colour-rendering characteristic evaluation for modern energy saving light sources is impossible, using only theoretical analysis. Colorimetry is located at the interface of physical optics and biology. The human visual system is too complicated for numerical simulation: it functions not only based on the laws of geometric optics, which are easy to model, but also based on complex psychophysiological processes. Therefore, any model must be validated experimentally by observers. The basis for carrying out colour experiments with the participation of observers is a chamber of visual evaluation and colour comparison, or a so-called chromatic room. A typical chromatic room represents a chamber separated into two sections, one of which is illuminated with the source under test, and the other with the reference light source. The inner surface of the room is covered with a grey matte paint to exclude any contrast phenomena. The surface, on which the samples are placed, light-grey to mid-grey, with a reflection factor of about 30%. The

Table. Results of the experiment on visual evaluation of colour rendition

Metrics / Light emitting diode light source	R_a	*CQS*	*NCRI*	FCI	*CRI–CAM02UCS*	Average arithmetic results of colour rendition quality evaluation by observers, points
«1»	93	80	88	71	77	8.3
«2»	45	40	44	44	45	3.8
«3»	38	32	32	21	32	2.7
«3+»	44	24	21	29	16	2.1
«123»	65	52	57	60	55	5.0

illuminated samples are placed as close as possible to each other, and a separating line between them is made as thin as possible. The illuminance level set for colour evaluation should be between 700–3000 lx and should be identical in both sections of the room. Higher levels are preferable for the evaluation of darker colours. The camera is located at such a height that the observation angle for an observer of medium height would amount to about 45% [17]. Based on the rules set forth, together with the Republican research-and-production unitary enterprise "The Centre of Light-Emitting Diode and Optoelectronic Technologies of the National Academy of Sciences of Belarus", a chamber for colour rendition visual evaluation (Fig. 2) was developed.

The tested LEDLSs were four light sources of white fluorescence with different CCTs. The reference source was a HIL operating in the CIE type *A* source mode.

LEDLS1 has a CCT of (2856 ± 150)K. It contains white broadband phosphor LEDs. The source CCT is selected so that it corresponds to the CIE standard type *A* source.

LEDLS2 has a CCT of (6500 ± 250)K. It contains white broadband phosphor LEDs. The CCT of the source is selected so that it corresponds to the standard source of the CIE *D65* type.

LEDLS3 has a CCT of (4500 ± 350)K. It contains full-colour (*RGB*-) LEDs. Their CCT was not selected specially.

LEDLS3+ is similar to LEDLS3, but has an improved colour rendition according to CIE. The CCT was not selected specially.

Additionally, the experiment was set up to allow for the possibility to switch on all the LEDLS simultaneously. This is a so-called LEDLS123.

The light sources, ballast and CDs, adjust and indication devices for the operating modes are placed in the top part, over the working area. Illuminance on the surface, where the samples are placed, is equal to (2000 ± 15) lx. The *Colour Checker* reference colours of *GretaghMacbeth* Company (24 colour samples from the Munsell's Atlas) were used as the comparison samples for the experiment, as well as fruits and brightly painted cans of soft drinks. An observer had to estimate the colour simularity of the left sample in comparison with the right one using a ten-point scale, where 0 means a no likeness at all, and 10 means absolutely identical. The left sample is illuminated with the source under test, the right sample – with the reference source. Before beginning the experiment, the observers answer a questionnaire (Fig. 3), in which they specify their psychological state according to a scale from one to ten, where the one means an absolute calm, and the ten means extreme anxiety. They specify any sight problems and their acuteness as well. They are also tested for chromatic blindness and defects of chromatic sight (Ishihara's test). The colour rendition quality evaluation results are written in the questionnaire by the administrator of the experiemnt for every observer.

The data obtained from the observers were compared with the numerical simulation results. To carry out the numerical simulation, a special pragramme was developed, which was able to provide the CRI R_a, *CQS, NCRI, FCI* and *CRI–CAM02UCS* calculations. These metrics were selected using the criterion "presence of clear algorithm of calculation of a colour rendition quality indicator". The measurements of the light source radiation spectrum (Fig. 4) were performed using a CS-1000 spectral radiometer of Konica-Minolta Company of the colorimetric device set of the National standard of luminous intensity and illuminance units of Republic of Belarus (НЭ РВ8–02).

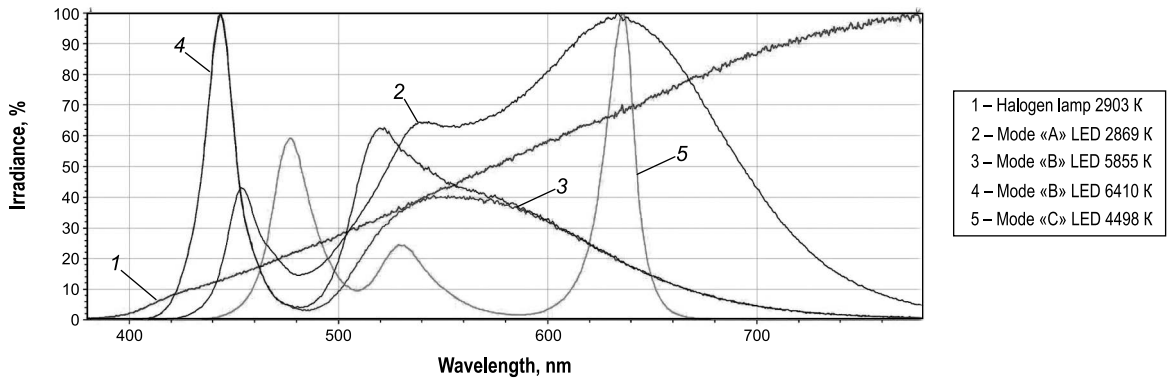

Fig. 4. Relative radiation spectra of reference and tested light-emitting diode light sources installed in the chamber of colour rendition visual evaluation

THE OBTAINED RESULTS AND THEIR CONSIDERATION

Thirty-eight people took part in the experiment (twenty-two women and sixteen men). The average age of the observers was 25; the oldest was 60, the youngest was 18 years old. After elimination by the negative psychological state criteria and/or by anomalies of colour perception according to the Ishihara's test, data collected from 30 observers were used for the calculations. The results are given in the Table.

It can be seen from the Table that the *CQS* metrics shows results closest to the experimental results. This method takes CRI R_a disadvantages into consideration to the maximum extent. The samples of the comparison with colours of a greater saturation than of the applied now, which were specially selected by the authors, and use of the newest generally recognised *CMCCAT2000* model of chromatic adaptation, as well as the original method of total chromatic shift calculation, made it possible to resolve almost all the issues set forward in the report [10]. At the same time, this metrics doesn't eliminate one of the main disadvantages of determining CRI R_a: application of several essentially different types of reference light sources. In our opinion, it is a significant disadvantage in the case of LEDLS colour rendition evaluation, because as it was said above, a situation can take place, when two visually completely identical LEDLSs obtain essentially different evaluations[1]. Hence, a question arises about the possible introduction of either a new reference light source, or of a tested light source uniform for all CCT values. The first version seems to be preferable but for as long as the lighting industry makes the decision about the main method of white light creation, it is too early to speak about standardisation of such a source conditionally named source of type *L* (*LED*). The mentioned method will dominate de facto, or de jure via the international standard. Therefore, we consider it possible to use CIE *A* radiation reproduced by the CCT 2856 incandescent lamp as the uniform reference radiation, or to use *D65* radiation simulating the light of the daylight sky in the northern hemisphere. In our opinion, the first radiation is more preferable, because an observer's perception of what constitutes natural colour has been developed under the influence of incandescent lamp light over the last century. Besides, *D65* radiation raises a question of the correctness of its application in places, where spectral characteristics of the daylight sky can differ considerably from the standardised (for example, in countries of Africa and South America).

CONCLUSION

An analysis of many research results has shown that the effective method of CIE colour rendition quality evaluation cannot be applied to light sources with a "complex" spectral composition. Instead of the effective metrics, different authors have offered

[1] Probably this situation arose, because the *CQS* method has inherited reference radiation sources from the method of R_a evaluation, in which as in a mirror, the history of development of artificial light sources was reflected. Coal lamps and incandescent lamps became the first radiation sources close by the spectral characteristics to the Plank radiator. Therefore, it was quite logical to compare their colour renditions with the colour rendition of Planck radiators. After the widespread introduction of fluorescent lamps, the family of reference sources was added to by *D* type sources (not only with *D65*) and calibration coefficient 4.6 was introduced into the formula of R_i calculation. At present, due to the introduction of the LEDLSs, a third revolution in light engineering is observed.

seven alternatives. Based on the analysis of the proposed methods, we have selected five of them using the criterion "presence of a clear algorithm for calculation of colour rendition quality indicator". Their accuracy was checked in experiments with observer validation. The obtained data have shown that the results closest to the observer results, are provided with the *CQS* metric.

REFERENCES

1. *Kirvel I.I.* Energy saving. An abridgement of lectures for students of all specialties of the Belarus State University of Informatics and Radio Electronics for all study forms. – Minsk: BSUIR, 2007. URL: http://www.bsuir.by/m/12_100229_1_65369.pdf (Addressing date: 03.03.2015).

2. *Kuzminov A.S.* Energy efficiency marking as a tool of decrease of power consumption of the household electrical appliance equipment // Energy saving technologies. 2010, # 4, pp. 45–50.

3. *Lishik S.I., et al.* On light-emitting diode lamps of direct replacement / /Svetotekhnika, 2010, # 1, pp. 48–54.

4. URL: http://technologyworld.blog.ru/80642627.html (Addressing date: 03.03.2015).

5. GOST 23198–94. "Electric Lamps. Methods of Spectral and Chromatic Characteristics Measurements".

6. ТКП 45–2.04–153–2009. Natural and artificial illumination. Building standards of design.

7. CIE (Commission Internationale de l'Eclairage): Method of Measuring and Specifying Colour Rendering Properties of Light Sources. 3ed CIE Publication № 13, 1994.

8. *Davis W., Ohno Y.* Approaches to Colour Rendering Measurement // Journal of Modern Optics. 2009, Vol. 56, No. 13, pp. 1412–1419.

9. Wood M. CRI and the Color Quality Scale, Part 2. URL: http://www.mikewoodconsulting.com/articles/Protocol%20Spring%202010%20-%20CRI%202%20CQS.pdf (Addressing date: 03.03.2015).

10. CIE177:2007. Technical report. Color rendering of white LED light sources.

11. *Khanh T.Q., Bodrogi P., Brückner S.* Rank-order based description of colour rendering: definition, observer variability and validation. CIE2010 "Lighting Quality & Energy Efficiency", 17.März 2010, Wien. Wien [Conference or Workshop Item], (2010).

12. *Hashimoto Yano, Shimizu Nayatani.* New method for specifying colour-rendering properties of light sources based on feeling of contrast // Colour Research & Application. 2007, Vol. 32, No.5, pp. 361–371.

13. *Cheng Li, Ming Ronnier Luo, Changjun Li.* Assessing Colour Rendering Properties of Daylight Sources Part II: A New Colour Rendering Index: CRI–CAM02UCS. URL: http://cie2.nist.gov/TC1–69/Leeds/CIE-CLi%202-final.pdf (Addressing date: 03.03.2015).

14. *Szabo F.* New Metric on Light Source Colour Quality: Colour Harmony Rendering Index. URL: http://www.create.uwe.ac.uk/norway_paperlist/szabo.pdf (Addressing date: 03.03.2015).

15. *Hirohisa Yaguchi, Nanako Endoh, Takayoshi Moriyama, Satoshi Shioiri.* Categorical Colour Rendering of LED Light Sources / CIE Expert Symposium on LED Light Sources: Physical Measurement and Visual and Photobiological Assessment, 2004.

16. *Smet, Forment, Hertog, Deconinck, Hanselaer*. Validation of a colour rendering index based on memory colours /CIE Conference on "Lighting Quality and Energy Efficiency", 2010, pp.136–142

17. Colours in industry. Under the editorship of R. Mak-Donald. Moscow: Logos, 2002, 596 p.

Dmitry V. Skums,
a physicist, graduated from the physical department of the Belarus State University in 2006. The scientist-keeper of national standards in the photometry and colorimetric field, the Belarus State Institute of Metrology

Lyubov D. Chaikova,
an engineer, graduated from the department of instrument engineering of the Belarus National Technical University in 2013. At present, she is an engineer in the department of physical-chemical and optical measurements of the Belarus State Institute of Metrology

Light & Engineering
Vol. 23, No. 4, pp. 22-29, 2015

Svetotekhnika
No. 4, 2015, pp. 41-46

VISUALIZATION AS ALTERNATIVE TO TESTS ON LIGHTING UNDER REAL CONDITIONS

Rafał Krupiński

Warsaw University of Technology, Faculty of Electrical Engineering, Lighting Division
E-mail: rafal.krupinski@ien.pw.edu.pl

ABSTRACT

This paper presents a lighting simulation method development that has taken place over more than a decade since these techniques started functioning. Although it has taken so much time, the photo-realistic computer visualization of lighting is still not so commonly applied. It may have been because a relatively small number of publications on this issue and a limited number of professional training courses devoted to its use for designing the lighting systems. Design offices, especially as far as the architectural structure floodlighting is concerned, still prefer traditional methods based on the tests with the use of a real lighting equipment in the real conditions. The paper compares these two methods, showing their advantages and disadvantages with an example of complex floodlighting project.

Keywords: illumination, floodlighting, lighting technology, computer graphics

INTRODUCTION

A lighting visualization is a computer graphics presentation of the lighting design image with the use of colour and luminance on the computer screen or another medium. The currently produced computer monitors can reproduce luminance values of around a few hundred cd/m^2, whereas the average luminances obtained in the floodlighting designs are between ten and twenty cd/m^2. Of course, apart from some exceptions, such as interior and street lighting, where we can face the images of luminaires whose luminance values considerably exceed this range.

In such cases the luminance evaluation could be made based on a similar principle as it is tried with the interior [1, 2] or street lighting [3]. However, in general, it can be said that the lighting technology is the area where computer simulations can be recognised as real rendering of the lighting state [4], and thus, it can be called photorealistic.

Lighting simulations in computer graphics have been known and performed for more than a decade. They are still being improved with new methods and functions enabling creating geometrical models which basis they are created. Also, better and faster lighting calculation algorithms have appeared. It is now possible thanks to a very rapid development of the computer equipment. When 3D visualization began functioning, it even took even between ten and twenty computing hours to make the simulation calculations for one lighting option. At present, depending on the level of complexity of the virtual scene, the amount of lighting equipment used, and of course, the speed of a computer, the calculations can take just a few minutes. Additionally, the dynamic simulations displayed on a computer screen are changing in time both, the lighting parameters and location of pointing luminaires, as well as video cameras. In short, the lighting animations are created.

FLOODLIGHTING DESIGN USING 3D COMPUTER GRAPHICS TECHNIQUES

The WUT (Warsaw University of Technology) Main Building floodlighting design made by the author was the first architectural floodlighting project

Fig. 1. Computer simulation of the WUT Main Building floodlighting – the first lighting simulation in 3D model in Poland made in 1996

in Poland, and perhaps in the world, carried out with the computer graphics method based on the realistic simulation of lighting equipment (Fig. 1).

3D computer applications and lighting companies were not ready for such projects in 1996. It can be said that it did not make sense to design the architectural structure floodlighting using the computer graphics, since only 19 luminaires were used. It was possible to do the test on the lighting concept under the real conditions successfully; however, we should remember, just on this option. At that time, it was an attempt to introduce a novel lighting design method in architecture that enabled analysing a large number of the floodlighting concepts in the virtual reality. The major problem with the computer applications was that they did not include the indirect illuminance component in the simulations. While illuminating the architecture, it is not a big mistake to ignore it, since the indirect illuminance component has a low impact on the simulation accuracy in most lighting designs. At present, while designing the architectural structure illumination based on this method, the calculations at the early project stages are often ignored, too. When selecting, positioning and directing the lighting equipment, the simulation of direct illuminance component only gives designers a sufficiently good presentation of their lighting vision "online" in practice. The graphics software did not allow them to correctly define the reflective and transmissive properties of materials of the real building. However, the biggest disadvantage of this method was a shortage of capabilities of reading out the basic lighting parameters – illuminance and luminance of the concept being made. And the

Fig. 2. Photorealistic simulation of office interior lighting

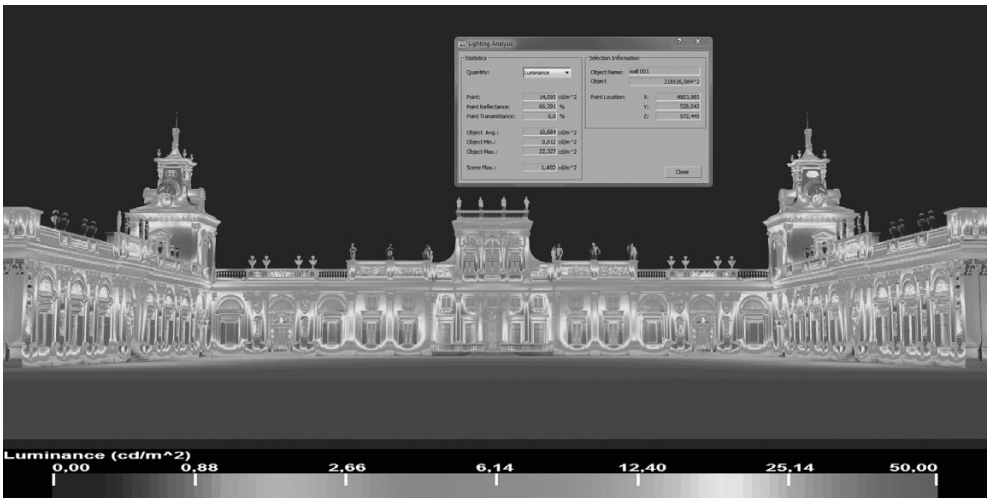

Fig. 3. Visualization of luminance distribution in the Wilanów Palace floodlighting design

lighting companies did not predict such a design mode. They did not make the photometrical files of their lighting products available. When simulating a floodlight or spotlight, the designer was forced to use a set of light sources available in the software. The applications only enabled defining the angles of variances in the useful beam for those individual virtual "lighting fixtures". The visualization was also based on the traditional units; such terms as luminous intensity and luminous flux were not used. The computer simulations were then just the images, on whose basis the illumination concepts could be assessed only. It was impossible to make a complete lighting analysis.

The current applications include all these parameters [5]. The indirect illuminance component simulation and proper material defining in a form of assigning the reflectance and transmittance as well as reflection character are not a problem any longer [6, 7]. As shown in Fig. 2, the visualization can successfully be used for designing the interior lighting and analysing its lighting system on the basis analogous to Fig. 3 luminance or intensity distributions [8, 9].

Practically, all lighting companies make a full photometrical file base of their produced luminaires available now. The files are mainly recorded in the IES (Illuminating Engineering Society) format and LDT – European equivalent file format specified in IESNA LM-63. All these facts enable, apart from the visual design evaluation, the quantitative assessment on the basis of colour images in a form of luminous intensity or luminance distribution. A specific colour represents a luminance value shown in the simulation legend. The presented results may also be shown in grey tones or as isolux or isocandela diagrams. On their basis, the average luminance level can be read out in both selected planes and points. It gives an opportunity to make a full analysis of the design, to check its accuracy with the quantitative average luminance recommendations [10] and the architectural structure floodlighting principles, both general [11] and detailed that take into account the architectural features [12, 13] or even creating the lighting mater plans [14]. Fig. 3 shows the luminance distribution of virtual floodlighting design.

On the basis of the photorealistic visualization, one of the latest projects designed by the author is the design of illuminating the Wilanów Palace Museum [15], Poland, often called the "Polish Versailles". Based on the earlier prepared 3D geometrical model, and after defining the earlier measured reflective and transmissive properties of materials, used for the construction of the palace, its multi-conceptual floodlighting design was created. This paper only presents the final concept with its three main options. The way leading to the final floodlighting projects was based on a selection of the lighting equipment from different companies, and its various positioning and directing. That could hardly be done during the field tests in the real conditions. The number of the lighting products used, depending on the option, was from 249 to 311 pieces. It is hard to imagine that any of the luminaire manufacturers could have such a big amount of the lighting equipment at their disposal to be able to carry out the tests under the real conditions.

Owing to the points and directions of observation of the building, it was decided to apply the floodlighting with a mixed method [11] in this concept. The elevations to the upper cornice level were lit

Fig. 4. Computer simulation of the Wilanów Palace floodlighting, option I

by the in-ground luminaire with metal halide lamps (HIT) each having the power of 70 W and maximum luminous intensity Imax = 3400 cd, with half peak divergence $\delta_{1/2} = 40$ deg and the colour temperature 3000 K. Option I of this concept assumes highlighting the column rhythm of the upper façade. The illumination of these architectural elements was also carried out by means of the in-ground luminaires with metal halide lamps having the same colour temperature. The lighting fixtures used along the upper cornice are characterised by a half-peak divergence of $\delta 1/2 = 10$ deg. and the light strip system with light-emitting diodes (LEDs) was installed to accentuate the reliefs and architectural balusters. The light colour was matched to the metal halide lamp colour temperature (3000 K). The main avant-corps was illuminated with general lighting method and with a higher luminance value than the other façades. The statues and lawns at the top of the building were illuminated with spotlighting method by means of small size LED luminaries. Two side towers were highlighted to the higher luminance level in order to emphasise their depth and height. Four spotlights equipped with metal halide lamps (HIT) were applied to each tower, i.e. two to their façades and two to the patina-covered helmets. To emphasise the bluish green patina-covered copper colour, the metal halide lamps of a higher colour temperature of up to 4200 K were used. Fig. 4 shows the computer simulation of this concept.

While performing this illumination concept, an annoying effect of uneven luminance on the cornice was noticed as a result of installing the lighting equipment accenting the effect of column and pilaster rhythm. The next step was an attempt to illuminate only the pilasters with the use of a different type of lighting fixtures, simultaneously emphasising the space between columns, where there are busts and statues exhibited. As shown in Fig. 5, unfortunately, the effect of luminance "burnt-outs" on the cornices was not eliminated completely. The talks with the conservator-restorer led to a consecutive change to the lighting design concept. It turned out that the illumination of figures and lawns at the top of the palace could not be carried out with the use of assumed lighting system due to the preservation maintenance of the building. Additionally, accentuating the pilaster rhythm and space between the columns was evaluated negatively, and therefore, a decision on withdrawing from using the spotlights to highlight that architectural detail was made.

Fig.6 demonstrates the final illumination design version. The created floodlighting is softened and consistent, and as shown in Fig. 3, describing the luminance distribution for this option. The most important thing is that the measured average luminance on the virtual object, is around 10 cd/m^2, and compliant with the recommendations included in the CIE report [10].

The discussed project shows how a powerful tool the virtualization of any illumination is in the lighting designer's hand. Of course, it has its disadvantages. It takes a relatively long time to design it and also creates the necessity of using complicated and expensive computer applications, which are difficult to learn and truly master. The time needed for creating a geometric model of the object considered according to a designer experience is about 100 h. After finishing that often laborious modelling work, the lighting design elaboration seems to be much easi-

Fig.5. Computer simulation of the Wilanów Palace floodlighting, option II, withdrawal from accenting column and pilaster rhythm

er than positioning light equipment on the spot. The designer task resolves itself into using photometrical files defined by luminaires makers and placing and directing the luminaires in an appropriate way. The shortage of capabilities to evaluate a glare effect still remains a limitation on the computer lighting simulation. It is connected with two basic features of the computer simulations. First of them are the maximum luminance values displayed by the projectors and computer screens, and the second is a lack of information what luminance the luminaries are characterised by. The files in IES or equal LDT format do not include the data. The luminance assessment in terms of discomfort glare, light pollution and its penetration into the building interior, generally enable only the same luminance measurements as made in the related fields [3]. The methods derived for the needs of glare evaluation in the street lighting can be basically shifted directly into the architectural structure illumination area, and thus, it is possible to assume that soon the problems will be solved.

However, all the disadvantages are disproportionately small compared to the advantages obtained. Based on the computer simulations, the designer has an opportunity to analyse the practically unlimited number of lighting options in terms of requirements and recommendations, without taking care of the amount of lighting equipment used. For example, it is also possible to apply the equipment being at the design stage to be dedicated to a given lighting solution. When the consultations with the conservator-restorers are required and if the building is subject to protection, this method has a big advantage by enabling the analysis of a large number of concepts without any time limits. It provides an opportunity to select the best design for both designer and investor.

TESTS UNDER REAL CONDITIONS

At the 2nd Royal Festival of Light in Wilanów, Warsaw, the organizers [16] decided to implement the final illumination concept on the basis of 3D model visualization when the event was held.

Fig. 7 shows the evening photography of the palace floodlighting. When comparing computer visualization to field test effect one should have regard that the picture had not been post-produced [17]. In that case, the graphical working had not been done. The palace floodlighting implementation can be compared to the common method for designing the illuminations based on the tests under real conditions. For two days before the Festival of Light, the company responsible for this project, collected and installed temporarily the lighting equipment of nearly 200 luminaires from Europe-wide different subsidiaries. However, the characteristics of luminous intensity distribution did not exactly correspond to the initial design. And the colour temperatures of the light sources were different from the assumed under the project. It is hard to expect the lighting companies to be able to collect the amount and type of equipment required for the project for a few-day show, especially that in some cases it was not standard. The lighting fixtures installation alone for a short time of the show could not be made exactly in the places included in the project. The facts show a weakness of applying this method, however, the obtained effect compared to the intended one

Fig. 6. Visualization of the final Wilanów Palace Museum floodlighting concept

can be found satisfactory. The high luminance values are above the upper cornice, but they are connected with the improper lighting equipment. Along the cornice, the LED light strip system consisting of two types of luminaires was applied, yet, none of types was compliant with the assumed functionality of the project.

Unfortunately, the palace towers did not receive the illumination included in the design – the implementation was impossible due to the lighting equipment available and its difficult mounting. It has to be noticed that the palace is under permanent preservation maintenance and any type of interference into its structure, even temporary, should be consulted.

While observing the elevation up to cornice level, comparing it to the design based on the photorealistic visualization and despite the existing differences, it should be considered that the similarity of the obtained effect in 3D model with the tests under the real conditions is very high.

Computer simulations were done in Autodesk 3ds Max Design software, which ranks among the most popular for creating virtual scenes. The effects that it enables are appreciated both by film producers as well as users creating still images and illumination designers.

The palace floodlighting test performed at the Festival showed reliability of the simulation methods. Of course, all depends on the visualization quality, calculation algorithms applied and degree of detail rendering in 3D model. As for the described design, the parameters were at a high level. They were both precisely presented in the 3D model, the main mass of the object, as well as the architectonic details of sculptures. Also, they were perfectively simulating the reflection transmission properties of the materials which had been earlier measured on the real object.

This method has many advantages which certainly aided to the spectacular nature of the show. According to the estimates from the organizers, 200 thousand people visited the three-day Festival of Light in Wilanów, and the palace illumination impressed them very much.

However, this method has a large number of disadvantages too. Its application is limited. While it is possible to imagine the tests on small structures under the real conditions, this method becomes useless for big buildings that require a high amount of lighting equipment. The Wilanów Palace, although it is a relatively low building, should be treated as extensive and rich in the architectural details. As for the tall buildings, it is hard to imagine using the tests under the real conditions, while implementing the concept of highlighting the architectural detail. Especially, when the spotlighting method for illuminating them is used and where the lighting equipment is mainly mounted on their façade. The next problem is a preparation time to implement the test. As for the described project, where accessibility to the places of luminaire location, was not too difficult, and also not carried out at considerable heights, the test under the real conditions was preceded by a two-day equipment installation. It is also unimaginable to make any changes to the project during the show. On the other hand, based on the photo documentation of its duration may be biased [17], especially for the people not taking part in it.

The method is applied to one floodlighting option, limiting itself on a number, types of the lumi-

Fig. 7. Photo of the Wilanów Palace Museum floodlighting test during the 2nd Royal Festival of Light in Wilanów, Warsaw [16]

naires available during the show as well as application of the equipment only currently produced by the lighting companies. The next issue, however, is a season of the year and the weather conditions under which the test can be done.

CONCLUSIONS

The Wilanów Palace Museum illumination/floodlighting design explicitly shows that designing the architecture illuminations on the basis of visualization in 3D model is currently the most convenient and reliable method. Any changes to the lighting concept and to the lighting equipment location are difficult, especially due to lamp discharge, as it takes time to cool and to restart them. Also, applying a different lighting system requires having a relatively large lighting equipment base during the tests under the real conditions. When comparing the visualization of the described design to its tests in the real conditions, of course, the differences are seen. However, based on long years of experience in lighting visualization, the author guarantees that using the luminaires included in the design, their proper positioning and directing, will accurately translate into the reality. It is hard to imagine an analysis of a few lighting options, based on the equipment from different lighting companies during the tests under the real conditions, even if they were not so complicated as it happened in this case. And, it is also hard to expect that the investor and conservator-restorer could make a decision on selecting the most appropriate lighting concept during the temporary show. The virtual visualization images can be displayed, printed and analysed without time limits.

The author continues improving it by implementing a few dozen floodlighting designs [18–20], as well as with its use for more than a decade of his work, thus creating and making this method the most popular. At present, it takes from a few, ten to hundreds of hours, to create a design in 3D model, depending on the complexity of the building or its structure; however, we should expect it to be shorter and shorter. Currently, the author is in the course of preparing a new simulation method that will reduce the time of designing the floodlighting to minimum and it will not require long hours of work on the 3D model. It also includes the excellent information on graphic applications from a lighting designer.

RETERENCES

1. Tashiro T., Kawanobe S., Kimura-Minoda T., Kohoko S., Ishikawa T., Ayama M. „Discomfort glare for white LED light sources with different spatial arrangements" Lighting Research and Technology, 2014, pp. 1–22.

2. Sweater-Hickcox K., Narendran N., Bullough JD., Frayssinier JP. „Effect of different coloured luminous surrounds on LED discomfort glare perception" Lighting Research and Technology 2013, V. 45, pp. 464–475.

3. Słomiński S., „Laboratoryjne pomiary luminancji LED-owych i sodowych wysokoprężnych opraw oświetlenia ulicznego pod kątem określenia olśnienia przykrego" Przegląd Elektrotechniczny, ISSN1506 6223, 2013, # 10, pp. 281–284.

4. Narboni R., „The old city of Jerusalem lighting master plan" Light & Engineering, 2012, V. 20, No. 1, pp. 50–57.

5. Krupiński R., Modelowanie 3D dla potrzeb iluminacji obiektów", Oficyna Wydawnicza Politechniki Warszawskiej, Warszawa, 2011, ISBN978 83 7207 961 9.

6. Krupiński R., „Istotne etapy wykonywania wizualizacji komputerowych oświetlenia i ich wpływ na dokładność", Przegląd Elektrotechniczny, ISSN00332097, 2009, #11, pp. 297–299.

7. Krupiński R., „Projektowanie iluminacji na podstawie trójwymiarowego obiektu geometrycznego", Przegląd Elektrotechniczny, ISSN1506 6223, 2012, #04a, pp. 212–214.

8. Żagan W, Krupiński R., „Oświetlenie pośrednie-wnękowe", Przegląd Elektrotechniczny, ISSN1506 6223, 2012, # 04a, pp. 204–208.

9. Dehoff P. "Lighting quality and energy efficiency is not a contradiction", Light & Engineering, 2012, V. 20, No. 3, pp. 34–39.

10. Guide for Floodlighting, CIE94–1993, ISBN978 3 900734 31 2.

11. Żagan W., „Iluminacja obiektów", Oficyna Wydawnicza Politechniki Warszawskiej, Warszawa 2003, ISBN83 7207 360 0.

12. Krupiński R., „Iluminacja zespołów obiektów architektonicznych", rozprawa doktorka Politechniki Warszawskiej, 2003.

13. Kołodziej M.,"Iluminacja neogotyckich obiektów architektury sakralnej", rozprawa doktorska Politechniki Warszawskiej, 2008.

14. Bystryantseva Natalia V. „Current state of urban luminous medium design", Light & Engineering, 2011, V. 19, No. 3, pp. 53–59.

15. Wilanów Palace Museum webpage www.wilanow-palac.pl.

16. Royal Festival of Light in Wilanów webpage www.festiwalswiatla.wilanow.pl.

17. Słomiński S. „The correct image of illuminated object registration – problems arising from software capabilities and equipment limitation" Przegląd Elektrotechniczny, ISSN0033 2097, 2013, #8, pp. 259–261.

18. Krupiński R., „Nowe projekty iluminacji zrealizowane w Zakładzie Techniki Świetlnej", Przegląd Elektrotechniczny, ISSN0033 2097, 2011, #04, pp. 63–65.

19. Krupiński R., „Iluminacja obiektów użyteczności publicznej na przykładzie ratusza w Jaworze", Przegląd Elektrotechniczny, ISSN0033 2097, 2014, #01, pp. 273–276.

20. Author's webpage www.rafalkrupinski.com.

Rafał Krupiński,
Ph. D., graduated from the Faculty of Electrical Engineering, Warsaw University of Technology in 2003. In his studies, he focused on lighting technology. He is a specialist of floodlighting using computer graphics simulations methods. While making these methods popular by implementing a few dozen floodlighting designs, with its use over more than a decade of his work, he continues by improving it. He also lectures at the Warsaw University of Technology at the Faculty of Electrical Engineering, Lighting Division, where he occupies the post of the Assistant Professor

Light & Engineering
Vol. 23, No. 4, pp. 30-32, 2015

Svetotekhnika
No. 5, 2015, pp. 33-34

EXTENSION OF THE LUMINANCE CONCEPT IN ROAD AND TUNNEL LIGHTING*

Axel Stockmar

LCI Light Consult International, Celle, GERMANY
E-mail: a.stockmar.lci@t-online.de

ABSTRACT

The visual impression of the luminance distribution of the road surface in front of a vehicle driver does not correspond necessarily well with the determined values of the lighting criteria obtained for the traditional angle of observation. To overcome these discrepancies it is proposed to extend the current luminance concept and to apply an additional angle of observation. This requires the knowledge of the reflection characteristics of the pavements for different angles of observation. For the determination of the expected uniformities at the design stage it is necessary to use a calculation grid which is about three times denser than the usual grid. The assumption of a different angle of observation has also a decent impact on the estimated veiling luminance and the resulting threshold increments in road and tunnel lighting.

Keywords: reflection characteristics of road pavements, road and tunnel lighting, road surface luminance

1. INTRODUCTION

The controlling criteria for the lighting of roads and tunnels for motorized traffic are the luminance level and uniformity of the carriageway and the limitation of disability glare. The use of the luminance concept requires the knowledge of the reflection characteristics of the road surface. Current pavements used on roads have reflection characteristics, which are not only different from CIE standard reflection tables [1] but are also dependent on the angle of observation. At reduced speed during night time driving the drivers' visual fixations tend more to parts of the road in a distance of about 30 m in front of the vehicle, i.e. an angle of observation of 3° below the horizontal. At a speed of 30 km/h the length of the area in front of a car lit by its own vehicle headlights is approximately equivalent to the stopping distance. At such a distance the luminance distribution experienced could be quite different from the expected luminance distribution calculated under the usual assumption of an angle of observation of 1° below the horizontal. To avoid these discrepancies between calculated results and the visual impression the current concept should be extended in such a way that different angles of observation are considered at the design stage.

2. LUMINANCE CONCEPT

Road surface luminance is determined following the conventions and methods as described e.g. in Technical Reports for road [2] and for tunnel [3] lighting. Conventions include positions of observers in transverse direction and positions in relation to the field of calculation for fixed and/or moving observers. Conventionally the eye height above the road surface is 1.5 m which, for an angle of observation of 1° below the horizontal, results in an observation point lying 86 m ahead of the observer.

* On basis of report published in Proceedings of the 28th CIE Session, 2015, Manchester

Similar conventions are specified for the calculation of veiling luminance and resulting threshold increments. The observer is positioned longitudinally at a distance in front of the field of calculation, which is equivalent to an angle of 20° above the horizontal for the centre of the first luminaire in front of the observer to be taken into account. For an angle of observation of 1° below the horizontal, the angle between the line of sight and the centre of the first luminaire will be 21°. The contributions are summed for all luminaires in the direction of observation up to a distance of 500 m.

3. REFLECTION CHARACTERISTICS OF ROAD SURFACES

The reflection characteristics of road surfaces are usually provided in (standard) tables of (reduced) luminance coefficients. The luminance coefficient is the quotient of the luminance of a surface element in a given direction by the illuminance on the element under specified conditions of illumination [2]. The angles, which used to describe the geometry of illumination and observation [1], are:

The angle α of observation measured between the direction of observation and the horizontal;

Azimuth angle β measured between the two vertical planes containing the directions of illumination and observation;

The angle γ of light incidence measured from the vertical to the direction of illumination;

The angle δ measured as a rotation of the direction of observation around the vertical.

The angle of rotation is considered as not influencing the values of the luminance coefficients and is set to 0°. For car, driving at reasonable speed, the observation angle of interest ranges from 0.5° to 1.5°. Measurements of luminance coefficients have traditionally be done at an angle of observation of 1° below the horizontal.

4. EXTENDED APPROACH

There is a trend to reduce the speed limits in urban areas, e.g. from 50 km/h to 30 km/h. At such speed, in particular during night time driving, the drivers' visual fixations tend more to parts of the road in a distance of about 30 m in front of the vehicle, i.e. a viewing direction approximately 3° below the horizontal. Measurements of road surface samples have shown significant differences of reflection characteristics at different angles of observation below the horizontal.

If the actual surface properties are taken into account during the design process it is often possible to achieve the required average luminance using less energy, and to determine uniformities, which correspond with the visual impression. Under the assumption that the values of measured luminance coefficients are valid +/-0.5° around the selected angle of observation, the area covered in front of the observer (at an eye-height of 1.5 m above the road surface) stretches from 57 m to 172 m for an angle of observation of 1°, and from 24.5 m to 34.4 m for an angle of observation of 3° below the horizontal. As the field of calculation, with a length usually equivalent to the luminaire spacing, is larger than the area considered for an angle of observation of 3°, the luminance distribution has to be evaluated assuming a moving observer. For modern luminaires with pronounced luminous intensity distributions it is necessary to apply a smaller spacing between grid points in longitudinal direction than the usual maximum of 3 m [2] or of the recommended 2 m [3], e.g. a spacing in longitudinal direction of 1 m or even less.

For an angle of observation of 3° below the horizontal, the angles between the line of sight and the light incident from the luminaires will increase, thus reducing the veiling luminance and, depending on the associated average surface luminance, also the threshold increments, which are of particular interest for counter beam lighting installations in tunnels.

5. EXAMPLES AND RESULTS

First measurements of complete r -tables at angles of observation of 1° and 3° below the horizontal have shown differences of up to +/ – 10% for the average luminance coefficient as traditionally defined [1]. There is some evidence that surfaces of lower specularity (e.g. class RI) tend to show reduced average luminance coefficients with an increased angle of observation, but this has to be confirmed by further measurements. Calculations of traditional tunnel lighting arrangements with symmetric or counter-beam luminaires reflect the expected differences of the average road surface luminance determined assuming a moving observer.

More or less independent of the geometry of the installations and of the luminous intensity distribution of the luminaires the calculated (maximum) veiling luminances are always about 20% lower at

an angle of observation of 3° compared to an angle of 1°. For a given limit the resulting threshold increments could lead to the development of different luminous intensity distributions for particular luminaire arrangements.

For the determination of realistic (corresponding with the visual impression) overall and longitudinal uniformities it is necessary to apply a dense mesh of grid points in both directions. For surfaces of higher specularity (e.g. class RIII) lit by luminaires with pronounced luminous intensity distributions (measured at a sufficient number of angular intervals) a considerable drop of the uniformities for an angle of observation of 3° has been found, provided the spacing between grid points was reduced to less than 1 m, preferably down to 0,5 m.

6. CONCLUSIONS

At reduced speed the drivers' visual fixations tend more to parts of the road in a distance of about 30 m in front of the vehicle, corresponding to an angle of observation of 3° below the horizontal. Measurements of road surface samples have shown significant differences of reflection characteristics at different angles of observation. To estimate perceivable uniformities at the design stage, it is necessary to consider additionally road surface luminance for an angle of observation of 3°. It is proposed to extend the current luminance concept to bring the determined values of the lighting criteria in line with the expected visual impression.

REFERENCES:

1. CIE2001. CIE144:2001. Road surface and road marking reflection characteristics. Vienna: CIE.
2. CIE2000. CIE140:2000. Road lighting calculations. Vienna: CIE.
3. CIE2010. CIE189:2010. Calculation of tunnel lighting quality criteria. Vienna: CIE.

Axel Stockmar,
Prof., Dipl. – Ing. in University of Applied Sciences and Arts in Hannover, LCI– Light Consult International

Light & Engineering
Vol. 23, No. 4, pp. 33-40, 2015

Svetotekhnika
No. 5, 2015, pp. 42-47

ADAPTIVE SYSTEMS IN ROAD LIGHTING INSTALLATIONS*

Giuseppe Rossi[1], Paola Iacomussi[1], Andrea Mancinelli[2], and Paolo Di Lecce[2]

[1] INRIM, Torino, ITALY,
[2] REVERBERI Enetec, Castelnuovo ne' Monti (RE), ITALY
g.rossi@inrim.it

ABSTRACT

The new revised European standards for road lighting will be published in July 2015 highlighting the importance of energy performance aspects in road installations. The adaptive lighting approach can increase energy saving and reduce the environmental impact if compared to traditional solutions with the same type of luminaires and installation layout.

For these reasons, the next revision of the Italian standard on the selection of lighting classes will consider adaptive installation suggesting peculiar requirements and control strategies as supplement to the European standard requirements.

The paper describes the development of a luminance and traffic detector for adaptive system and the results of measurements carried out in more than one year on two experimental road lighting installations representative of an high volume traffic road (starting lighting class M2) and of a medium volume traffic road (starting lighting class M3).

Keywords: photometry, road lighting, energy saving

1. INTRODUCTION

The adaptive lighting concept is defined in (CEN, 2014) as "*temporal controlled changes in luminance or illuminance in relation to traffic volume (e.g. veh/5 min), time, weather or other parameters*".

For example, adaptive road lighting installations are able to maintain constant at the requested value the road surface luminance or illuminance despite the installation ageing, considering:

- A wide variation range of key parameters (luminous intensity depreciation of luminaire, variability of the road surface reflection properties, instability of the column voltage, etc.);
- The change of the installation lighting class according to design constraints (for example traffic volume);
- Actual conditions instead of hypothetical ones linked for example to the weather conditions or emergency situations.
- Conceptually we can classify an adaptive system, in ascending order of performances, as:
- **Open loop system**: the lighting class change is controlled considering a statistical estimation of the traffic volume. For example, in the Italian standard (UNI, 2012) the lighting class can be decrease by one level (i.e. from M2 to M3) if the estimated traffic volume is less then 50% of the maximum capacity of the road and by two levels (i.e. from M2 to M4) if the estimated traffic volume is less then 25% of the maximum capacity. The lighting class change starts at a given hour of the night according to decision the designer describes in a risk evaluation report. Generally, in these systems the luminance or illuminance average value is not stable during the installation life, therefore, the installation shall be over dimensioned to consider lamps and luminaires ageing and statistical variability of key parameters (tolerances in the luminaire photometric characteristics, weakness in road surface characterization, etc.). The

* On basis of report published in Proceedings of 28th CIE Session, 2015, Manchester

new revision of the European standard gives guidelines (tolerance analysis) to mathematically evaluate a reasonable figure of the over dimensioning needs (CEN, 2015a).

• **Close loop system**: the lighting class change is controlled using real time measurements of one or more influence parameters like volume and typologies of traffic or weather conditions. A close loop system gives the correct lighting level required by standards for the measured traffic volume and/or weather conditions. If compared to the open loop solution, generally this control method gives a remarkable long terms reduction in the road lighting installation energy consumption, quantified by the annual energy consumption indicator (AECI) defined in (CIE, 2015b). As a matter of fact, the statistical estimation adopted in open loop system need a safety margin and often the designer has difficulties to correctly determine local or seasonal variability of the traffic volumes. Sometime the short term comparison of the energy consumption between open and closed loop installation could be negative (i.e. more energy consumed by the closed loop installation) because of unpredicted situations, but this increment of cost for a limited period of time is largely compensated by the assurance of traffic safety conditions also during otherwise critical situations.

According to the (CEN, 2014) definition a constant light output (CLO) system (CEN, 2015b) is not strictly an adaptive system, but CLO is a functionality an adaptive system could have to improve its energy saving performances. The CLO functionality aims to compensate for the light loss caused by ageing of the light sources. The stabilization of the luminous flux emitted by the luminaire is obtained changing the value of a control quantity (i.e. the lamp voltage for sodium high pressure lamps or the device current for LED sources) and by the knowledge of the characteristic curve *control quantity – luminous flux*.

We can distinguish between two different approaches:

• **Passive**: for the light source installed in the luminaire the usual (i.e. at a constant and nominal value of the controlling parameter) reduction of the luminous flux with working time (ageing function) is statistically known and it is compensated using an *a-priori* definition of the variation rule with time of the controlling quantity. The accuracy of this approach depends on the measurement uncertainty of switch-on time, on the accuracy of the knowledge of the ageing function, on the source manufacture tolerances and on the influence of other not measured parameters, like the luminaire temperature, mains supply instability, thermal stress.

• **Active**: a quantity correlated with the real luminous flux emitted (i.e. the illuminance on a lighted surface inside the luminaire, the lamp current or voltage at constant luminaire voltage) is continuously sampled and the control quantity is changed according to the characteristic curve *control quantity – luminous flux*. In a well-designed luminaire, the accuracy of this approach is greater then the accuracy of a passive system. In the case of a photometric correlated quantity, the approach accuracy mainly depends on the measurement uncertainty of the transducer for this quantity. Key parameters are the transducer stability with time and temperature, its repeatability between switch-on and off cycles and its ageing. Of course a correct transducer calibration in absolute units is too expensive and generally not technically justified or required. As a consequence, the luminaire emits a luminous flux with a value inside the standard tolerances (IEC, 2004), and it is this unknown value but within the tolerance limits (usually between the rated value and –10% of the rated value) that is maintained stable during the luminaire operating life or between maintenance actions.

In road lighting installation this approach has several weak points:

• Only the luminous flux of the light source is maintained constant, but the luminous flux and the luminous intensity distribution of the luminaire also depend on the ageing of the optical components and the influence of dust inside and outside the luminaire.

• The over-dimensioning of the road lighting installation should not be avoided but only reduced. Practically only the influence of the lamps ageing (lumen maintenance) can be deleted in the maintenance factor evaluation. The influence of the a.c. mains supply conditions can be reduced using luminous flux controllers that usually are a more simple solution.

• For motorized traffic (CIE, 2010) and European standards (CEN, 2015c) the lighting level is quantified by the maintained average road luminance value given in the M set of lighting classes. Therefore, the variability and ageing of the road surface characteristic in reflection (CIE2001) are important factors that should be considered in order to guar-

antee the standard requirements with the minimum energy consumption.

To overcome these limitations REVERBERI Enetec developed a detector (LTM) able to measure the motor traffic volume and road average luminance. The research programme REGOLO obtained the financial contribution of Regione Lombardia (Italy) and was done in collaboration with INRIM (the Italian National Metrological Institute) that characterized the metrological performances of the detector and of the road lighting installations and Provincia di Bergamo that provided the test sites (selection and management of the road lighting installation).

The LTM detector permits to realize a close loop adaptive system able to:

- Select the correct lighting class according to the traffic volume;
- Detect weather conditions;
- Maintain the road luminance equal to the maintained average value required by standard for the given lighting class;
- Detect anomalous situation like the presence of car queues and wet road surface.

2. EUROPEAN STANDARD REQUIREMENTS

The new European standard for measuring the lighting performance or road installation (CEN, 2015a) gives requirements according to the measurement aims and in its normative annex D considers measurement systems for adaptive road lighting. To avoid technically unjustified costs for luminance measurement, the standard suggests strategies to simplify the measurement system and the operating conditions without compromising the measurement aims. The measurement uncertainty of the controlling system should be evaluated considering not only the instrumental contributions but also the contributions due to installation conditions should be considered in order to be sure to guarantee the maintained value of the photometric quality parameters as required in (CEN, 2015c).

These simplifications can modify the road lighting design approach too and their consequences should be clearly understood.

Set measurement: the set measurement is defined as "*measurement carried out in an installation to determine the values of parameters used by an automatic measuring system for control purpose*" (CEN, 2015a) and it can be considered as a sort of calibration of the detector carried out in the field and in its actual operating conditions. This procedure avoids or reduces the necessity of a complete characterization of the detector in laboratory, it takes into account also the peculiar position of the detector respect to the observer position defined in the standard (CEN, 2015d) and the detector – road surface distance.

Particular parameters: if the control system does not modify the installation uniformity values, it is possible to measure directly the average road luminance but avoiding the influence of road marking. Formally this is the measurement of a particular parameter as defined in (CEN, 2015d). The measurement can consider the entire grid zone, a significant part of it or more than one grid zone. This simplifies the optical system, reduces spatial resolution requirements of the sensor and its alignment procedure. Instrument constants that link the peculiar parameters measured to the standard ones shall be known. These values can be obtained from the set measurement.

Detector position: of course it is not possible to put the luminance detector in the position defined in the standard (CEN, 2015d). The correlation between the road luminances considering the detector real position and the standard observer can be obtained using the set measurement or peculiar calculations. Also statistical knowledge of the road surface photometric characteristic with different angles of observation can be used, but this approach usually increases the measurement uncertainty. Practically there are two technical possibilities in selecting the new position of the luminance detector and a compromise between the *pro* and *contra* of the two solutions should be considered.

A luminance meters with a narrow measurement cone can be used at a greater height than the standard observer. The meters measures the luminance on a road surface at a proportionally greater distance so that the angle of view of the meter is $(89 \pm 0{,}5)°$ to the normal to the road surface. This solution tries to maintain the standard view condition, but works at greater distance, so the influence of the atmospheric luminance or attenuation is higher and the mechanical stability of the detector becomes critical especially in windy zones.

The luminance meters at a greater height than the standard observer frames a zone of the road surface with an angle lower then the standard $(89 \pm 0{,}5)°$. As the observation angle decreases the specular component of the reflectance of road surface decreases and

Table 1. Description of the two experimental installations

Installation	Mornico	Treviolo
Position (Latitude Nord)	45° 35' 23,16"	45° 39' 43,98"
Position (Longitude East)	9° 49' 0,05"	9° 36' 30,52"
Description of road	Two lane road with single side luminaire arrangement	Four line road with central reservation and central luminaire arrangement
Type of lamps	Metal Halide	High pressure sodium
Lighting classes	M3 – M4 – M5	M2 – M3 – M4

the road surface becomes like a lambertian surface. In this conditions the detector measure a luminance proportional to the illuminance on the road surface instead of the luminance in standard conditions

Detector characteristics: the detector should be characterized considering the quality parameters define in (ISO/CIE, 2014). But some simplification can be adopted.

The calibration of the luminance meter can be omitted if the set measurement concept is adopted and if this measurement guarantees the traceability of the controlled parameter. In this situation the set measurement gives a sort of calibration factor to the control system that take into account not only the characteristics of the detector but also its position and the road lighting installation conditions.

The deviation of relative spectral responsivity from the $V(\lambda)$ function (f'_1) is less important if the set measurement concept is adopted, but during the life of the road lighting installation the spectral emission of the luminaires can change as well as the spectral reflectance of the road surface. For these reasons it is preferable to minimize the value of f'_1 or to adopt strategies to minimize its influence in the measurement uncertainty like the correction of the measured value considering the type of lamp and its correlated colour temperature.

Luminaires or extraneous and obtrusive lights framed or not framed by the detector can influence its reading due to inter-reflection in the lens or between the lens and the protective glass in the detector box. The parameter $f_{2,\,u}$ becomes very important especially in urban road lighting installation. Any characterization of the detector concerning this aspect shall be done with the detector in its box and with all the screens installed.

Other not photometric characteristic can become very important. The detector will work at very different temperature conditions (winter – summer, day – night) for long period of time. Its stability, long term ageing, repeatability, the influence of working temperature and humidity generally different form those present during the set measurement, the possible presence of condensation or moisture in its lens, the thermal stress are aspects that should be considered in evaluating the measurement uncertainty. The use of a thermally stabilized box can reduce the influence of these conditions.

Extraneous and obtrusive lights: Extraneous and obtrusive lights may not be avoided during measurements. During the set measurement the influence of extraneous and obtrusive lights may be evaluated, for example, some measurements can be carried out with the road lighting installation switched off.

3. PROPOSAL FOR STANDARD REQUIREMENTS

A new revision of the Italian standard (UNI 2012) is in development and will consider in details the close loop adaptive systems with luminance control.

Many aspects are not considered in the European standards but some normative requirements are necessary to avoid unsafe conditions. The main points under discussion are described in the following where only the opinion of the authors is given.

Extraneous and obtrusive lights: they could increment the road surface luminance but also the glare condition. The detector cannot evaluate the glare to which the observer is exposed because its position is completely different and it is quite impossible to determine the correlation between the measured glare and the observer glare. In the risk analysis the designer should evaluate the presence of extraneous and obtrusive lights and decides the possible set of lighting classes. The adaptive system controls the road luminance considering the real road luminance as sampled.

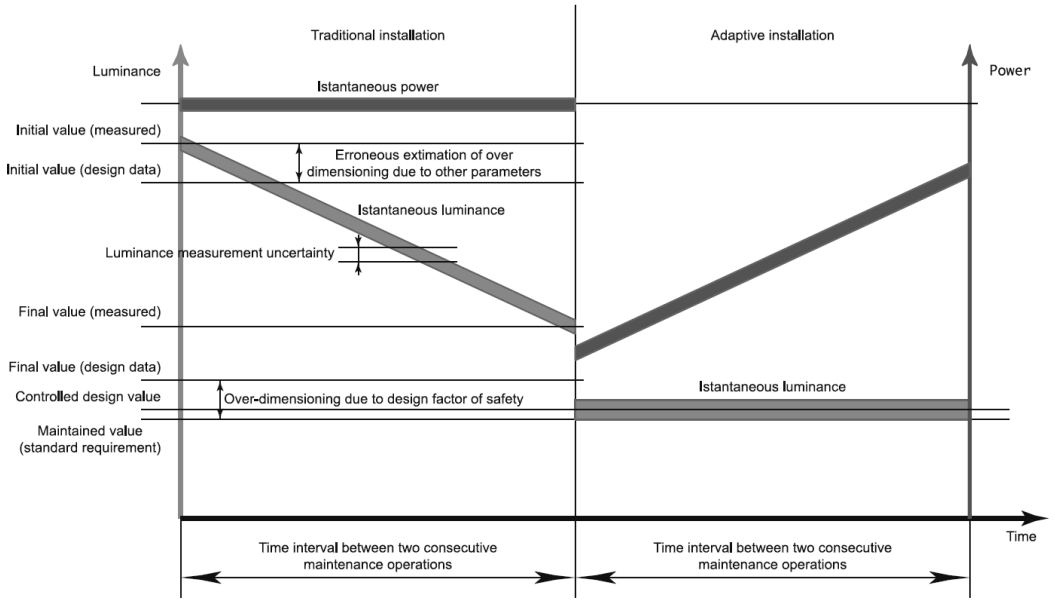

Fig. 1. Comparison between a traditional road lighting installation (left) and an adaptive solution (right). The luminance and the power consumption versus time of the two systems have been drawn

Presence of rain, fog or snow: the reading of the luminance meter becomes unreliable because the instrument performances may change but also the atmospheric attenuation and diffusion change dramatically. If required by the standard, the designer shall select the lighting classes that should be used in these situations. The detector should be able to identify these anomalous situations and the correct lighting class activated using the control coefficient or factors adopted previously for the same lighting class.

Traffic volume: it could be evaluated in a given relatively long period of time (for example 15 min) and then the lighting class modified according for the next 15 min or it could be sampled in a short period of time (for example 1 min) and a moving average evaluated considering for example 10 samples. Sudden variation of luminance shall be avoided so the decrement of luminance should be done with a long time constant while the increment requires a short time constant for safety reasons. A continuous variation of luminance proportional to the measured traffic volume could be a permitted procedure to avoid sudden variation of luminance and decrease energy consumption without a perceptible decrease of traffic safety.

Unwanted operating conditions: when the measurement conditions give wrong results the control system shall maintain safety condition i.e. shall adopt control strategies that guarantee the required value of the average luminance for the correct lighting class.

Typical situations are the stabilization period of the lamp after the evening switch-on of the installation, climatic conditions that do not represent the conditions required by design and management of the road lighting installation, the detector working conditions (temperature, humidity, condensation or moisture on light transmitting surfaces) outside its operating range.

Detector failure: also in this situation the luminance reading is unreliable. As before, the control system shall maintain safety condition of road traffic.

4. ROAD LIGHTING INSTALLATION DESIGN

To obtain the best performances of a close loop adaptive systems with luminance control, the designer of the road lighting installation should consider that the system will always operate near the minimum average luminance value required by the standard. The installation over-dimensioning can been divided into two group of components:

The components described by the maintenance factor that hypothesizes a continuous reduction of the lighting level with time (CIE, 2003).

The components due to other parameters. In the design phase this component can be statistically evaluated using the tolerance algorithm described in (CEN, 2015a) considering for example the tolerance in manufacturing of the photometric characteristic of luminaires and light sources with reference to rated

value, the influence of ambient temperature, the layout tolerance of road lighting installation and of the installation of the light source and the uncertainty of the road surface photometric characteristics.

Also in this application, the measurement uncertainty shall be minimized and a compromise between detector and control system cost and measurement accuracy should be carefully considered. As the compliance with standard requirements shall be verified considering the expanded measurement uncertainty of the measure (CEN, 2015a), the measurement uncertainty should be considered in the over-dimensioning (second group) of the installation, as clearly highlights in Fig. 1.

In Fig.1 a traditional installation is compared to an adaptive solution considering for simplicity a single luminous class. The traditional installation works at constant power consumption. Its luminance decreases from the initial values to the final value that, for a wrong estimation of the over-dimensioning, is greater then the standard maintained value.

The adaptive system works at constant luminance. Its energy consumption increases with time but it is always lower than that of the traditional system. In this case the over- dimensioning has no consequences in the management cost. It represents a cost only in the installation phase.

The measurement uncertainty of the control system represents a cost in term of additional energy consumption. For this reason this uncertainty shall be specified in the road installation project, because it influences the installation energy performances.

5. THE MEASUREMENT OF ROAD SURFACE LUMINANCE

The detector used in the LTM system is a colour camera (Bayer filter) with a CMOS sensor, an infrared filter and a long focal lens.

The optical system is designed to operate between 60 m to about 200 m (Fig. 2) and the road surface point luminance is obtained considering the weight sum of the reading of the four close pixels of the Bayer filter.

The spectral responsivity of the single colours of the Bayer filter has been measured using a modified Perkin Elmer Lambda 900 spectrometer with the lens and the protective glass in front of the detector. Then the weight coefficient for every colour has been evaluated to minimize the f'_1 value.

To increase the accuracy of luminance measurements, the luminance value obtained is multiplied by different calibration factors considering the lamp type and its correlate colour temperature. The selection of the lamp type is done automatically in the field considering the ratio between the signals of the three colour of the Bayer filter.

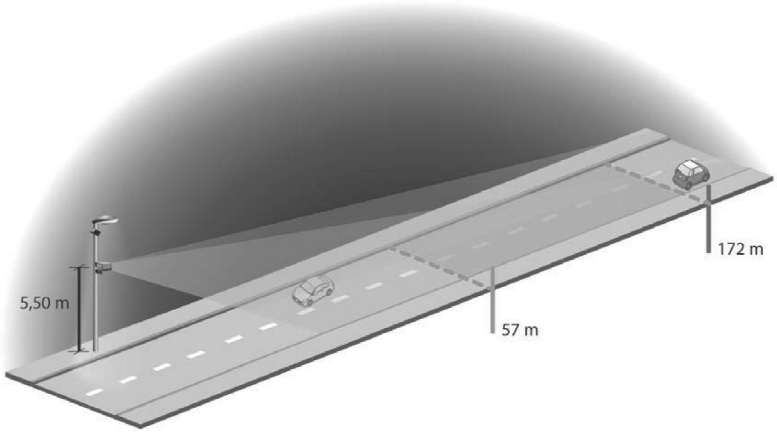

Fig. 2. Typical conditions of installation of the LTM detector

Fig. 3. The road lighting installation at Mornico (left) and at Treviolo (right)

The corrected luminance value is then multiplied by the calibration factor obtained from the set measurements.

The measurement zone of the road is selected during the installation of the system observing the acquired imagines.

In a well-design system the main contribution to the measurement uncertainty should arise from the set measurement. Considering a measurement uncertainty of 3% for this measurement the system is able to work with a 5% uncertainty.

The same sensor is used to measure the traffic volumes using a proprietary algorithm to count the number of vehicle in the given time interval. If compared with traditional systems considered exacts, the count uncertainty is less then 10%. The image analysis algorithm counts the vehicles but it is also able to detect if there are vehicle in the zone selected for the luminance measurement or if the headlamps of vehicles can influence the luminance measurement. The two acquisition processes (for luminance measurement and for vehicle detection) are carried out with different integration times of the detector to reduce the influence of saturated pixels or noise.

6. EXPERIMENTAL DATA

Two experimental road lighting installation (Table 1 and Fig. 3) has been tested for more than one year. The installations represent two typical not urban situations.

The more interesting results have been find in the Treviolo road. The differences in the traffic volumes at the same time between the two carriages (in the morning high traffic volume in the town direction and vice-versa in the evening) justifies the realization of two independent system because the energy saving can be as great as 25% respect to a single system installation. This situation is clearly shown in Fig. 4 where all measurements are given without averaging process. The road luminance has been controlled to the level required by design (open loop system). The traffic volume is quite different in the two directions and there are situation when the a-priori selection of the lighting class does not guarantee safety.

7. CONCLUSIONS

The experimental results show the great potentiality of adaptive system with a continuous control

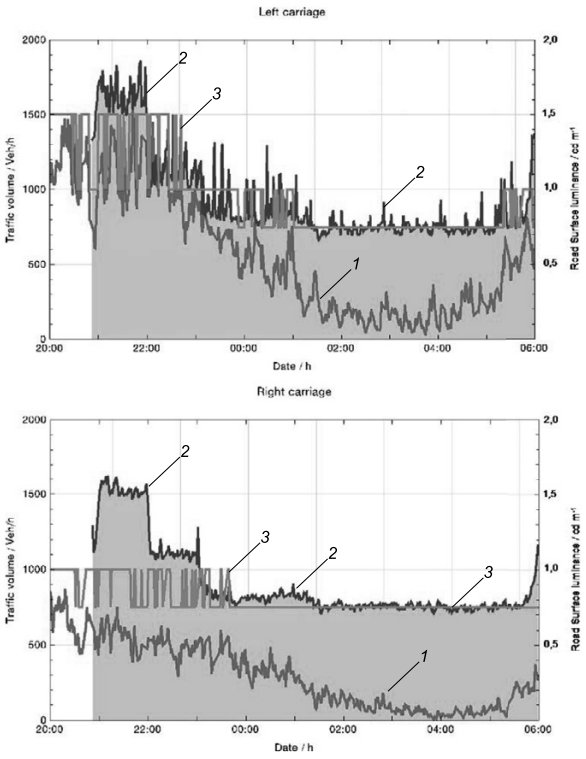

Fig. 4. Example of the traffic volume and operating condition of the Treviolo installation during the 12 August night. The curve 1 is the measured traffic volume, the curve 2 the measured road luminance and the curve 3 the standard luminance required considering the measured traffic volume

of the road luminance level, but highlight the necessity to follows clear rules for the luminance control to optimise the energy saving and the traffic safety: the energy consumption reduction is also strongly correlated to these choices. Unconventional control strategies, like the continuous but filtered variation of the luminance with traffic volumes could adopted but the require a revision of the national standard.

In the two experimental installations, if compared to the condition before the installation of the LTM system, the energy consumption has been reduced for about 35%.

REFERENCES

1. CEN2014. CEN TR13201–1:2014. Road lighting – Part 1: Guidelines on selection of lighting classes. Brussels: CEN.

2. CEN2015a. EN13201–4:2015. Road lighting – Part 4: Methods of measuring lighting performance. Brussels: CEN.

3. CEN2015b. EN13201–5:2015. Road lighting – Part 5: Energy performance indicators. Brussels: CEN.

4. CEN2015c. EN13201–5:2015. Road lighting – Part 2: Performance requirements. Brussels: CEN.

5. CEN2015d. EN13201–5:2015. Road lighting – Part 3: Calculation of performance. Brussels: CEN.

6. CIE2001. CIE144:2001. Road Surface and Road Marking Reflection Characteristic. Vienna: CIE.

7. CIE2003. CIE154:2003. The Maintenance of Outdoor Lighting System. Vienna: CIE.

8. CIE2010. CIE115:2010 2nd Edition. Lighting of Roads for Motor and Pedestrian Traffic. Vienna: CIE.

9. IEC2004. IEC EN60969:2004–4. Self-ballasted lamps for general lighting services – Performance requirements. Geneva: IEC.

10. ISO/CIE2014. ISO/CIE19476:2014. Characterization of the Performance of Illuminance Meters and Luminance Meters. Joint ISO/CIE International Standard. Geneva: ISO.

11. UNI 2011. UNI 11431:2011. Luce e illuminazione – Applicazione in ambito stradale dei dispositivi regolatori di flusso luminoso (Light and Lighting – Use of luminous flux controllers in road lighting). Milano: UNI.

12. UNI 2012. UNI 11248:2012. Illuminazione stradale – Selezione delle categorie illuminotecniche (Road lighting – selection of lighting classes). Milano: UNI.

Andrea Mancinelli,
has degree in engineering and experiences in electronic development for high precision instrumentation devices. He was project leader for different projects involving in the electronics development of instrumentation boards. In Reverberi Enetec since 2011, was the Project Manager of a ERDF Funded Project, namely "Regolo" (POR FESR funds, Lombardy, Italy). The project was articulated along 2 years and was involved in the R&D development of the innovative sensor for Luminance, Traffic and Meteo, also known as LTM sensor. For Regolo project, Mr. Mancinelli coordinated a team and collaborated with the Italian Research centre INRiM (situated in Turin) and with Bergamo Province. Regolo, as many other internal Reverberi R&D projects have been managed by Mr. Mancinelli

Paola Iacomussi,
Doctor in physics, is a senior researcher at INRiM, Department of Optics. She is the Italian member of CIE in Division 8 and expert in photometry, and works for art illumination

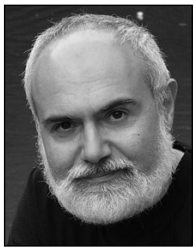

Giuseppe Rossi,
Ph.D. in Metrology, is a senior researcher at INRiM, Department of Optics. He is the Italian member of CIE Division 4 and expert in photometry, optical characterization of materials and road lighting installation

Paolo Di Lecce,
graduated in electric engineering in 1985, he was appointed with a Master in Business administration in 1990. After several years spent in important electric companies as a Director, he became Managing Director in Reverberi Enetec, company working in the fild of Light Energy Saving. Member of the Board of aiDi (italian lighting association), he published several articles in technical magazines and the chapter about energy saving and remote Control in the "Manuale di illuminazione" of Prof. Pietro Palladino

Light & Engineering
Vol. 23, No. 4, pp. 41-46, 2015

Svetotekhnika
No. 6, 2015, pp. 8-11

PHOTOBIOLOGY – PRESENTATION OF A BLUE LIGHT HAZARD IN VIVO EXPERIMENT ON THE RAT*

Pierre Boulenguez[1], Imene Jaadane[2], Cristophe Martinsons[1], Samuel Carré[1], Sabine Chahory[3], and Alisio Torriglia[2]

[1] Centre Scientifique et Technique du Bâtiment, Grenoble, FRANCE,
[2] Institut National de la Santé et de la Recherche Médicale, Paris, FRANCE,
[3] Ecole Nationale Vétérinaire d'Alfort, Alfort, FRANCE,
E-mail: Pierre.Boulenguez@cstb.fr

ABSTRACT

An animal experiment was conducted aiming at a better understanding of blue-light retinal toxicity. Freely moving Wistar rats were exposed to intense, blue-rich light for up to eighteen hours. Their retinas were analysed using transmission electron microscopy, Western Blot, immunofluorescence, and Terminal transferase dUTP nick end labelling. This paper details the dosimetry aspects of the experiment and summarizes the biological results.

Keywords: blue light hazard, Wistar rat, dosimetry

1. INTRODUCTION

1.1. Blue Light Hazard

Blue light hazard (BLH) denotes an incompletely understood phenomenon by which radiations in the blue-end of the spectrum induce lesions in the layer of photoreceptors and retinal pigment epithelium (RPE).

Damages of rapid onset following high-dose exposure (retinal dose > 20 J/cm^2) have long been described [3]. Low-dose chronic exposure has also been suspected, since seminal studies, to play a role in age-related macular degeneration (AMD).

No epidemiological study confirmed this connexion so far, but it now known that A2E, a protein found in druse of lipofuscin (the hallmark of AMD) reacts with blue light [1].

1.2. Solid State Lighting

Concerns over the BLH have intensified because of the advent of "white-light" LEDs as general lighting service (GLS) sources. A typical Indium gallium nitride (InGaN) LED indeed emits significantly more blue-light per lumen than competing sources (Fig. 1).

1.3. Exposure Limit Values

The BLH action spectrum of Fig. 1 was determined through animal experiment. In [2], Van Norren surveyed nineteen such experiments and noted the following models: rat (9), macaque (7), rabbit (2), and squirrel (1).

The International Commission on Non-Ionizing Radiation Protection (ICNIRP) relied on these studies, and mostly on [3], to estimate that toxicity begins at a retinal dose of 20-30 J/cm^2 of BLH-weighted radiation [4]. Taking a substantial safety factor into account, a safe-dose threshold was set at 2.2 J/cm^2; indeed defining the guideline exposure limit value (ELV) for the BLH.

The so-called "spatially-averaged BLH-weighted radiance" (SABLHWR) is generally employed

* On basis of report published in Proceedings of the 28th CIE Session, 2015, manchester

Table 1. Different sources used for the experiment.

	XP-E Blue	XP-E Royal Blue	NCSE119A	NCSB119
Type	LED	LED	LED	LED
Brand	Cree	Cree	Nichia	Nichia
Dominant wavelength (nm)	473	449	507	473

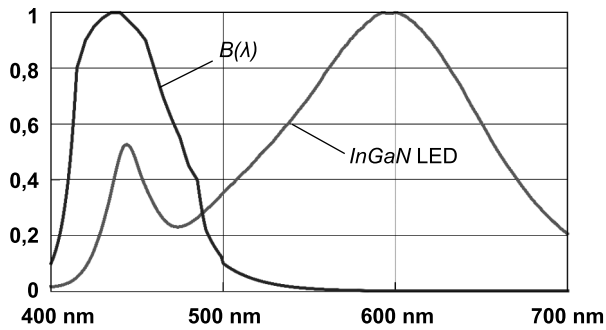

Fig. 1. InGaN LED spectrum and BLH action spectrum

Fig. 2. Outbred albino Wistar rat

to verify that any given source would not induce an excess of the ELV for the user [5]. SABLHWR, related to spectral radiance, accounts for voluntary and involuntary eye movements and pupillary constriction. The accuracy of its assessment is essential for the classification of a source into a photobiological risk group [6].

2. IN VIVO EXPERIMENT

In this context, a new animal experiment was conducted in order to gain at a better understanding of blue-light retinal toxicity.

2.1. Animal Model

The experiment was conducted on the Wistar rat (Fig. 2). The strain is often considered as the golden standard general multipurpose model organism, and has been used in ophthalmological studies since its inception [7].

In the context of blue-light retinal toxicity, the translation of the model to human being remains a matter of debate. Some frequently discussed aspects are the fact that the rat is a nocturnal animal, deprived of macula, that the eye repair mechanisms are less efficient, and that the Wistar strain is albino. It is nonetheless considerably easier to work with than other animals (*e.g.* macaques).

All experimental and animal care procedures were approved by the animal use and care committee of the veterinary school of Maison Alfort (ENVA).

2.2. Illumination Procedure

Groups of six-week-old males, freely moving in their cage, were exposed for up to eighteen hours using the illumination device of Fig. 3.

The device was made up of eighteen source modules, each consisting of four LEDs (see Table 1), allowing the spectral distribution of the stimulus to vary. Each group of rats was exposed to a single spectral distribution.

2.3. Dosimetry

The dosimetry was performed based on measurements within the cages (section 2.3.1), and on a model relating these measurements to the retinal dose of BLH-weighted radiation (section 2.3.2).

2.3.1. Measurements

Spectral irradiance within the cages was measured using a diffusing head fibre spectrophotometer. Illuminance uniformity in the plane of the eyes, given by the ratio $\frac{E_{v,min}}{E_{v,ave}}$, was about 0.7 for all sources.

Fig. 3. Multispectral illumination device, top: the cages were placed below an emitting surface; bellow left: eighteen source modules are positioned above the surface; bottom right: a source module is made of four LEDs

The average spectral irradiance in the plane of the eye will be noted E_λ in the following.

2.3.2. Retinal Dose

Retinal irradiance was dependent upon the head glaze of the animals. To compute the overall dose, it was estimated that: (a) on average, a rat keeps his head aligned with his body, and (b) the eye can be approached as half a globe with focal length f as diameter (as in [2]).

As only the upper surface was emitting light (*cf.* Fig. 3), a horizontal to corneal irradiance correction factor was applied:

$$E_{\lambda,cor} = \frac{E_\lambda}{2} \text{ [W/nm·m}^2\text{]}.$$

Retinal spectral irradiance was then approached as:

$$E_{\lambda,ret} = \tau E_{\lambda,cor} \frac{A_{cor}}{A_{ret}} \text{ [W/nm·m}^2\text{]},$$

where τ is the transmittance of the ocular media, A_{cor} is the effective area of the illuminated cornea, and A_{ret} the area of the illuminated retina. The former area was estimated as:

$$A_{cor} = \frac{\pi d_p^2}{4} \text{ [m}^2\text{]},$$

where d_p is the diameter of the pupil. The retinal area A_{ret} was approached as half that of the ocular globe:

$$A_{ret} = 2\pi f^2 \text{ [m}^2\text{]}.$$

The average spectral retinal irradiance was thus estimated as:

$$E_{\lambda,ret} = \tau E_{\lambda,cor} \frac{d_p^2}{8f^2} \text{ [W/nm·m}^2\text{]}.$$

The values for d_p, f, and τ were taken according to [2] ($d_p = 5$mm, $f = 5.525$mm, and $\tau = 0.58$ at 403nm), consistently with the values found in [8]. Other values for d_p were proposed by [9] ($0.4\text{mm} \le d_p \le 1.2\text{mm}$) and [10] ($d_p = 0.5$mm). An explanation for this discrepancy might be due to the difference between the real and the (magnified) entrance pupils.

Average retinal irradiance was deduced from the average spectral retinal irradiance using numerical integration:

$$E_{ret} = \Delta_\lambda \sum_{i=1}^{n} E_{\lambda,ret,i} \text{ [W/m}^2\text{]},$$

with $\Delta_\lambda = 1$ nm. The retinal dose was finally given by: $D_{ret} = tE_{ret}$ [J/m^2], where t is exposure time.

These formulas were calculated using the software of Fig. 4. While uncertainties remain in these calculations (due to assumption on head glaze notably), it is expected that the ratios of doses between the different spectral distributions remain correct.

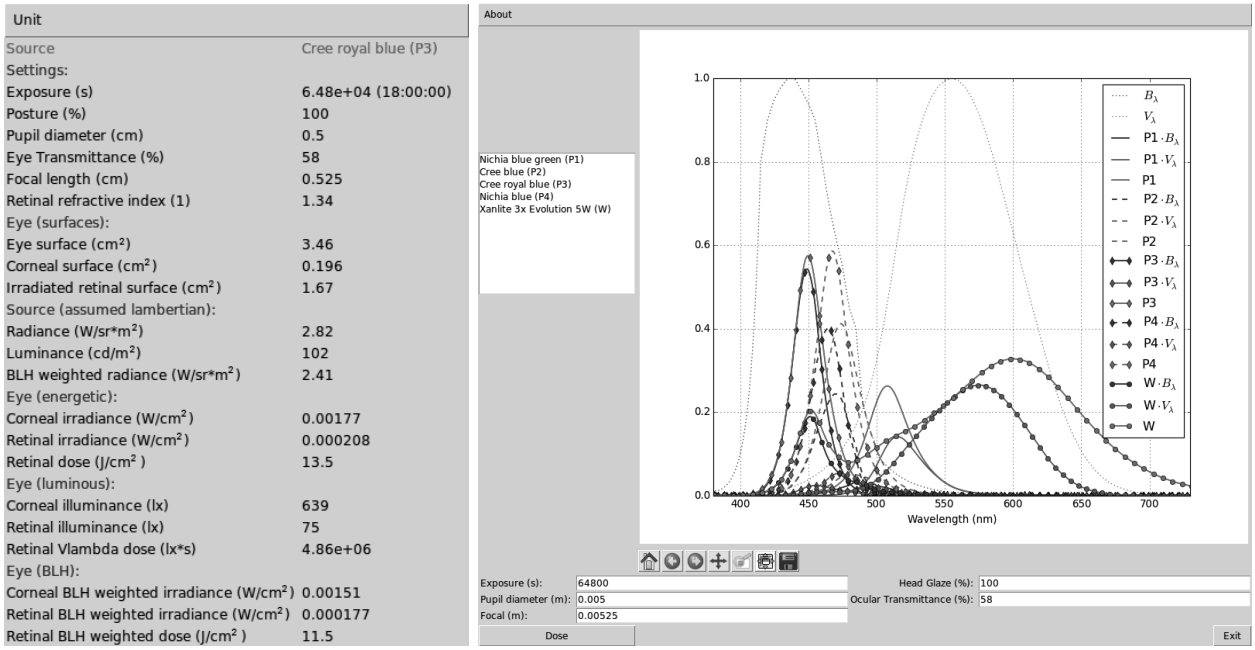

Fig. 4. BLH dosimetry software

2.4. Biological Analysis

A fundus examination was performed immediately after exposure. The rats were ethically sacrificed. Their eyes were enucleated, fixed in paraformaldehyde, washed, and embedded in optimal cutting-temperature for cryosection [11].

The retinas were next analysed using Western Blot, immunofluorescence, Terminal transferase dUTP nick end labelling (TUNEL), and transmission electron microscopy.

The fundus examination showed no bleaching, but important chemosis, indicating an oedema of ocular tissues. This sign of eye irritation was probably due to exudation from abnormally permeable capillaries, and conjunctive vasodilation.

This hinted at microscopic photochemical lesions because no macroscopic damage to the retina was detected . The presence of an important oxidative damage was identified, involving proteins and nucleic acids, as well as an important amount of cell death.

The presence of necrosis was detected by staining cells with propidium iodide. A significant amount of photoreceptors were labelled, much more than photoreceptors that are TUNEL positive; indicating that permeabilization of the plasma membrane precedes degradation of deoxyribonucleic acid.

The existence of this necrosis easily explains the oedema, which is not sub-retinal but interstitial. This could also explain the presence of an early inflammatory reaction, probably due to the release of damage-associated molecular-pattern molecules.

CONCLUSIONS

This paper reports on an animal experiment on blue-light retinal toxicity. Freely moving Wistar rats were exposed for up to eighteen hours to intense, blue-rich light. Their retinas were analysed using Western Blot, immunofluorescence, Terminal transferase dUTP nick end labelling (TUNEL), and transmission electron microscopy.

Wavelength dependant loss of photoreceptors, activation of caspase-independent apoptosis, necroptosis, and necrosis were observed [11].

Two issues particularly relevant to the lighting community were emphasized: the design of an illumination device allowing animals to move freely in their cage; and blue-light hazard dosimetry.

A new iteration of the experiment is currently being performed, using other spectral distributions, and an improved illumination device that alleviates the assumption on head glaze in the dosimetry.

ACKNOWLEDGEMENTS

The Retina LED experiment was an interdisciplinary collaboration between biologists and ophthalmologists from the National Institute of Health and Medical Research (INSERM), veterinary ophthalmologists from the National veterinary School

of Alfort (ENVA), and physicists from the Scientific and Technical Centre for Building (CSTB). It was funded by the "Agence de l'environnement et de la maîtrise de l'énergie" (ADEME).

REFERENCES

1. ARNAULT E., BARRAU C., NANTEAU C., GONDOUIN P., BIGOT K., VIÉNOT F., GUTMAN E., FONTAINE V., VILLETTE T., COHEN-TANNOUDJI D., SAHEL J.A., PICAUD S. 2013. Phototoxic action spectrum on a retinal pigment epithelium model of age-related macular degeneration exposed to sunlight normalized conditions. *PLoS One* 8(8).

2. VAN NORREN D., GORGELS TG. 2011. The action spectrum of photochemical damage to the retina: a review of monochromatic threshold data. *Photochemistry and Photobiology* 87(4), pp. 747-753.

3. HAM W. T. Jr, MUELLER H. A., SLINEY D. H. 1976. Retinal sensitivity to damage from short wavelength light. *Nature 260*, pp. 153-155.

4. ICNIRP. 2005. Adjustment of guidelines for exposure of the eye to optical radiation from ocular instruments: statement from a task group of the International Commission on Non-Ionizing Radiation Protection (ICNIRP). *Applied Optics* 44(11), pp. 2162-2176.

5. CIE S 009:2002. Photobiological safety of lamps and lamp systems. European Standard 62471.

6. BOULENGUEZ, P., CARRE, S., PERRAUDEAU, M., MARTINSONS, C. 2013. Blue light hazard of LEDs – Comparison of the photobiological risk groups of fifteen lamps assessed using the uniform spectrum assumption and a new hyperspectral imaging method. Proceedings of the CIE Centenary Conference "Toward a new century of light", Paris.

7. CLAUSE B. T. 1993. The Wistar rat as a right choice: Establishing mammalian standards and the ideal of a standardized mammal. *Journal of the History of Biology* 26, pp. 329-349.

8. HUGHES A. 1979. A schematic eye for the rat. *Vision Research* 19, pp. 569-588.

9. M.T. BLOCK. 1969. A note on the refraction and image formation of the rat's eye. *Vision Research 9(11)*, pp. 705-711.

10. SLINEY D. H. 1984. Quantifying retinal irradiance levels in light damage experiments. *Current Eye Research* 3(1), pp. 175-179.

11. JAADANE I., BOULENGUEZ P., CHAHORY S., CARRÉ S., SAVOLDELLI M., JONET L., BEHAR-COHEN F., MARTINSONS C., TORRIGLIA A. 2015. Retinal damage induced by commercial light emitting diodes (LEDs). *Free Radical Biology & Medicine*. S0891-5849(15)00158-6.

12.ICNIRP. 2013. Guidelines on limits of exposure to incoherent visible and infrared radiation. *Health Physics* 105(1), pp. 74-96.

Pierre Boulenguez
received a master's degree in computer science in 2002 from the University of Marne-la-Vallée and a Ph.D. degree in computer science from the University of Paris-Est in 2010. Following a Post-Doc at the CNRS/University of Poitiers in 2010, he joined the Health and Comfort Department of the Center for Building Science and Technology (CSTB) in 2012. His fields of interest include computer vision, near-field photometry, optical scattering, imaging radiometry, and photobiology

Imene Jaadane
is a postdoctoral researcher at Institut de la Santé et de la Recherche Médicale (INSERM). She is a Doctor in molecular biology and eye physiopathology of Paris Descartes University. She works on molecular mechanisms of cell death in retinal degeneration and phototoxicity study of light emitting diodes

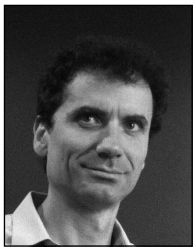

Christophe Martinsons
is head of the lighting and electromagnetism division at the Center for Building Science and Technology (CSTB). He currently conducts research in the fields of optics and lighting in order to promote energy-efficient buildings while providing the best visual comfort for users. Christophe Martinsons has been leading several studies concerning health and environmental aspects of solid-state lighting for governmental agencies such as the French agency for food, environmental and occupational health and safety (ANSES) and the International Energy Agency (IEA)

Samuel Carré
received a master's degree in computer science in 1993 and a Ph.D. degree in 1998 from University of Rennes 1. In 1998, he joined the lighting engineering team at the Center for Building Science and Technology (CSTB). His current research interests include physics based lighting simulation, global illumination in building environments, GPU-based rendering, and computer vision

Sabine Chahory
received her D.V.M. degree from the National Veterinary College of Alfort (Paris, France) in 1995, and pursued a residency in Veterinary Ophthalmology from 1999 to 2003. She was a Diplomate of the European College of Veterinary Ophthalmology (ECVO) since 2004. She received her Ph.D. in Cell and Molecular Biology (Paris, France) in 2007. She currently works as an assistant professor at the Ophthalmology unit, National Veterinary College of Alfort, France. Her fields of interest are light-induced retinal degeneration

Alicia Torriglia
is a Doctor in Medicine and Ph.D. in Science. She is Research Director at the Institut de la Santé et de la Recherche Médicale (INSERM). Her field of expertise concerns the molecular mechanisms of cell death in the retina

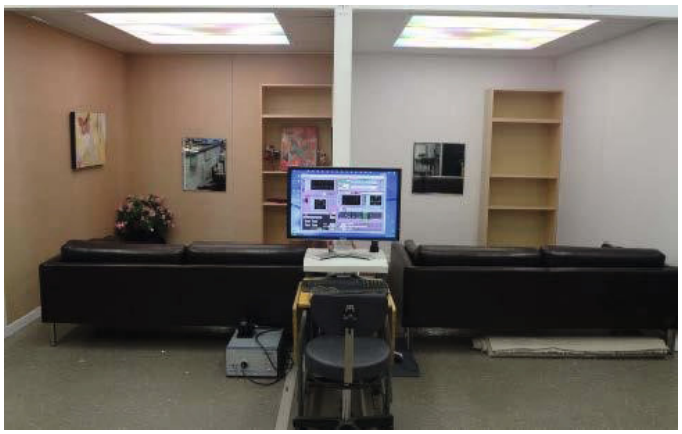

Fig. 1. View of the two cubicles of NIST Spectrally Tunable Lighting Facility

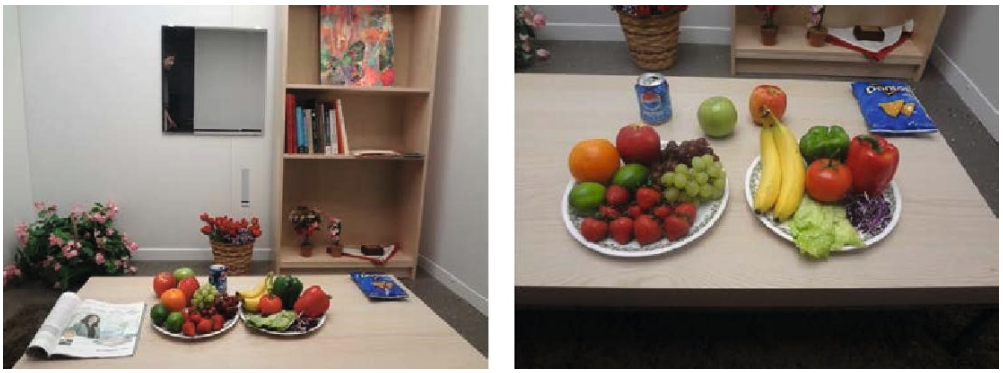

Fig. 5. The set-up of the STLF cubicle with objects on the table used in the experiments

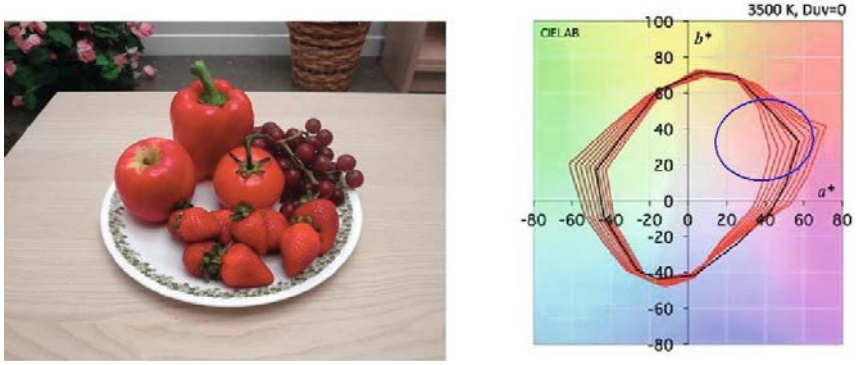

Fig. 6. Photo of the red samples only and the CIELAB plots of the chroma saturation setting of lights at STLF

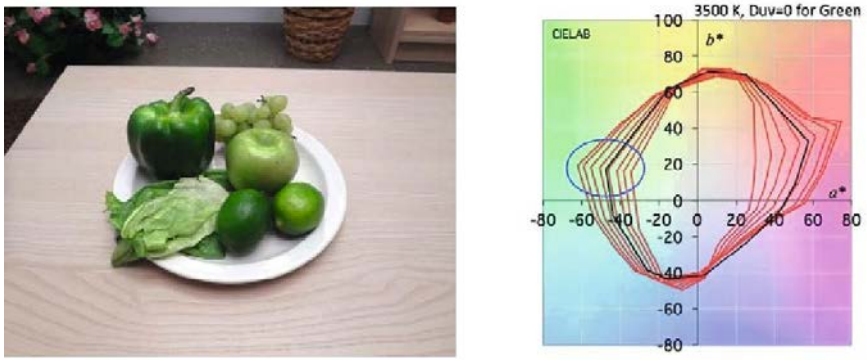

Fig. 7. The photo of the green samples only and the CIELAB plots of the chroma saturation setting of lights at STLF

Fig. 1. Computer simulation of the WUT Main Building floodlighting – the first lighting simulation in 3D model in Poland made in 1996

Fig. 2. Photorealistic simulation of office interior lighting

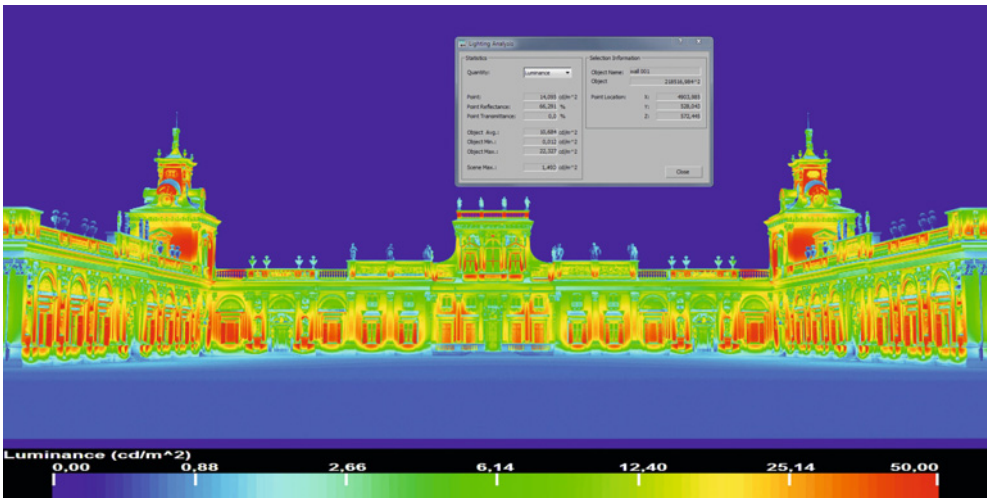

Fig. 3. Visualization of luminance distribution in the Wilanów Palace floodlighting design

Fig. 4. Computer simulation of the Wilanów Palace floodlighting, option I

Fig.5. Computer simulation of the Wilanów Palace floodlighting, option II, withdrawal from accenting column and pilaster rhythm

Fig. 6. Visualization of the final Wilanów Palace Museum floodlighting concept

Fig. 7. Photo of the Wilanów Palace Museum floodlighting test during the 2nd Royal Festival of Light in Wilanów, Warsaw [16]

Photobiology – Presentation of a Blue Light Hazard in Vivo Experiment on the Rat

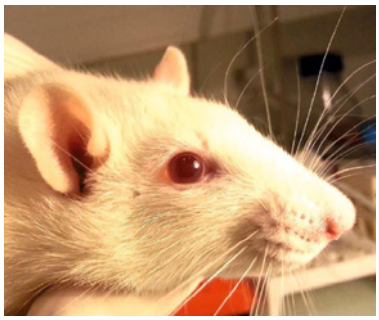

Fig. 2. Outbred albino Wistar rat

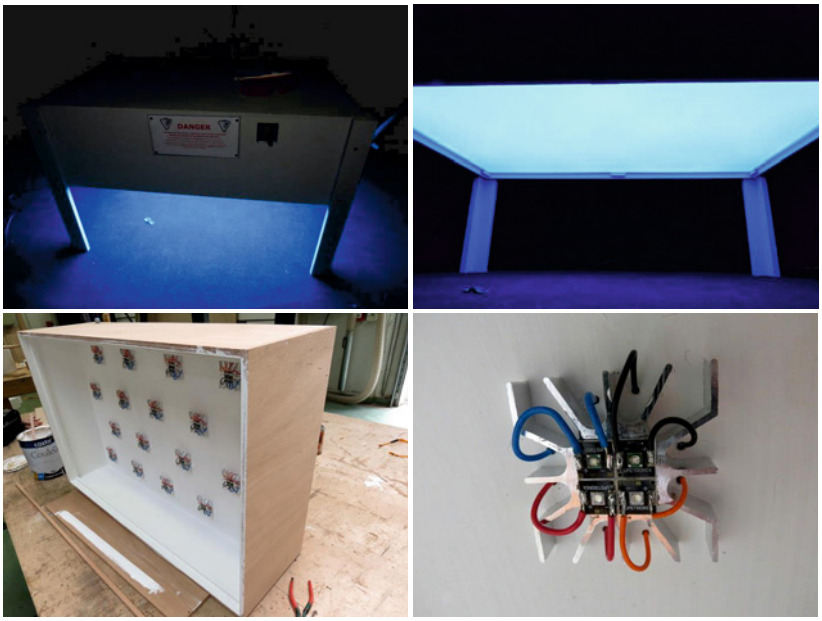

Fig. 3. Multispectral illumination device, top: the cages were placed below an emitting surface; bellow left: eighteen source modules are positioned above the surface; bottom right: a source module is made of four LEDs

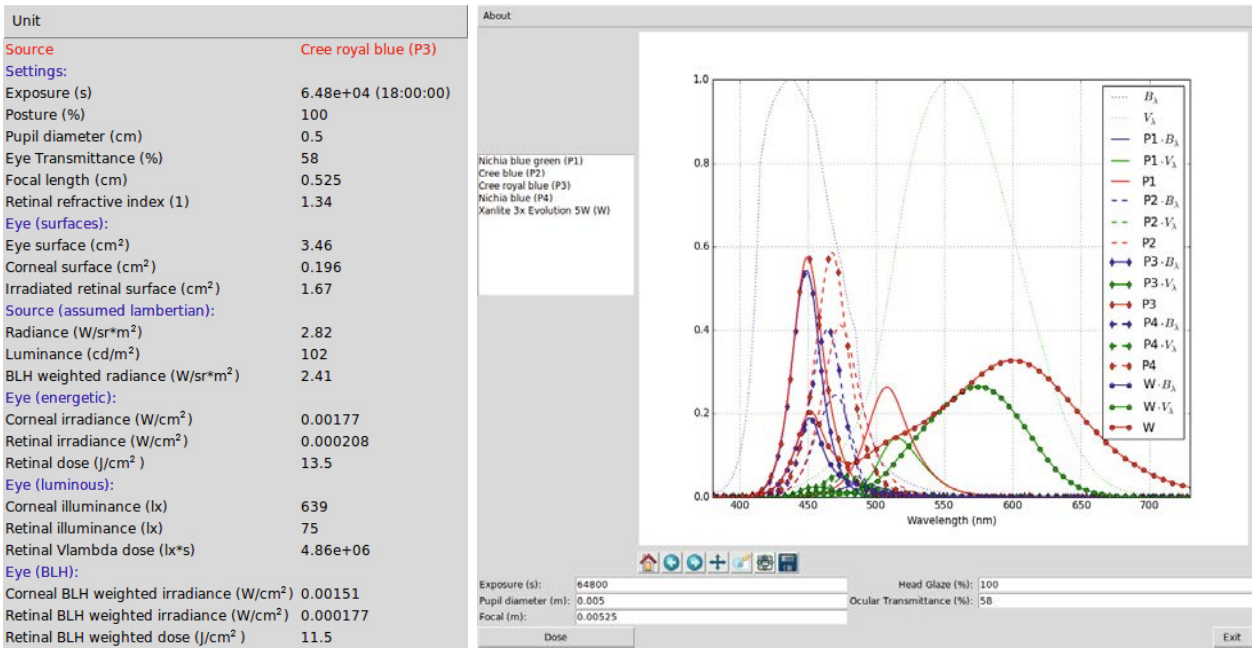

Fig. 4. BLH dosimetry software

Light & Engineering
Vol. 23, No. 4, pp. 51-54, 2015

Svetotekhnika
No. 2, 2015, pp. 45-47

ONCE MORE ON THE SUBJECT OF PREVENTIVE UV–IRRADIATION AS A MEANS TO ELIMINATE "SOLAR STARVATION"

Galina N. Gavrilkina, Elena I. Ilyinna*, and Henri S. Sarychev

VNISI Open Company, Moscow
**NIIOT Open Company, Ivanovo*
E-mails: gavrilkinagn@mail.ru, svetosar@mail.ru, niiotsvet@mail.ru

ABSTRACT

Reducing respiratory disease incidence and strengthening the human immune system is possible by the use of ultra-violet irradiation during autumn and winter periods. The article confirms that UV irradiation standards accepted in Russia don't contradict the international standards on safety of lamps and lamp systems.

Keywords: preventive ultraviolet irradiation, ultra-violet irradiation (UVI), erythema spectrum area, irradiation dose, UVI standards

In accordance with [1], the International Commission on Illumination (CIE) classifies UV in the optical radiation spectral area of 100–400 nm as follows:

UV-A is from 315 to 400 nm,

UV-B is from 280 to 315 nm,

UV–C is from 100 to 280 nm.

All of the specified radiation intervals are potentially dangerous, however, the degrees of danger are different. The greatest risk is concentrated in the UV–C interval, which is an area of optical radiation bactericidal influence. This area is almost always used in the case of a full isolation of a person. The UV-B middle interval of UV radiation is aggressive enough and at the same time, if irradiation is strictly dosed, can be very helpful. Even since publication of the unique monograph of A. Meyer and E. Zeitz [2], UV-B has been named preventive radiation. Finally, UV-A is the most "soft" ultraviolet, which admits sufficient irradiation levels, as shown in standard [3].

It should be noted that CIE standard S009/E: 2002 "Photobiological Safety of Lamps and Lamp systems" [3] distinguishes only two areas of UV spectrum: 200–400 nm (with a strict regulation of the irradiation actinic dose of no more than 30 J/m^2) and UV-A area (315–400) nm admitting a high enough limit of the dangerous irradiance equal to 10 W/m^2 during irradiation time t > 1000 s.

UV-B area especially distinguished in [1], which is carefully studied and widely applied, has appeared to be outside of this standard [3]. And this standard [3] has admitted a high irradiance level, many times exceeding an effective irradiation level of 30 J/m^2 within UV-A (315–400) nm limits, as if there is no UV-B area of erythema radiation (280–315 nm), which was admitted for practical use more than 50 years ago [2].

There should be a very special attitude to this spectrum area. This is precisely the short-wave earth sunlight area, in which life on earth developed, and all organisms produced a huge set of photobiological reactions, having become vital. In the middle of the twentieth century, this was confirmed by numerous experiments. Deficiency of the wholesome UV irradiation (a so-called "solar starvation") was identified by research among children in different climate areas of the USSR, by inspection of ship crews making regular routes in the Northern regions, as well as when analysing impacts of space flight. Some authors consider the consequences of UV-radiation deficiency as an illness of the civilization [4, 5, 6].

During the last decade, primarily American scientists [7–10], revealed the leading role of vitamin

Table 1. Recommended by standards and calculated doses of actinic exposition with UFL

Source	Photoreaction	Recommended dose of actinic exposition for 8 h, J/m^2 in spectral area	Calculated dose of actinic exposition for 8 h with LE type lamp, J/m^2
CIE S009/E:2002 [3]	UV danger	30 (200–400)	30 (280–400)
CIE S009/E:2002 [3]	UV-A	10 000 (315–400)	–
CIE S009/E:2002 [3]	UV danger	30 (200–400 nm)	30 (280–400 nm)
CIE S009/E:2002 [3]	UV-A	10 000 (315–400 nm)	–
МУ 5046–89 (Russia [12])	Erythema preventive UV irradiation	140*)	140 (280–400)
CIE S007/E: 1998 [17]	Erythema UV irradiation	150–600 (250–400)	140 (280–400)
CIE Journal, 1986 [18]	Photo keratitis	100 (230–320)	48 (280–320)
	Photo conjunctivitis	50 (230–290)	5.2 (280–290)
The sun (south of Russia, midday, summer) [16]	Sunburn, preventive maintenance, vitamin D	120 (mW/m^2) (290–400)	–

*) UVI intensity is calculated taking into account the necessity to observe an established dose for a specific duration of irradiation

D being the "solar vitamin" not only in the maintenance of natural calcium metabolism, but also practically in all organs of human beings. In particular, a deficiency in vitamin D raises the risk of cancer of the mammary gland, the large intestine, and the prostatic gland, as well as risk of multiple sclerosis, diabetes, and other diseases.

Finally, in the recent report by Sliney D.H. at the CIE conference "Lighting Quality and Energy Efficiency", April, 2014 [11], it was declared a necessity to introduce some corrections in [3].

It should be recalled that, according to [12][1], during the autumn and winter periods, people who are fully or partially lacking natural sunlight and have a constant deficiency of UV radiation, whether due to the geographical parameters of their residence (located to the north of 57.5^0 N) or due to the characteristics of their working conditions (underground, buildings without natural light or with its deficiency located to the north of 42.5^0 N), should be exposed to a preventive UV irradiation. In addition, in [12, 17], requirements for UV-irradiation, erythema and energy irradiance, wavelength area, irradiation dose and period are specified. Radiation of wavelength shorter than 280 nm is not permitted. That is to say that precisely the interval of UV radiation, which facilitates the formation of vitamin D so necessary for a human body, is not permitted.

Nothing has changed since: neither climate, nor the northern territories of the Russian Federation, nor nature of UV influence on the human body. Moreover, the number of rooms with a sunlight deficiency has increased in recent years. Trade enterprises, storages facilities with tightly closed window openings, public catering enterprises, laundries and repair shops in basement rooms, industrial enterprises, warehouses with huge areas without sunlight but with round-the-clock operation of personnel, have appeared in cities. According to NIIOT Open Company in the city of Ivanovo, as a result of the certification of workplaces for working conditions carried out in the Russian Federation in accordance with the Labour code requirements, a significant number of workplaces were identified, the natural illumination working conditions of which were classified as 3.2 (harmful) because of the unavailability of natural illumination. According to standard legal acts of the Russian Federation [12, 13, 14], one of methods of overcoming "light starvation syndrome" and to decrease the harm caused by working conditions in rooms without natural light and in buildings located in northern territories, is preventive UV irradiation.

The efficiency of application of the preventive ultra-violet irradiation in rooms without natural light

[1] The first instructions on preventative measures against light starvation of people #547–65 were adopted in the USSR in 1965, the second ones [12] were adopted in 1989, and they are effective to the present day, i.e. these recommendations have existed for about 50 years.

was confirmed by the practice of its introduction.

An analysis of disease incidence amongst workers of industrial enterprises has shown that UVI application at workplaces reduced respiratory diseases in the mean by 18.7% with a reduction in the incapacity for work time by 24.6% in comparison with non-irradiated people [15, 18].

All of this confirms the necessity to revive UV preventive maintenance in Russia [12, 14]. This is not a question about special sunrooms, where people obtain a necessary dose over a short time (this is a separate direction in medicine). We only consider preventive installations with a long-term influence using illumination and irradiation devices operating eight-hour working days along with normal luminaires. Such devices contain both illumination, and erythema lamps.

In Table 1, recommended (by the standards) and calculated doses of actinic exposure of some photoreactions are given, which were obtained with erythema lamps of LE (LE15, LE30, LE Mercury 40) type radiating in UV-(B+A) interval and do not generate any UV–C radiation at all, i.e. radiation shorter than $\lambda = 280$ nm. The spectrum of LE type lamp is given in [16].

The calculation results show that LE type lamps and erythema irradiators developed on their basis meet not only the functional requirements [12], but also the safety requirements as specified in the CIE and IEC standard [3].

Irradiators with erythema lamps of LE type were manufactured not so long ago in the Russian Federation. These were as follows: LEBO10–3x18 (1x15)-004 УХЛ 4 and ЭСП 24 ДР 1x40 УХЛ 4 for different suspension heights. The listed irradiators were applied in our projects: Novomoskovsk AC (production shops without natural light), VNIPIneft Open Society, Ryazan Oil Refining Joint-Stock Company (operational rooms), Sosnovy Bor (Pine forest) atomic station (rooms of this atomic station near St. – Petersburg), Technopolis Holding Open Company, Ektel Open Company, etc.

In our opinion, improvement of these irradiators based on use of light emitting diodes instead of fluorescent lamps, will not reduce the reliability of these irradiating installations and their radiant safety.

CONCLUSIONS AND PROPOSALS

1. The Russian UVI standards recommended by Methodical Instructions [12] are not contrary to the international standard on safety of lamps and lamp systems established by CIE and IEC [3].

2. It is necessary to introduce some corrective amendments into CIE and IEC [3] standard making more precise the wavelength areas and admissible UVI standard doses for preventive maintenance.

3. To consider the expedient introduction of the information stated in p. 2 into Federal Law #426–03 about the special evaluation of working conditions, which was adopted by the State Duma on December, 23rd, 2013 without the proposed corrections.

4. To recommend VNISI Open Company and the CIE Committee of the Russian Federation to publish the special information in lighting and medical (labour medicine) journals of the Russian Federation; to present the results from CIS countries and Scandinavian countries of this type of work and to propose collaborative efforts in this sphere of lighting research.

REFERENCES

1. International lighting dictionary, the third edition, Moscow, Russky Yazyk, 1979.

2. A.Meyer and E.Zeitz. Ultra-violet radiation (generation, measurement and application in medicine, biology and technology), Inostrannaya Literatura Publishing House. Moscow, 1952.

3. IEC62471/CIE S009/E&F:2002 (bilingual edition) Photobiological Safety of Lamps and Lamp Systems Dual IEC/CIE Logo Standard.

4. Ultra-violet radiation, Moscow: Meditsina, 1971.

5. Konev S.V., Volotovsky I.D. Photobiology, Minsk, Publishing House of the BSU, 1979.

6. Panferova N.E. Perspectives of application of ultra-violet radiation in long-time space flights // Space biology, Medicine.1986, #1, pp. 4–71.

7. M. Holick. Sunlight, UV-B radiation, vitamin D_3 and your health, Expert Symposium on Light and Health, 30 Sept. –2 Oct.2004, Vienna, Austria.

8. Holick M.F. “Historical and new perspectives on the biologic effects of sunlight and vitamin D on health”. Proceedings Lux Europa, Berlin, 2005, pp. 20–24.

9. M. Holick, “Sunlight, Vitamin D and health: A D- lightful story”//Solar Radiation and Human Health, The Norwegian Academy of Science and Letters, 2008.

10. Luis Tavera-Mendosa, John White “Solar vitamin”, Biology // # 2, February 2008.

11. Sliney D.H. Almost all lamps are safe, but safety of new lamps is questioned, Light & Engineering, V22, #4, pp.15–23.

12. Methodical instructions. Preventive ultra-violet irradiation of people (with use of artificial sources of ultra-violet radiation. MI 5046–89 of July, 27th, 1989.

13. Manual P 2.2.2005–06, 2014. "The manual on hygienic evaluation of factors of working environment and labour process Criteria and classification of working conditions".

14. Code of rules: СП 2.2.1.1312–03. "Hygienic requirements to design of new and reconstructed industrial enterprises (amended and revised #1)".

15. Belyaev I.I., Borodinova A.A., Mamontova N.V. Decrease of respiratory disease incidence, using ultra-violet irradiation, Svetotekhnika, 1983, #7, pp.9–10.

16. Afanasyeva R.F, Barmin V.V., Gavrilkina G.N, Mudrak E.I., Sarychev G.S. Preventive ultra-violet radiation using, Svetotekhnika. 2001. # 1, pp. 18–20.

17. CIE S007/E:1998 "Erythema Reference Action Spectrum and Standard Erythema Dose".

18. Sarychev G.S. Irradiating lighting installations (a monograph), Energoatomizdat, Moscow, 1992.

Galina N. Gavrilkina,
Ph.D., graduated from Moscow Power Energy Institute (MPEI) in 1962, lead scientist in Open Company "VNISI of S.I. Vavilov"

Elena I. Ilyinna,
Ph.D., graduated from Ivanovo Energy Power Institute of V.I. Lenin. At present, she is the Head of the Laboratory of industrial illumination in Open Company "NIIOT" (Scientific and Research Institute of Labour Protection), Ivanovo

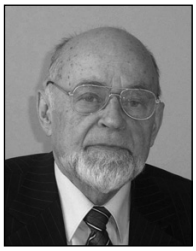

Henri S. Sarychev,
Dr. of technical science, graduated from MPEI in 1956, at present, he is the Head of the laboratory in VNISI, Academician of the Academy of Electrotechnical Sciences of the Russian Federation

Light & Engineering
Vol. 23, No. 4, pp. 55-62, 2015

Svetotekhnika
No. 4, 2015, pp. 47-52

SPECTRAL ASPECT WHEN USING LIGHT-EMITTING DIODE IRRADIATORS FOR SALAD PLANT CULTIVATION UNDER PHOTOCULTURE CONDITIONS

Andrei A. Yemelin[1,2], Leonid B. Prikupets[1,2], and Ivan G. Tarakanov[3]

[1]VNISI of S.I.Vavilov Open Company
[2]BL TRADE Open Company
[3]Russian State Agrarian University – MAA of K.A.Timiryzev FSEE, Moscow
E-mail: prikup@vnisi.ru

ABSTRACT

The authors state that there is currently no alternative to the experimental method of searching for an optimum spectrum of optical radiation to cultivate some plant types. Photobiological research was performed for salad photoculture conditions in a phytothron at the Russian State Agrarian University (RSAU) – Moscow Agrarian Academy (MAA). Irradiators with high pressure sodium lamps (HPSL), and with white and colour (red-dark blue) LEDs were used in the experiment. The obtained results hold out a hope of a decreasing electric energy costs by up to 40–45% when using red-dark blue phyto-irradiators with light emitting diodes to cultivate salad in industrial greenhouses.

Keywords: light emitting diode, photoculture, irradiating installation, light curves, salad-greengrocers cultures, photobiological experiment, HPSL, photosynthesis photon flux

1. INTRODUCTION

The emergence of light-emitting diode radiation sources holds out a hope for the ambition of photobiologists, light engineers and greenhouse cultivation specialists, which seeks to create light sources with an optimal spectrum for the cultivation of some types of plants [1–3]. A logical choice as the first object of study, are greengrocer salad cultures, because these are plants with a short vegetation period (25–30 days), which generate useful biomass: leaves.

The final reaction of the plants for influence of optical radiation (OR) can be expressed, with some assumptions, as an integral function, more likely being a conditional mathematical illustration:

$$N = q \cdot \eta_{эф} \times T \int_{400}^{700} E_v(\lambda) \cdot \alpha(\lambda) \cdot K_ф(\lambda) \cdot d\lambda, \qquad (1)$$

where $E_v\ (\lambda)$ is irradiance spectral concentration on the cone surface from a radiation source of photosynthetic active radiation (PAR) area (400–700 nm), $\alpha(\lambda)$ is the spectral absorption factor of the leaves, $K_ф(\lambda)$ is the spectrum of photosynthetic influence, N is the dry weight of plants, T is the duration of irradiation, η_{ef} is the efficiency of synthesis of dry biomass, q is the useful-energy value of dry biomass.

Characteristic spectral functions *of* $K_ф(\lambda)$ and $\alpha(\lambda)$ are presented in Fig. 1. Their configuration has motivated a variety of lighting equipment manufacturers to propose irradiators with a combination of red and dark blue LEDs to cultivate greengrocer salad cultures. The portion of radiation in the red spectrum interval (630–690 nm) amounts to 65–95%, and in the dark blue interval to (430–470 nm) – the others amount to 5–35% [4–6].

It was repeatedly claimed that use of new red-dark blue irradiators with LEDs can achieve energy efficiency and greater production capacity of plants

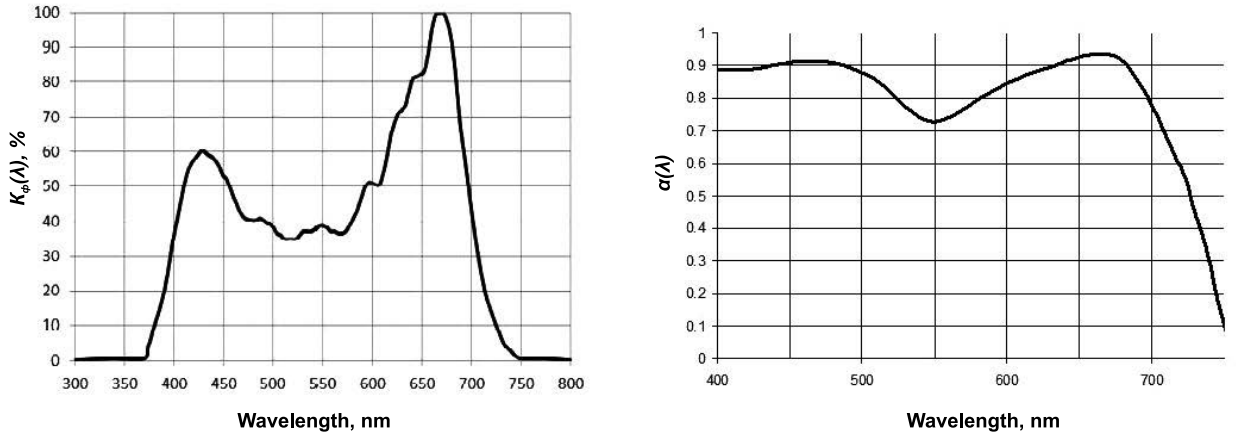

Fig. 1. Relative spectrum of photosynthesis influence (a) and spectral factor of leaves absorption (b)

Fig. 2. Appearance of the ДО01–80x01–05 Galad irradiator

in comparison with HPSL luminaires currently applied in greenhouse plant growing.

It should be noted that for a long time before the introduction of the new devices, practical photobiology had proved that in most cases there was no correlation between photosynthesis intensity and plant production capacity, and the problem of photosynthesis integration with growth in the production process to a great extent depends on the arrangement and regulation of donor-acceptor relations [7].

When searching for an optimum OR spectrum for a certain type of plant, there is currently no alternative to the experimental method.

Experimentation can yield the results, based on which substantiated requirements of LED phytoirradiators lighting parameters can be developed.

Trials performed at several research centres have been an important and necessary stage of the process. As a rule, trials have compared efficiency of salad cultures at one level of illuminance (irradiance) using both traditional light sources and colour LEDs [8, 9]. The results obtained did not confirm any radical benefits of colour combinations of irradiators with LEDs and did not take into account the energy parameters of the irradiating installations (II).

Having reviewed these previous studies, the authors decided to carry out their own photobiological research in the phytotron of the department of plant physiology at the RSAU – MAA of K.A. Timiryazev.

2. METHODS, CONDITIONS OF THE RESEARCH AND EQUIPMENT USED

The plan of the research provided for a photobiological experiment according to the classical procedure, which allowed obtaining "light curves" of salad plant production capacity, in other words of production capacity's dependence on the illuminance (irradiance) level of radiation sources with different spectra. In order to minimize the costs, it was decided to use three illuminance (irradiance) levels only for each spectral version and to perform vegetation series in threes.

The temperature in the phytothron was maintained at 24 ± 2° C during the day-time and 18 ± 2° C at night; air humidity was at 85 ± 5%; the photoperiod amounted to 18 hours a day. Salad plants were grown in threes using a substratum based on a neutralised terrestrial peat filled with fertilizers. Plants were watered daily until the first drop.

Containers with plants were placed on tables, each 100×100 cm in size. Three types of irradiators were used in the experiment: analogues of HPSL irradiators by *Osram* company of the *PlantaStar* series of 400 and 250 W (control) power usually applied in

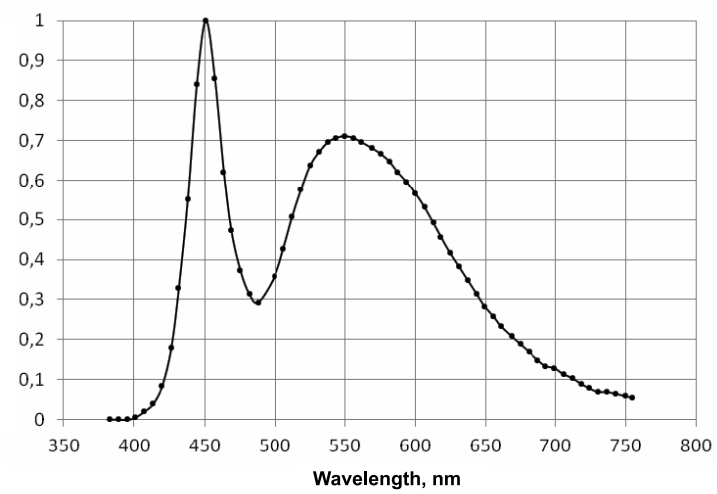

Fig. 3. Relative spectral concentration of horizontal irradiance at 1.5 m distance from ДО01–80–01 irradiator with white LEDs

greenhouses to cultivate salad; a luminaire of ДО01–80x1–04 *Galad* type with white LEDs (its correlated chromatic temperature (CCT) was 5000 K); and an experimental irradiator made on its basis with a combination of red and dark blue LEDs.

This irradiator (Fig. 2) consisted of four "lines" of 20 W each, the general power consumption was 95 W. LEDs of *XR-C* series of 1 W power of *Cree* company (USA) of red and dark blue light were used. Thus the portion of red radiation amounted to 70% and dark blue – to 30%. Spectra of the irradiators are given in Figs. 3 and 4. Slope angle of the side modules of DO01–80x1–04 LED device lines could be changed, which turned out to be rather convenient to provide a required illumination (irradiation) uniformity of the technological surface.

The irradiators were suspended at a necessary height over the table surface, and the height was adjusted within 50–120 cm, which allowed providing the required illumination (irradiation).

All sorts of salads were grown within 25 days from a sprout obtained under identical conditions, to final products. Average green and dry weight of the useful biomass (leaves) for a container, were determined upon completion of the vegetation period using standard methods. Biological repeatability was quadruple: (four containers for a version).

Within a representative technological area of salad cultivation, change of illuminance (irradiance) didn't exceed ± 10% of the average value. In Fig. 5, pictures of phyto-installations with different irradiators are given. For the research, two sorts of sal-

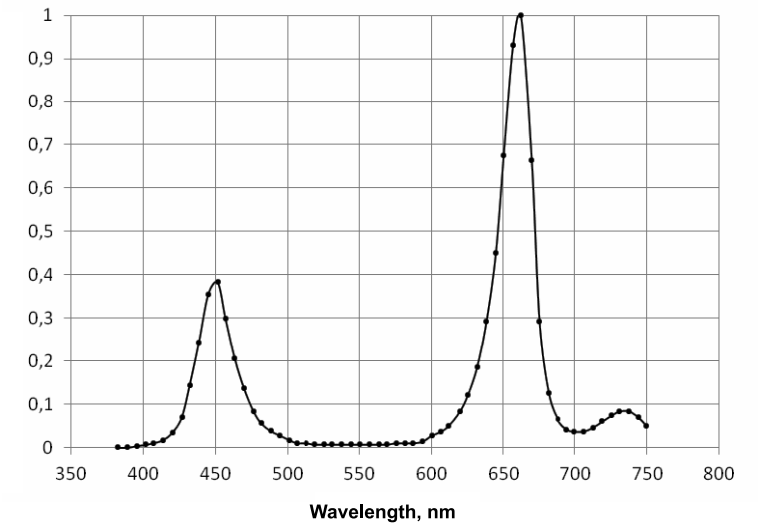

Fig. 4. Relative spectral concentration of horizontal irradiance at 1.5 m distance from ДО01–80–01 irradiator with red-dark blue LEDs

Fig. 5. Pictures of the phyto-installations mounted in order to carry out experiment in the RSAU – MAA. From left to right: with red-dark blue and white LED irradiators and with HPSL irradiators

ad: Aficion and Karmezi, were selected, which had high production capacity and were used in industrial greenhouses.

Based on our expert evaluations and of the technology requirements to the "salad lines" of industrial greenhouses, an illuminance variation interval within 8–18 klx was accepted for HPSLs and white LEDs. Because of the fact that use of the light value system for irradiators with red-dark blue spectrum was not possible, we used a photosynthesis photon value

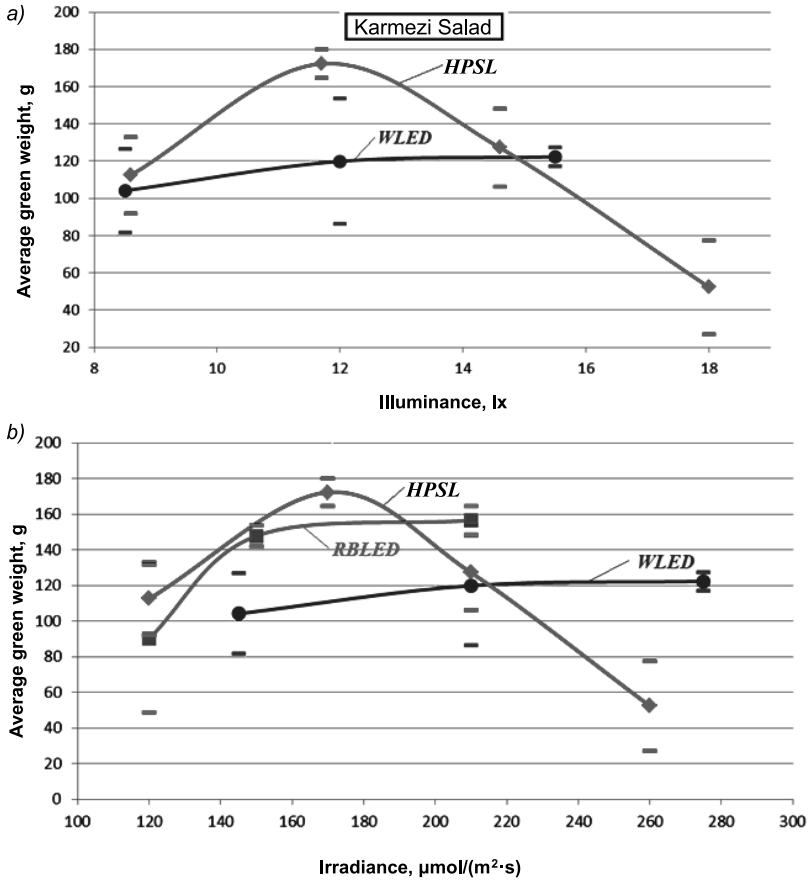

Fig. 6. Production capacity dependence of Karmezi salad (g/container) on illuminance (a) and on photosynthesis photon irradiance (b) of white (WLED) and red-dark blue (RBLED) irradiators with LEDs and of irradiators with HPSL (HPSL)

Table

Irradiator version	*H,* (μmol/(·s^{-1})/W	η_{ir}	U_{ID}
Irradiator with HPSLs	1.85	0.9	0.9
Irradiator with red-dark blue LEDs	2.24	1	0.9

system for irradiance measurement, as used in the Netherlands, the USA and in some other countries. Unfortunately, it is not propagated in Russia yet. Irradiance in this system is determined as the surface density of photon flux and measured in μmol/m^{2}s units. Based on an analysis of these foreign studies and of our own evaluations, an irradiance interval of 100–300 μmol/m^{2}s was chosen in this case. Certainly, to obtain comparable data, for measuring irradiance from irradiators with HPSLs and with white LEDs, the photosynthesis photon system was also used along with the photometric system. An experimentally determined relation between illuminance measured in klx and irradiance measured in μmol/(m^2·s), for irradiators with HPSLs and white LEDs was described as follows:

$$E_v^{HPSL}\ [\text{lx}] \approx 68\text{–}75 \cdot E_{ppf}^{HPSL}\ [\mu\text{mol}/(\text{m}^2\cdot\text{s}],$$

$$E_v^{white\ LED(5000K)}\ [\text{lx}] \approx$$

$$\approx 55\text{–}60 \cdot E_{ppf}^{white\ LED\ (5000K)}\ [\mu\text{mol}/(\text{m}^2\cdot\text{s}].$$

To measure illuminance, we used a TKA-LUX luxmeter of TKA company, St. – Petersburg, and to measure photosynthesis irradiance we used *Quantum Meter* device of *Spectrum Technologies, Inc*. company, USA.

3. ANALYSIS OF THE RESEARCH RESULTS

The research results are presented in Figs. 6 and 7 as a series of light curves connecting production capacity *N* of plants with illuminance E_v or with pho-

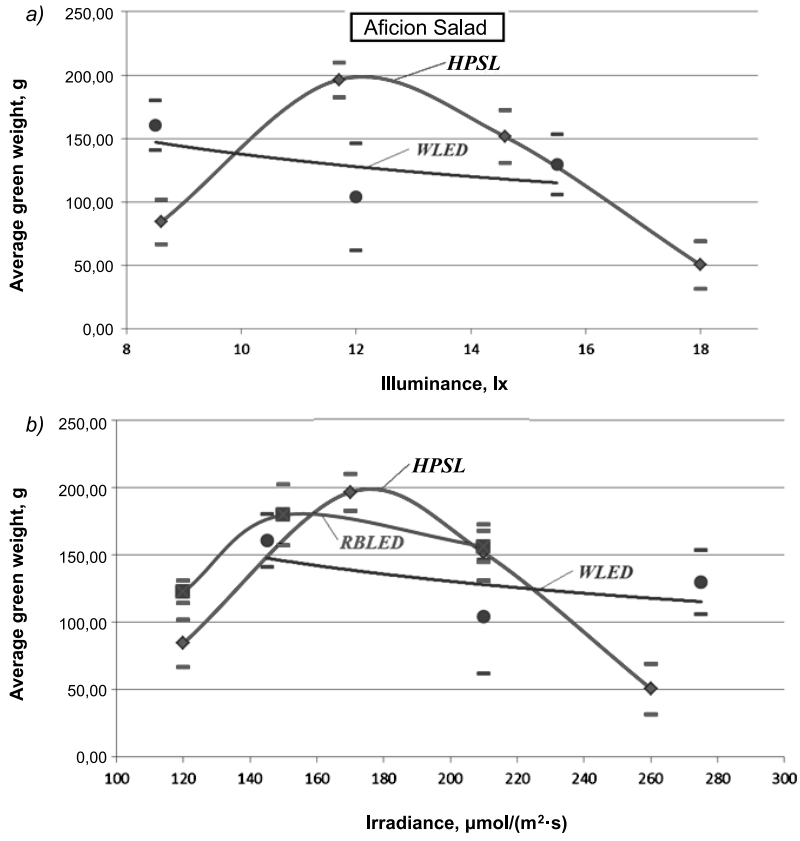

Fig. 7. Production capacity dependence of Aficion salad (g/container) on illuminance (a) and on photosynthesis photon irradiance (b) of white (WLED) and red-dark blue (RBLED) irradiators with LEDs and of irradiators with HPSL (HPSL)

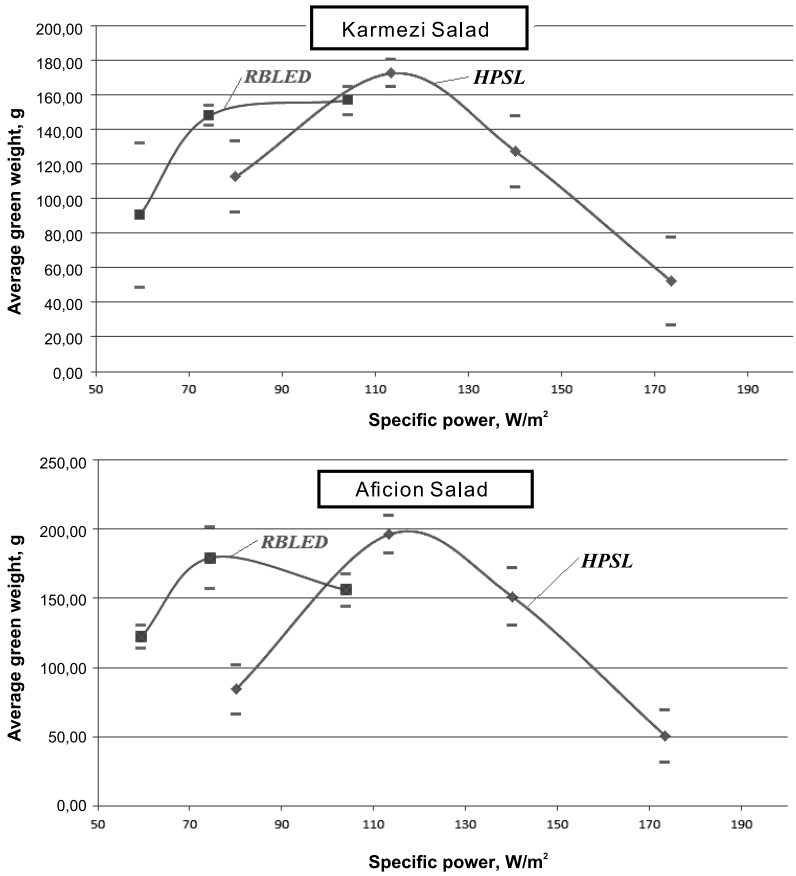

Fig. 8. Production capacity dependence of different salad sorts on specific installed power of the phyto-installation with red-dark blue LED (RBLED) irradiators and with HPSL (HPSL) irradiators

tosynthesis photon irradiance E_{ppf}. Producing capacity in our case is an average weight of the useful biomass of salad plants of one pot similar to the used in industrial hothouses.

An analysis of the obtained data allows speaking both about general mechanisms of plant reaction to the illuminance (irradiance) level and to the spectrum, and about differences for each salad sort. It should be noted that light curves obtained for irradiators with HPSLs only and in some measure, with red-dark blue LEDs have a "classical" form (an evident maximum of the producing capacity) for all sorts of salad.

In spite of a prolonged use of irradiators with HPSLs for salad photoculture, there are practically no published data reasoning the choice of preferable illuminance for salad lines in greenhouses. For example, in the centre of Russia it can fluctuate from 8 to 14–15 klx in different greenhouse facilities. Our experiments show that the greatest producing capacity of all three salad sorts is provided when using HPSL irradiators with E_v of about 12 klx (~ 170 μmol/(m^2·s)), which certainly is of the utmost interest to greenhouse facilities.

A maximum, or close to maximum, production capacity in the experiments with red-dark blue LEDs, was reached at a slightly lower photon irradiance (of about 150 μmol/(m^2·s)) for both investigated salad sorts. The production capacity results reached when using white light LED radiation with CCT of 5000 K, were inferior to the ones reached with HPSLs and red-dark blue LEDs.

As a whole, the spectrum version correspondent to the HPSLs appeared to be more effective, because it provided the highest plant efficiency. This somewhat contradicts the perfunctory concepts, which have arisen lately, that an optimum spectrum of a radiation source should be close by the form to the spectrum of photosynthesis influence. It should be noted that the photosynthesis process takes no more than 5–8% energy of the absorbed radiation, and the production capacity of plants is a complex product of exposure of a wide spectral interval radiation. In particular, HPSL near-infrared radiation absorbed by

the leaves and influencing temperature and transpiration of the latter, is very important for salad cultures, which are leaf plants.

The obtained salad producing capacity dependences on spectral characteristics and on the intensity of the radiation incident onto the cone (Figs. 6 and 7) are to a certain extent "refined", because they do not take into consideration the energy consumption ensuring a needed illumination (irradiation) level.

The necessity of practical use of the research results requires an accomplishment of the correspondent calculation evaluations for the main compared types; that is for irradiators with HPSLs and red-dark blue LEDs. These evaluations were carried out according to the expression:

$$P_1 = \frac{E_{ppf}}{H \cdot \eta_{ir} \cdot u_{ID}},$$

where P_1 is installed specific power of a greenhouse IDs, W/m^2; E_{ppf} is photosynthesis photon irradiance, μmol/(m^2·s); H is photosynthesis photon flux of the radiation source relative to the power and active losses sum in the ballast (photosynthesis photon efficacy), (μmol ·s^{-1})/W; η_{ir} is irradiator efficiency; u_{ID} is ID usage coefficient.

When calculating, the highest of the reached H values were used both for 600 W power HPSLs of *PlantaStar* [10], and for the similar parameter of red-dark blue irradiators with LEDs [11], as well as the η_{ir} and u_{ID} data reached in practice. The specified values are given in the Table.

In Fig. 8, N dependences on P_1 for two main compared versions for the Karmezi and Aficion salads are given.

As it can be seen, replacing the E_{ppf} scale with the P_1 scale leads to a certain transformation of the light curves. It has become more obvious that the nearest by production capacity data of salad cultures, taking any errors into account, can be obtained when using irradiators with red-dark blue LEDs at the installed power by 30–35% smaller than in the event of HPSL irradiators. This essentially raises energy-efficiency of the salad photoculture technology, where electric power costs usually reach 50% of the prime cost. It should be also noted that according to the current forecasts [11], photon efficacy of red and dark blue LEDs may increase in years to come by 30%, which will allow lowering specific installed power of IDs with LEDs by 40–45% in comparison with HPSLs.

The answer to the question, what then interferes with mass introduction of LED irradiators into greenhouse plant growing, is obvious. The price difference of the LED irradiators and of the traditional HPSL irradiators is so substantial, that the repayment period of this replacement will be not less than six or even seven years [12]. The financial events of the latter time only aggravate this situation.

REFERENCES

1. *Prikupets L.B., Tihomirov A.A.* Spectrum optimisation when cultivating vegetables under conditions of an intensive photoculture // Svetotekhnika. – 1992. – # 3. – p. 5–7.

2. *Tikhomirov A.A, Lisovsky G. M, Sidko F.Ya.* Spectral composition of light and producing capacity of plants. – Novosibirsk: "Nauka", 1991. – 167 p.

3. *Tarakanov, I., Yakovleva, O., Konovalova, I., Paliutina, G., Anisimov, A.* Light-emitting diodes: on the way to combinatorial lighting technologies for basic research and crop production // Acta Horticulturae. – 2012. – Vol. 956. – P. 171–178.

4. Light emitting diode illumination for hothouses. Phillips Catalogue, edition 09/2013.

5. URL: http://kodosvet.ru/led-light-fixtures от 25.02.2015 (Addressing date: 15.03.2015).

6. Plant Growth with LED Lighting. Parus Catalogue (South Korea), edition 05/2014.

7. *Mokronosov A.T.* Interrelation of photosynthesis and growth function // In the book: Photosynthesis and productional process. Moscow: Nauka, 1988. – p. 109–121.

8. *Sase, S., Mito, C., Okushima, L., Fukuda, N., Kanesaka, N., Sekiguchi, K., Odawara, N.* Effect of overnight supplemental lighting with different spectral LEDs on the growth of some leafy vegetables // Acta Horticulturae – 2012. – Vol. 956. – P. 327–333.

9. *Lee, J.S., Lim, T.G., Kim, Y.H.* Growth aqnd phytochemicals in lettuce as affected by different ratios of blue to red radiation // Acta Horticulturae. – 2014. – Vol. 1037. – P. 843–-848.

10. PlantaStar Lamps. Osram catalogue, 2014.

11. *Ton ten Haaf* (Light Interaction (Holland)), All about supplementary lighting / A report at the scientific and technical seminar of the Hothouse of Russia Association, Maloyaroslavets, 13.03.2014 .

12. *Prikupets L.B., Yemelin A.A.* Use of irradiators based on light emitting diodes for the salad photoculture: economic aspect // Hothouses of Russia. – 2013. – # 2. – p. 66–68.

Andrei A. Yemelin,
M.Sc. Graduated from the Magistracy of the Chair "Lights and Engineering" of the Moscow Power Institute National Research University cum laude in 2014. An engineer of VNISI of S.I. Vavilov Open Company and a technical adviser of BL TRADE Open Company

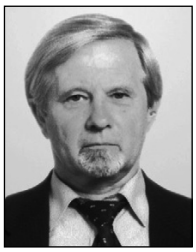

Leonid B. Prikupets,
Ph.D. Graduated from the Moscow Power Institute cum laude in 1970. A chief of the laboratory of VNISI of S.I. Vavilov Open Company and a technical adviser of BL TRADE Open Company

Ivan G. Tarakanov,
Doctor of Biology, professor. Graduated from the MAA of K.A.Timiryazev in 1978. The Head of the Chair «Physiology of plants» of the RSAU – MAA FSEE of K.A. Timiryazev

Light & Engineering
Vol. 23, No. 4, pp. 63-69, 2015

Svetotekhnika
No. 6, 2015, pp. 33-35

EVALUATING THE UNCERTAINTY OF THE SPECTRORADIOMETRIC APPROACH FOR THE CALCULATION OF SSL LUMINAIRES CHROMATICITY COORDINATES

Alexander A. Sharakshane, Anton S. Sharakshane, and Raisa I. Stolyarevskaya

LLC "Editorial of Svetotekhnika Journal", Moscow
E-mail: lights-nr@inbox.ru

ABSTRACT

The accuracy of chromaticity coordinates measurements, which are effective values, connected with the CIE tabulated functions and with a specific colour space, depends on the measuring devices used and on the spectral distribution of the energy characteristics of the radiators. These devices can be both integral, and spectral. In this paper, limit evaluations of colour coordinates *x* and *y* determination error are considered for lighting devices with light emitting diodes under laboratory test conditions. The evaluations are based on measurements of irradiance spectral distribution created by an LED luminaire, taking into account the uncertainty of the spectral characteristics of a standard source, which is used for spectrometer calibration. The research was performed by analysing linear errors and using the stochastic simulation method.

Keywords: chromaticity coordinates, colour stimuli (coordinates), irradiance spectral distribution, standard lamp, colour space, chromatic locus, limit evaluations of chromaticity coordinate uncertainty, random errors, stochastic simulation, error correlation

1. INTRODUCTION

When analysing the methods and measuring devices in the fields of photometry and colorimetry, which are the most important and expansive directions of lighting science connected with the visual perception of optical radiation by a person (CIE tabulated functions), the differences and benefits of various approaches should be clearly understood. One of the main benefits is the resulting uncertainty of the measurement results.

Light and chromatic measurements can be achieved using the following methods:

– A comparison of the measured radiation source with a standard lamp of light or chromatic values by means of an integral comparator;

– A direct measurement of light and chromatic characteristics using a photometric head, a photometer, a luxmeter or a colorimetric head as well as a colorimeter;

– A measurement of the spectral distribution characteristics of the radiator and calculation of the photometric and colorimetric values.

In the latter case, the CIE tabulated addition functions don't contribute any error.

The method of source comparison is only significantly more accurate when the spectral characteristics of the compared radiators are identical.

In event of direct measurements based on the detector approach, the theory and practice of light and chromatic measurements assumes use of standard light measuring lamps operating in the CIE A type mode of a source for photometer calibration. For this case, correction multipliers must be applied [1, 2], which exclude the regular component of correction quality error of the receiving channels, in accordance with the CIE tabulated functions. While for the case of light measurements we deal with one tabulated function, relative spectral luminous efficiency for chromatic measurements requires three such func-

tions. This significantly complicates the direct integral measurement of chromatic characteristics of the light sources with spectral distribution of energy characteristics different from the A type sources.

In the case of the spectroradiometric approach, the main regular not excluded measurement error is an error of the standard light-measuring lamp of energy characteristics (spectral irradiance concentration, SIC), spectral radiance concentration (SRC), (spectral radiant intensity concentration SRIC), or spectral flux distribution, the reproduction of which is absent in the Russian accuracy chart (calibration test circuit) [3]). Within the spectrum visible interval, error limits of SIC, SRC and SRIC of the working measuring instruments doesn't exceed ± 4% for the absolute values of the spectral characteristic. These values were used when solving the task set, although for colorimetric calculations it was enough to know the relative spectral concentration and the limits of its measurement's total error in the visible wavelength interval.

The state calibration test circuit for measuring instruments of colour coordinates and chromaticity coordinates, as well as of whiteness and point brilliance indicators [4] regulates errors of transmission of chromaticity coordinate units of self-luminous objects from the state primary standard (SPS) to secondary standards, working standards and working measuring instruments. For the radiators, limits of admitted absolute errors ($\Delta_x = \Delta_y$) when measuring chromaticity coordinates at a level of the working measuring instruments, amount to 0.004–0.020.

The main goals of the research were as follows:

– Determination of the maximum possible limit of the regular error component connected with the standard lamp for calibration of the spectrometer, and in this case it is a light-measuring SRC lamp at a level of the working measuring instrument;

– Comparison of the analysis results with error limits of the calibration test circuit for measuring instruments of chromatic values regarding self-luminous objects [4];

– Comparison of the analysis results with the allowances regulated by Russian Standard 54350–2011 "Lighting devices. Lighting requirements and test methods" [5].

2. THE ANALYSIS

Source chromaticity coordinates x, y are calculated according to the formulae:

$$x = \frac{X}{X+Y+Z}, y = \frac{Y}{X+Y+Z}, \tag{1}$$

where *X, Y, Z* are colour stimuli. Colour coordinates themselves depend on the distribution of the radiation spectral concentration $\phi_{e\lambda}(\lambda)$ of a source and can be represented by the formulae:

$$X = \int_{380}^{780} \phi_{e\lambda}(\lambda)\bar{x}(\lambda)d\lambda,$$

$$Y = \int_{380}^{780} \phi_{e\lambda}(\lambda)\bar{y}(\lambda)d\lambda,$$

$$Z = \int_{380}^{780} \phi_{e\lambda}(\lambda)\bar{z}(\lambda)d\lambda,$$

where $\bar{x}(\lambda)$, $\bar{y}(\lambda)$, $\bar{z}(\lambda)$ are addition functions of the CIE1931 standard colorimetric system [6], (section 11.13.2).

Approximately

$$X = \sum_{\lambda} \phi_{e\lambda}(\lambda)\bar{x}(\lambda)\Delta\lambda,$$

$$Y = \sum_{\lambda} \phi_{e\lambda}(\lambda)\bar{y}(\lambda)\Delta\lambda, \tag{2}$$

$$Z = \sum_{\lambda} \phi_{e\lambda}(\lambda)\bar{z}(\lambda)\Delta\lambda,$$

where $\Delta\lambda$ is wavelength pace.

According to [8], the addition functions look like in Fig.1.

As an example of the source, we will use here a light emitting diode CREE MK-R3500K. The relative spectral distribution $\phi_{e\lambda}(\lambda)$ for this source obtained by means of interpolation according to [7], looks like shown in Fig.2.

Chromaticity coordinates calculated by this distribution with a pace of $\Delta\lambda$=5 are equal to:

$$x_{\text{CREE MK-R 3500K}} = 0.405001,$$
$$y_{\text{CREE MK-R 3500K}} = 0.389928.$$

Let's suppose that at some λ value during $\phi_{e\lambda}$ measurements, $\delta\phi_{e\lambda}$ error is made, and in formulae (2), the $\phi_{e\lambda} + \delta\phi_{e\lambda}$ value is used instead of the exact $\phi_{e\lambda}$ value. Such a local error of $\phi_{e\lambda}$ leads to errors in the x, y coordinate calculations, which using the linear approach amount to:

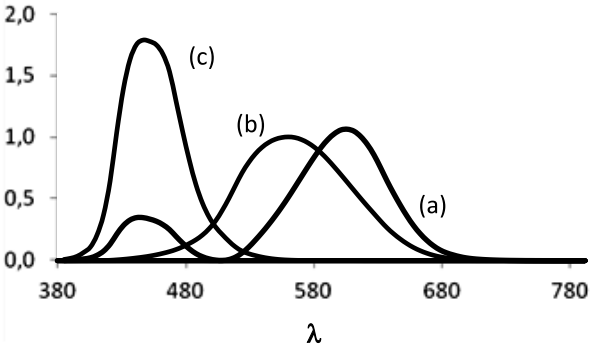

Fig. 1. Addition functions in the standard colorimetric system: (a) $\bar{x}$; (b) $\bar{y}$; (c) $\bar{z}$

$$\delta x = \frac{\partial x}{\partial \phi_{e\lambda}} \delta \phi_{e\lambda}, \delta y = \frac{\partial y}{\partial \phi_{e\lambda}} \delta \phi_{e\lambda},$$

where

$$\frac{\partial x}{\partial \phi_{e\lambda}} = \frac{\bar{x}(Y+Z) - X(\bar{y}+\bar{z})}{(X+Y+Z)^2}, \quad \frac{\partial y}{\partial \phi_{e\lambda}} = \frac{\bar{y}(X+Z) - Y(\bar{x}+\bar{z})}{(X+Y+Z)^2}. \tag{3}$$

Values of derivatives $\frac{\partial x}{\partial \phi_{e\lambda}}$ and $\frac{\partial y}{\partial \phi_{e\lambda}}$ depend on the colorimetric system (via addition functions $\bar{x}(\lambda)$, $\bar{y}(\lambda)$, $\bar{z}(\lambda)$) and on the source (via colour stimulus *X, Y, Z*). And for this source they depend on the wavelength λ. With this λ value, $\frac{\partial x}{\partial \phi_{e\lambda}}$ and $\frac{\partial y}{\partial \phi_{e\lambda}}$ characterise the value and sign of small *x* and *y* changes accordingly due to $\phi_{e\lambda}$ small change.

For the CREE MK-R3500K source, derivatives $\frac{\partial x}{\partial \phi_{e\lambda}}$ and $\frac{\partial y}{\partial \phi_{e\lambda}}$ as λ functions look like shown in Fig. 3.

One should note a complex and non-monotonic nature of these functions, especially of $\frac{\partial x}{\partial \phi_{e\lambda}}$.

Let's assume that when measuring $\phi_{e\lambda}$ at each λ value, an error within ±4% of the measured value is possible. Then the biggest total *x* error is formed, if at every λ, error of $\phi_{e\lambda}$ is equal to 0.04 $\phi_{e\lambda}$ and has the same sign as $\frac{\partial x}{\partial \phi_{e\lambda}}$. That is

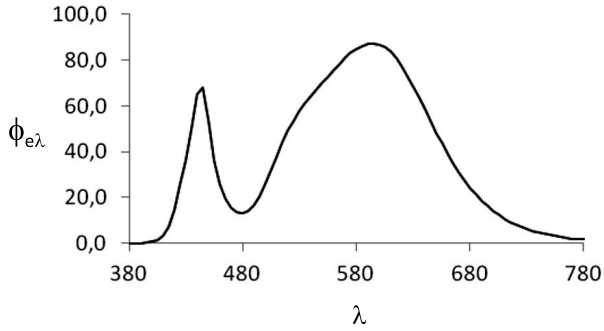

Fig. 2. Distribution of radiation spectral concentration of light emitting diode CREE MK-R3500K

$$\delta \phi_{e\lambda} = \operatorname{sgn}\left(\frac{\partial x}{\partial \phi_{e\lambda}}\right)(0.04\phi_{e\lambda}),$$

where sgn is the "signum" function equal to ±1 depending on the argument sign.

Thus, equation

$$\phi_{e\lambda} + \operatorname{sgn}\left(\frac{\partial x}{\partial \phi_{e\lambda}}\right)(0.04\phi_{e\lambda}) \tag{4}$$

represents a distribution of spectral concentration of a source with 4% errors, which are "maximum unfavourable" for *x* chromaticity coordinate calculation.

Similarly, equation

$$\phi_{e\lambda} + \operatorname{sgn}\left(\frac{\partial y}{\partial \phi_{e\lambda}}\right)(0.04\phi_{e\lambda}) \tag{5}$$

represents a distribution of spectral concentration of a source with 4% errors, which are "maximum unfavourable" for calculation of *y* chromaticity coordinate. For the CREE MK-R3500K source, distributions (4) and (5) are shown in Fig. 4.

Substituting (4) instead of $\phi_{e\lambda}$ to formulae (2) and (1), we find coordinates (x, y) of *P* point, which realises the highest possible value for the *x* coordinate. As a result, it is a 4% error for $\phi_{e\lambda}$. For the CREE MK-R3500K source, point *P* coordinates appear to be equal to $(x = 0.412957, y = 0.390721)$, and maximum total *x* error amounts to $\delta x_{£}^{\max} = 0.007956$, or near 1.96% of the true *x* value.

Substitution of (5) to formulae (2) and (1) gives point *Q* having maximum raised *y* coordinate; for CREE MK-R3500K, point *Q* has coordinates: *y* = 0.404176, *x* = 0 398099, and the maximum total

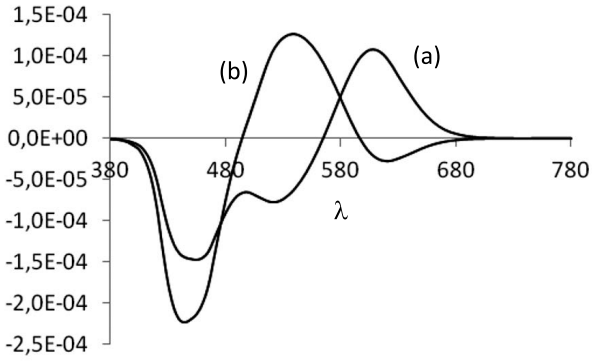

Fig. 3. CREE MK-R3500K: (a) $\frac{\partial x}{\partial \phi_{e\lambda}}$; (b) $\frac{\partial y}{\partial \phi_{e\lambda}}$

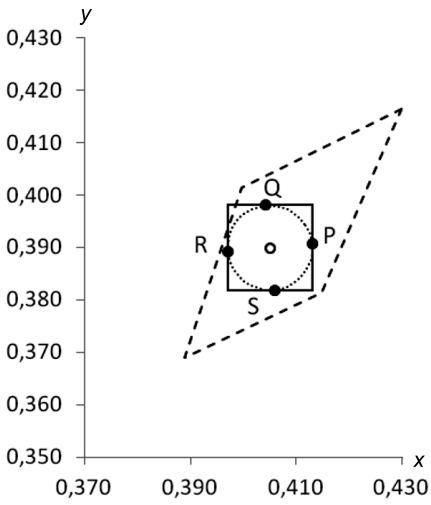

Fig. 5. Possible errors when calculating (*x, y*) coordinates owing to 4% $\phi_{e\lambda}$ error for the CREE MK-R3500K source: check mark as a circle in the centre is light emitting diode CREE MK-R3500K; P is point with a highest possible x coordinate; Q is point with a highest possible y coordinate; R is a point with lowest possible x coordinate; S is a point with lowest possible y coordinate. The dotted line is an approximate boundary of possible positions of (*x, y*) point. The dashed line is quadrangle of maximum deviations according to the CIE recommendations.

y error amounts to $\delta y_{£}^{\max} = 0.008171$, or 1.98% of the true y value.

Fig. 5 shows points P and Q, as well as points R and S, symmetrical to points P and Q relative to the true point of the CREE MK-R3500K. They implement lowest possible x and y values accordingly.

Horizontal and vertical straight lines drawn through points P, Q, R and S limit the rectangle, into which the calculated point should be necessarily placed (x, y) with any radiation spectral concentration errors lying within the limit of ±4% of $\phi_{e\lambda}$ for

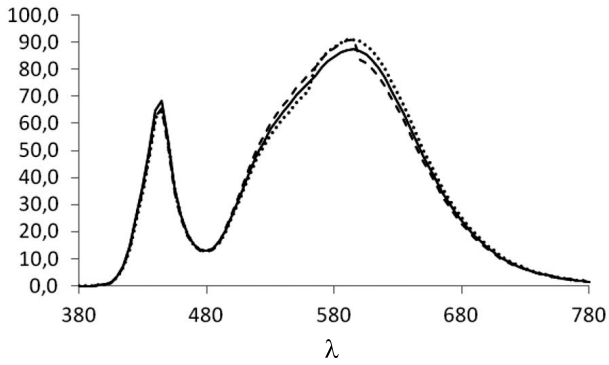

Fig. 4. Distributions of radiation spectral concentration of light emitting diode CREE MK-R3500K with 4% errors leading to highest possible *x* coordinate (dotted line) and y coordinate (dashed line), in comparison with the true distribution (solid line)

every λ. In a real situation, the entire rectangle is not "achievable" for (x, y) point. An approximate boundary of the area, in which the (x, y) point can lie in case of a 4% error, is shown in this figure by the dotted line; its exact configuration and possible connection with Mac-Adam's ellipses demands additional research. In Fig. 5, a quadrangle of maximum deviations from the АЧТ 3500K point according to the CIE recommendations is also shown by the dashed line [8]. It should be noted that possible deviations due to the 4% error for $\phi_{e\lambda}$, just get into this quadrangle.

Maximum *x, y* coordinate errors, which are caused by especially constructed disturbances of radiation spectral concentration distributions (4) and (5), are only theoretically possible; in practice, $\phi_{e\lambda}$ determination errors have a random nature and do not follow signs of the derivatives $\frac{\partial x}{\partial \phi_{e\lambda}}$ and $\frac{\partial y}{\partial \phi_{e\lambda}}$. Moreover, errors at various wavelengths λ compensate each other to a great extent. This effect is expressed to the maximum if these errors are independent random values.

Let's assume that $\delta\phi_{e\lambda}$ error at every λ is a random value distributed according to the normal law with zero mathematical expectation: $\mu_{\delta\phi_{e\lambda}} = 0$ (non-systematic normal error). Mean-square deviation $\sigma_{\delta\phi_{e\lambda}}$ is to be set so that $\pm 0.04\phi_{e\lambda}$ is correspondent to the interval. That is $\sigma_{\delta\phi_{e\lambda}} = \left(\frac{0.04}{3}\right)\phi_{e\lambda}$.

Total errors of x, y in a linear approach, are expressed using derivatives (3) as the sums as follows:

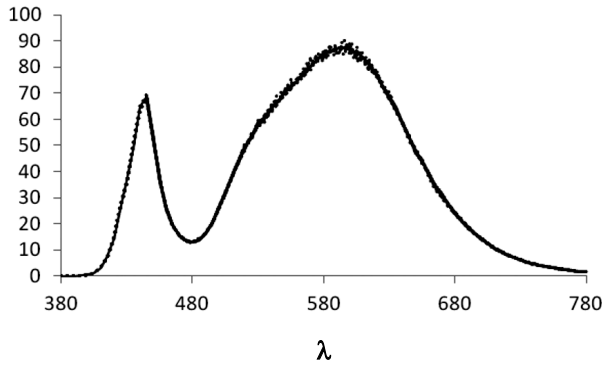

Fig. 6a. Radiation spectral concentration distribution of the CREE MK-R 3500K source with random independent errors distributed according to the normal law with $\mu_{\delta\phi_{e\lambda}} = 0$, $\sigma_{\delta\phi_\lambda} = \left(\frac{0.04}{3}\right)\phi_{e\lambda}$: the solid line is the true distribution, the dotted lines are distributions with errors

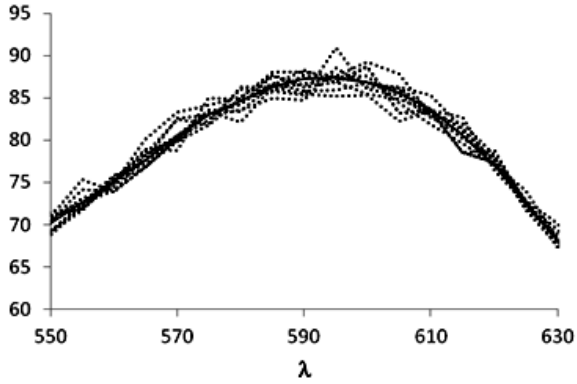

Fig. 6b. Spectral distribution of radiation of the CREE MK-R3500K source with random independent errors (the central fragment of the diagram is given in an increased scale)

$$\delta x_\Sigma = \sum_\lambda \left(\frac{\partial x}{\partial \phi_{e\lambda}}\right)\delta\phi_{e\lambda},\ \delta y_\Sigma = \sum_\lambda \left(\frac{\partial y}{\partial \phi_{e\lambda}}\right)\delta\phi_{e\lambda}.$$

If $\delta\phi_{e\lambda}$ local errors at different wavelengths can be considered independent, then $\delta x_£$ and $\delta y_£$ are normal random values with zero mathematical expectation and mean-square deviations, which can be expressed by the formulas:

$$\sigma_{\delta x_\Sigma} = \sqrt{\sum_\lambda \left(\frac{\partial x}{\partial \phi_{e\lambda}}\right)^2 \sigma^2_{\delta\phi_{e\lambda}}},$$

$$\sigma_{\delta y_\Sigma} = \sqrt{\sum_\lambda \left(\frac{\partial y}{\partial \phi_{e\lambda}}\right)^2 \sigma^2_{\delta\phi_{e\lambda}}}.$$

The calculation for the CREE MK-R3500K source gives:

$\sigma_{\delta x_\Sigma} = 0.000456;\ \sigma_{\delta y_\Sigma} = 0.000523.$

Comparing these values with the maximum possible errors $\delta x_\Sigma^{\max}$ and $\delta y_\Sigma^{\max}$ found previously, a conclusion can be drawn that at random independent $\phi_{e\lambda}$ errors, x, y errors will be less by approximately two orders.

Correlation coefficient of random values δx_Σ, δy_Σ is given by the formula:

$$r = \frac{\mathrm{cov}\left(\delta x_\Sigma, \delta y_\Sigma\right)}{\sigma\delta x_\Sigma,\ \sigma\delta y_\Sigma}.$$

where, with $\delta\phi_{e\lambda}$ independence assumption,

$$\mathrm{cov}\left(\delta x_\Sigma, \delta y_\Sigma\right) = \sum_\lambda \left[\left(\frac{\partial x}{\partial \phi_{e\lambda}}\right)\left(\frac{\partial y}{\partial \phi_{e\lambda}}\right)\sigma^2_{\delta\phi_{e\lambda}}\right].$$

A mixed distribution of random values δx_Σ and δy_Σ has concentration [9]:

$$f(\delta x_\Sigma, \delta y_\Sigma) = \frac{1}{2\pi\sigma_{\delta x_\Sigma}\sigma_{\delta y_\Sigma}\sqrt{1-r^2}} \exp$$

$$\left[-\frac{1}{2\sqrt{1-r^2}}\left(\frac{\delta x_\Sigma^2}{\sigma^2_{\delta x_\Sigma}} - \frac{2r\delta x_\Sigma \delta y_\Sigma}{\sigma_{\delta x_\Sigma}\sigma_{\delta y_\Sigma}} + \frac{\delta y_\Sigma^2}{\sigma^2_{\delta y_\Sigma}}\right)\right].$$

Lines of the concentration level are so-called ellipses of dispersion, which big semi-axis for the CREE MK-R3500K source is inclined to axis x at an angle of about 62°.

Dependence of random errors on x, y coordinates when measuring $\phi_{e\lambda}$, can be simulated using the random number generator. Fig. 6 and 7 show results of such stochastic simulation.

3. CONCLUSION

The linear analysis and stochastic simulation made it possible to evaluate the error of determining chromaticity coordinates of light-emitting diode LDs based on the measurement of their relative spectral characteristics. The evaluation was made based on the assumption that limits of admitted relative errors of SIC working measuring instruments should not exceed ± 4% in a wavelength interval of 0.3–1 μ [3].

The results of the analysis testify that limits of measurement error of chromaticity coordinate using

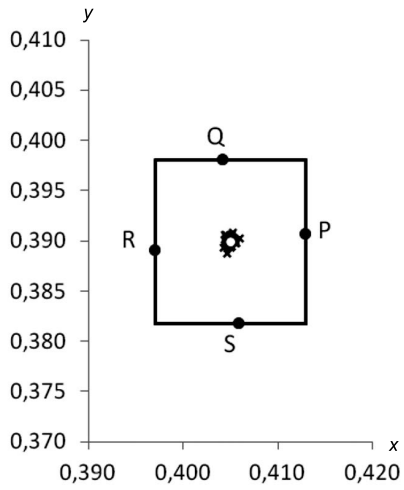

Fig. 7a. Influence of random errors of the source spectral concentration distribution on *x, y* coordinates. The circle in the centre is CREE MK-R3500K. The criss-crosses are points (*x, y)* calculated using $\phi_{e\lambda}$ with independent random errors distributed according to the normal law with

$$\mu_{\delta\phi_{e\lambda}} = 0 \text{ and } \sigma_{\delta\phi_\lambda} = \left(\frac{0.04}{3}\right)\phi_{e\lambda}$$

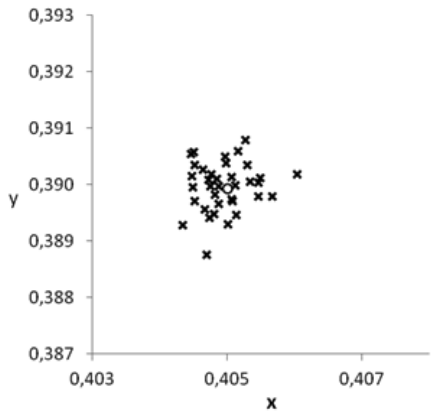

Fig. 7b. Influence of random errors of the CREE MK-R3500K source spectral concentration distribution on *x, y* coordinates (the central fragment of the diagram is given in an increased scale)

calculations based on measurement of spectral irradiance distribution, don't exceed ~ ± 0.008. This value corresponds to the requirements of standard [4] for working measuring instruments of chromaticity coordinates of self-luminous objects, and it is much narrower than the allowances regulated by standard [5], namely admissible quadrangles of chromaticity coordinates for lighting devices, i.e. for products.

REFERENCES

1. CIE S023/E:2013 Characterization of The Performance of Illuminance Meters and Luminance Meters.

2. CIE179:2007 Methods for Characterising Tristimulus Colorimeters for Measuring the Colour of Light.

3. GOST 8.195–2013. State system of securing measurement unity State hierarchical chain for measuring instruments of spectral radiance, spectral radiant intensity, spectral irradiance concentration, radiant intensity and irradiance within wavelengths interval of 0.2 to 25.0 microns.

4. GOST 8. 205–2014 State system of securing measurement unity State hierarchical chain for measuring instruments of colour stimuli and chromaticity coordinates, indicators of whiteness and point brilliance.

5. GOST P 54350–2011. Group E83. The National Standard of the Russian Federation. Lighting devices. Lighting requirements and test methods.

6. http://www.cie.co.at/publ/abst/datatables15_2004/CIE_sel_colorimetric_tables.xls. CIE.

7. http://www.cree.com/~/media/Files/Cree/LED Components and Modules/XLamp/Data and Binning/XLamp-MKR.pdf.

8. CIE recommendations 15:2004. Colorimetry, the 3rd edition.

9. Venttsel E.S., Ovcharov L.A. The theory of probability and its engineering applications. – Moscow, Vysshaya Shkola, 2000.

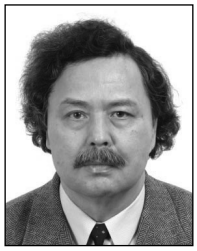

Alexander A. Sharakshane,
Ph.D. phys.-math., graduated from Moscow Institute of Physics and Technology in 1976, Associate Professor at Department of Mathematics of Plekhanov Russian University of Economics

Anton S. Sharakshane,
Ph.D. phys.-math., graduated from physical faculty of Moscow State University named by M.V. Lomonosov in 2001. At present, he is a scientific editor of Light & Engineering Journal

Raisa I. Stolyarevskaya,
Dr. of technical science, graduated from the physics faculty of Kazan State University in 1968. At present, she is the editor of Light & Engineering Journal and a scientific consultant at VNISI, country member of CIE Division 2

Light & Engineering
Vol. 23, No. 4, pp. 69-74, 2015

Svetotekhnika
No. 4, 2015, pp. 18-22

DEGRADATION OF LIGHT EMITTING DIODES: THE CONNECTION BETWEEN OPERATING CONDITIONS, AND ACTUAL AND DECLARED SERVICE LIFE

Dmitry Yu. Yurovskikh

The Representative office of Cree Hong Kong Limited, Moscow
E-mail: Dmitry_Yurovskikh@cree.com

ABSTRACT

The article explores the service life of light emitting diodes and their luminaires. Approaches to the evaluation of service life are proposed, and some principal causes of product failures dependent on specific operating conditions are considered. Recommendations are given regarding what is important when evaluating the durability of light-emitting diode luminaires.

Keywords: light emitting diodes, service life, luminaires with light emitting diodes, failure criteria, *Electrical Overstress*

Today it can be stated confidently that the light-emitting diode illumination revolution has occurred. Light emitting diodes (LED) have found their way into street, office, trade, household and industrial illumination, as well as into households and the communal services sphere. There are several reasons for this, which are widely known.

However, consumers take the declared levels of reliability and durability of luminaires with LEDs (LEDL) incredulously. This is natural, because in such spheres as street, industrial and trading illumination, LEDL introduction is a significant investment as their payoff period is quite slow: as a rule, no less than a year. LEDL failure is much more unpleasant, than the failure of a simple lamp, at least because lamp replacement is a simple process, which the consumer can manage single-handed. On the other hand, LEDL replacement or repair demands involvement of a service company or of the LEDL manufacturer. This is due to the fact that the lamp concept in itself cannot be used with LEDLs. LEDL failure is equally unpleasant both for the user, and for the lighting equipment supplier, who has to repair or to replace the LEDL. Therefore, both manufacturers, and consumers should understand, what LEDL service life means and what it depends on. Consumers frequently have a limited understanding of the difference between the LED and LEDL concepts. In this article, we discuss not only LED properties and durability, but also LEDL service life as a whole.

The service life of a luminaire with a traditional light source is the time of its operation to the moment of catastrophic failure, i.e. a full termination of the operation, for example, because of burnout of the light source or ballast malfunction. Relative to LEDLs, we apply the concept of parametric failure because burnout of the light source in a LEDL is rarely considered. When it is said that service life of a white LED, is 50 thousand hours according to the *L70* level, it means that after this period, the LED continues to function, but its luminous flux becomes less than 70% of the rated (initial) luminous flux. In other words, designers of a lighting installation (LI) should know, how long the LEDL produce a high enough proportion of its rated (initial) luminous flux, rather than how much time needs to pass until the light source fails. Incidentally, some LED manufacturers today refer not to the standard level of 70% as the design level, but higher performance thresholds of 80% or even 90% (Fig. 1).

There is a reason for this: if the designer calculates the illumination level for the LI service life

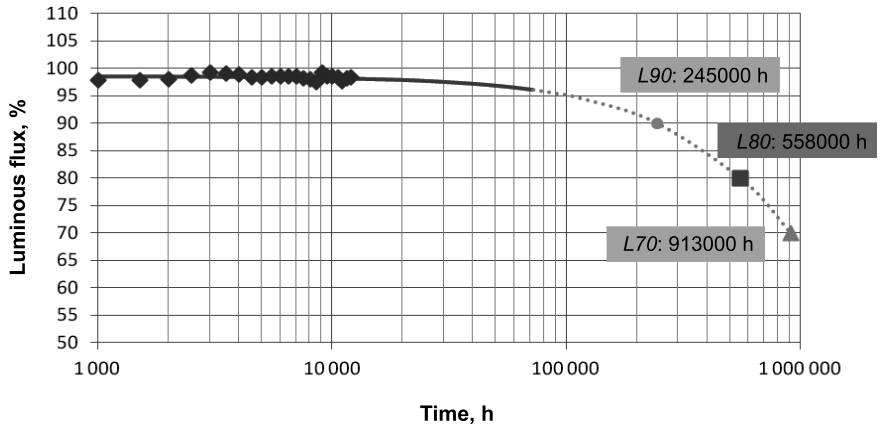

Fig. 1. Evaluation of a luminaire's service life by the decrease in luminous flux

end, he/she should provide for an illuminance reserve from the very beginning. Therefore, when calculating in accordance with the *L70* level, the initial reserve should amount to (100/70–1) = 0.428, i.e. about 43% of the required illuminance (Fig. 2). And when computing in accordance with the *L90* level, the reserve of (100/90–1) = 0.111, i.e. 11% only is enough.

Therefore, the simple application of criterion *L90* reduces the necessary initial illuminance reserve (luminous flux) by 32% (from 43 to 11%) and accordingly reduces the LI assurance factor (and consequently, the cost and the power). This is an interesting "secondary" effect [1].

However, let us return to LEDL service life. The period, during which degradation (decrease) of LEDL luminous flux doesn't exceed a threshold value is generally considered to be the LEDL's service life. It is known that the most significant indicators determining service life (degradation speed) of any LED is temperature and the current density of its crystal. Both parameters have clear upper limitations caused by the LED production technology[1]. There are also limitations of the combination of these factors, i.e. the speed of luminous flux decrease depends on a combination of temperature and current density of the crystal.

In 2008, the North American Illuminating Engineering Society (*IES*) offered a generalised measurement technique of luminous flux for discrete LEDs, LED matrices and separate LED modules: *LM-80–08* [2]; today it is the generally accepted method for measuring dynamics decrease and luminous flux values. The *LM-80* technique requires the manufacturer to submit data for a measurement period of at

[1] For example, the maximum regulated working temperature of a crystal manufactured on a silicon or sapphire substrate, as a rule does not exceed 125–135^{0}C, and the temperature of the crystal manufactured on a carbide-silicon substrate can reach 150^{0}C.

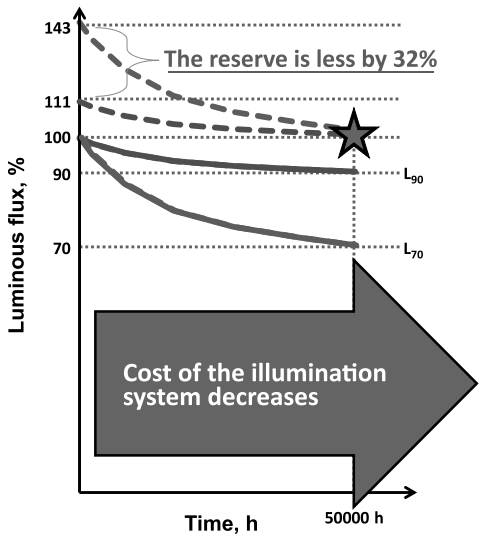

- Two LED luminaires, one with L_{70} evaluation, another with L_{90} for 50,000 h
- When designing, illuminance for the service life end is calculated
- The choice of LEDs with L90 requires less light emitting diodes by 32%, less optics, less aluminium and less power

Fig. 2. Comparison of luminaires with different criteria of service life evaluation

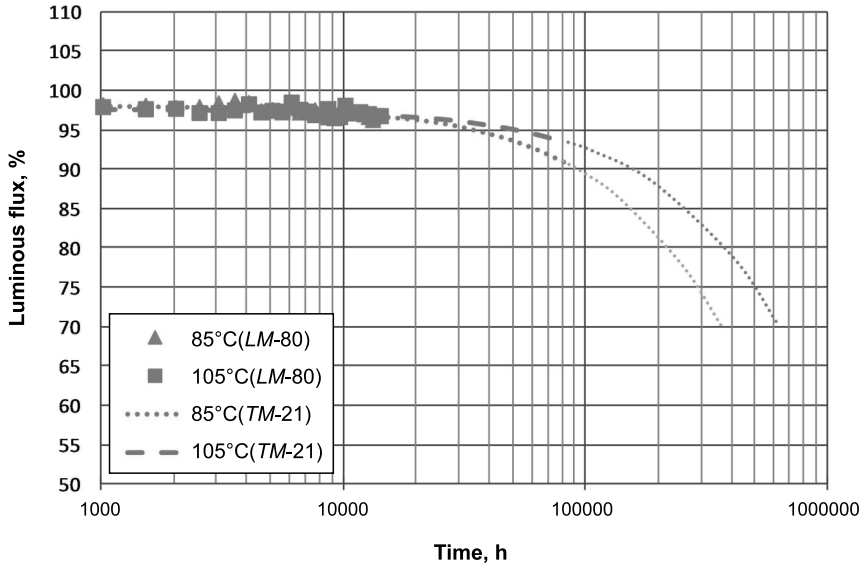

Fig. 3. A diagram of luminous flux reduction from measurement results in accordance with LM-80; extrapolation and service life forecast in accordance with TM-21

least 6000 h, and preferably, no less than 10000 h. Measurements are performed with several values of the LED current and with regulated temperatures in the soldering point (at the LED lead): 55, 85ºC and with a temperature selected by the LED manufacturer, for example, 105ºC. In parallel with this, *IES* has also proposed measurement techniques of luminous flux, input power, luminance distribution and LEDL chromaticity coordinates (CC): *LM-79–08* [3]. However, using these methods, only the fact of change (decrease, degradation) can be noted in lighting parameters of LEDs or their products at the moment of measurement, whereas we actually need an authentic forecast of luminous flux decrease to determine service life according to the selected *L70, L80* or *L90* levels. To determine the service life, a method of forecasting luminous flux change over time was developed by means of processing mathematical data obtained in accordance with *LM-80–08*: TM-21–11 method [4, 5]. Later experimental data provide a more exact extrapolation than earlier data. Therefore, with the availability of data for 6000–10000 h of the measurement, the data for the last 5000 h are used for the calculation, and in case of longer measurements, the data used are obtained during a later measurement period. Hence, the standard which regulates service life of LEDs, LED-matrices or separate LED modules cannot exceed a six fold duration of these measurements[2]. It should be

[2] For example, for *Cree* LEDs of *XP-G2* series, there are data in accordance with Fig. 3 obtained during 14112 h in the measurement process under the *LM-80* standard with 500mA current and temperature in the soldering point T_{sp} = 105ºC. The

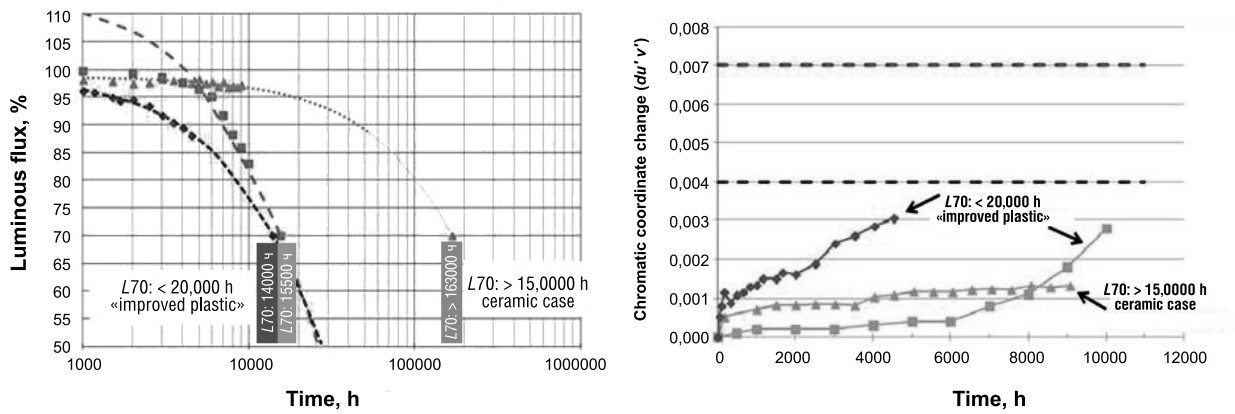

Fig. 4. Dynamics of luminous flux decrease and drift of chromaticity coordinates with temperature in the soldering point T_{sp}=105ºC

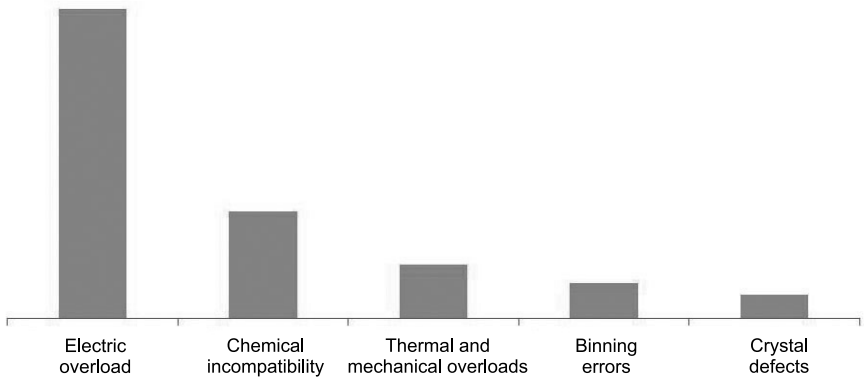

Fig. 5. Distribution of failure causes of light emitting diodes in luminaires

taken into consideration that with different combinations of the crystal current and temperature, different service lives are obtained.

Luminous flux decrease is certainly not the only criterion determining LEDL failure. The second important criterion is chromaticity coordinates (CC) (coordinates namely, not the correlated chromatic temperature). It appears that CC also depends on current, temperature and time. This type of failure is much more perceptible, because human sensitivity to colour is much more acute than to luminance. The *LM-80* also prescribes CC measurement of LEDs, LED matrices and separate LED modules (but not LEDLs as a whole) during a minimum of 6000 h. However, the technique says nothing either about an admissible CC change, or about extrapolation of the measurement results. It appears that the only international standard regulating admissible CC change is *Energy Star*® [7]. It states that CC should not change more than by 0.007 (i.e. within the seven-step McAdam's ellipse[3]) during 6000 h. This standard is probably acceptable as a foundation, but for high-quality light, a more strict regulation is needed since the service life of modern LEDs is much more than 6000 h. When developing criteria of LED service life evaluation, it should be notes that most people do not notice a change in CC within two- or three-steps McAdam's ellipse (i.e. CC change by 0.002–0.003) [8].

We have determined what should be considered as LED failure and what data should be submitted by the LED manufacturer to confirm the declared service life. The LEDL manufacturer should clearly understand, in what temperature mode their products will operate and what will be the temperature in the soldering point (i.e. in the contact point of the LED with the printed-circuit board), etc. This is very important, because luminous flux decrease and CC displacement at a high temperature strongly depend on the technology of crystal production and on the LED casing material. For example, LEDs with a plastic case, even using improved plastic, do not maintain high temperatures for a long time: the LED case material changes its light-reflecting power, and the LED luminous flux at a high crystal temperature can decrease for 15000–16000 h, and CC can exceed the bounds of the two-step McAdam's ellipse (Fig. 4). One can find a method of the temperature measurement in the soldering point, for example, here: www.cree.com/xlamp_app_notes/solder_point_temp.

However, this is not the whole story: even whilst having a set of the LM-80 and LM-79 photometric characteristics and knowing the LED average current and temperature, we still cannot confidently predict the LED service life of a LEDL. The fact is that LED failure can be caused not only by a disturbance of the temperature mode. Even if the thermal mode is normal, there is still a considerable number of factors, which can influence LED service life. As it can be seen from Fig. 5, apart from temperature mode, overwhelmingly the greatest number of failures are caused by electrical overstress (*EOS*) [9]. This can be a pulse, the power of which exceeds an admissible maximum for the given LED and has a duration of 100–1000 ns, unlike electrostatic dis-

obtained design service life by *L90* level is more than 233000 h, but in accordance with *TM-21,* the manufacturer can declare service life in accordance with *L90* 77600 h only, i.e. only six times exceeding the measurement period (see the Table).

[3] It is generally assumed that the single-step McAdam's ellipse limits CC field on the CIE x-y chromatic diagram, in which human eye perceives colours being identical.

The McAdam's ellipse step corresponds to geometric average CC change *u ', v '* by 0,001 on the chromatic diagram *u '-v '*.

Table

A forecast of service life of the *Cree XP-G2* light emitting diodes with 500 mA current and temperatures in the soldering point T_{sp} = 85 and 105°*C*

Current	*Tsp*	Test duration	*α*	*β*	Calculated service life	Reported service life (h)		
						L90	L80	L70
500 mA	**85°C**	13,608 hrs	9.148E-07	0.9798	>245,000 hrs	**>81,600**	**>81,600**	**>81,600**
	105°C	14,112 hrs	5.271E-07	0.9762	>233,000 hrs	**>77,600**	**>77,600**	**>77,600**

charge, the duration of which is within the 10^{-3} – 10 ns limits. LED damages caused by an *EOS* can be both imperceptible, and catastrophic, i.e. they can lead to the LED full failure. When an *EOS* causes little damage but occurs repeatedly (for example if a LED control device (CD) periodically generates short current pulses), the LED becomes unfit for use in due course. *EOS* reasons are as follows: transient processes, low voltage of breakdown of the printed-circuit board or CD, topology errors of the printed-circuit board or of LEDL arrangement, etc. LED failure probability due to *EOS* is strongly dependent on temperature.

One more common cause of LED failure is chemical incompatibility. More often LEDs are used with secondary optics or tightly closed by a cover, and in such cases some material (glue or gasket) is applied to provide tightness and/or fixation of the optics and of the protection cover. When heating during the operation, this material can give off fumes, creating the probability of a reaction with the silicone, phosphor, and in the case of LED, these substances can change the properties of the LED, which could cause a decrease of luminous flux and CC change. If LEDs with plastic cases or containing silver conductors are used in LEDLs affected by corrosion gases, in particular by sulphurous ones, such LEDs also degrade much faster (by luminous flux, and by CC) than the LEDs with ceramic substrate cases.

A widespread reason of a premature LED failure is damage when mounting on the printed-circuit board or in the process of subsequent operations with soldered LED-modules.

Besides LED failure or degradation, one shouldn't forget that the optics used, the diffuser or the protection cover (protection glass), can in due course also change their optical and physical properties, which inevitably influences the LEDL lighting parameters.

When estimating LEDL service life, it is necessary consider all of the parameters influencing both LED degradation, and service life of the LEDL as a whole. For this reason, it is important to know LED and CD temperatures (especially of electrolytic capacitors – the "weakest link" in the CD structure), and estimate LED temperature mode, considering working current and available data in accordance with *TM-21–11*. It follows that obligatory checks of the process and of the soldering quality, as well as of chemical compatibility of the used substances, heat-conducting materials and glues are necessary. Certainly, the use of LEDs with plastic cases should be treated with caution, especially if it concerns street or industrial LEDLs. It is also necessary to check the data on LEDL CD input voltage interval, because the wider the voltage interval, the bigger network voltage oscillations will cause LEDL instability. Anti-lightning protection should be checked according to the *EN61000–4–5*. A protection against short-term voltage pulses up to 6 kV and higher is recommended. Data on CD service life in the temperature mode, in which it works in a given LEDL are also necessary. It is necessary to carry out tests for "hot switching on", breakdown of CD, printed-circuit board and LEDL, as well as to measure start-up current and to analyse LI transient processes. Crucially, the data on the CD parameters should be confirmed by the test reports. In some cases, independent tests of LEDL samples are expedient in professional test laboratories and centres. Quite detailed recommendations for reliable LEDLs to be selected are given in publication [10].

CONCLUSIONS

The real service life both for LEDs and LEDLs depends on many factors. It is entirely possible that an LEDL consumer will not carry out a careful check or demand all the necessary documents confirming the declared reliability and durability. But manufacturers and sellers of lighting products with LEDs need to keep all that in mind and to follow the rec-

ommendations, at least so as to provide warranty for their products and to make power-service contracts with a confidence in generating profit.

REFERENCES:

1. Degradation of light emitting diodes. Connection between service conditions, real and predicted service life / A report at an open discussion of the Lighting Trade Association. URL: http://www.lta.ru/images/Presentations/%D0%A1%D0%A2%D0%90_%D0%BA%D1%80%D1%83%D0%B3%D0%BB%D1%8B%D0%B9_%D1%81%D1%82%D0%BE%D0%BB_2014–11.pdf (Addressing date: 02.04.2015).

2. Approved Method: Measuring Lumen Maintenance of LED Light Sources* + Addendum A. URL: http://www.ies.org/store/product/approved-method-measuring-lumen-maintenance-of-led-light-sources-1096.cfm (Addressing date: 02.04.2015).

3. Approved Method: Electrical and Photometric Measurements of Solid-State Lighting Products. URL: http://www.ies.org/store/product/approved-method-electrical-and-photometric-measurements-of-solidstate-lighting-products-1095.cfm (Addressing date: 02.04.2015).

4. Projecting Long Term Lumen Maintenance of LED Light Sources + Addendum. URL: http://www.ies.org/store/product/projecting-long-term-lumen-maintenance-of-led-light-sources-1253.cfm (Addressing date: 02.04.2015).

5. The elusive "life" of LEDs: How TM-21 contributes to the solution. URL: http://www.ledsmagazine.com/articles/2012/11/the-elusive-life-of-leds-how-tm-21-contributes-to-the-solution-magazine.html (Addressing date: 02.04.2015).

6. Cree XLamp Long-Term Lumen Maintenance. URL: http://www.cree.com/xlamp_app_notes/lumen_maintenance (Addressing date: 02.04.2015).

7. ENERGY STAR Luminaires Final Draft Version 1.0 Specification. URL: http://www.energystar.gov/sites/default/files/specs//Luminaires_V1_0_Final_Draft%20_Specification.pdf (Addressing date: 02.04.2015).

8. Color Maintenance of LEDs in Laboratory and Field Applications. URL: http://apps1.eere.energy.gov/buildings/publications/pdfs/ssl/2013_gateway_color-maintenance.pdf (Addressing date: 02.04.2015).

9. Analysis on Failure Modes and Mechanisms of LED. URL: http://www.csaa.org.cn/uploads/xiazai/lwj/ICRMS'2009/section_09/09–15.pdf (Addressing date: 02.04.2015).

10. The communique by results of the second Round Table of the Lighting Trade Association (LTA) of 13.11.2014. URL: http://www.lta.ru/index.php/novosti/46-communice-2014 (Addressing date: 02.04.2015).

Dmitry Yu. Yurovskikh,
a test engineer. Graduated from the MAI in 1996. A regional sales manager of Cree Hong Kong Limited Representative Office, Moscow

Light & Engineering
Vol. 23, No. 4, pp. 75-80, 2015

Svetotekhnika
No. 5, 2015, pp. 23-27

NEXT GENERATION GONIOPHOTOMETRY

Jürgen P. Weißhaar

Opsira GmbH, Weingarten, Germany
E-mail: weisshaar@opsira.de

ABSTRACT

In these times of steadily reduced product life times and a rapidly changing choice of available light source it is mandatory to be able to measure the photometric and colorimetric properties of sources and luminaires in an effective, quick and precise way. Modern approaches in computer aided optics design of luminaires demand high-grade measurement data of the sources very early in the development process to support a design of the lighting systems that's efficient and close to reality.

Manufacturers of sources as well as luminaire makers and vendors need to obtain these information quickly, easily and efficiently. The new approach described in this paper, the next generation goniophotometry, combines the advantages of various conventional goniophotometer methods, comprising much more flexibility, multiple functions and a top of the line precision in only one single device.

Keywords: goniophotometer, light source, luminaire, robogonio, CA – computer aided, DUT – device under test, LID – luminous intensity distribution, CHMSL – central high mounted stop lamp

1. INTRODUCTION

The use of goniophotometers has always been a fundamental measuring method in lighting technology. They have been used for photometric measurements of sources or lumiaires for almost 100 years now.

At the beginning, but also until today, the basic approach with a goniophotometer is the measurement of the angular dependant luminous intensity distribution (LID) of the device under test (DUT), e.g. a luminaire. The detector is a simple photometer measuring in the far field of the DUT.

Forced by the development of steadily more complex as well as more compact lighting systems, but also driven by the use of high performance optics design software packages running on powerful computers, the goniophotometer applications diversified.

This paper introduces a worldwide new technology of using one single device to derive the data of the sources as a seed for the optics design process as well as to perform all the necessary measurements on the resulting products (luminaires, head lamps, signal lamps, etc.) to obtain the well known luminous intensity distribution and much more.

One of the various applications of this goniophotometer approach is the creation of polychromatic ray files to enable the optics engineer to perform optics simulations that are very close to reality in due consideration of the emission angle dependant spectral power distribution of the sources.

2. GONIOPHOTOMETER OVERVIEW

Traditionally goniophotometers are distinguished in their way how the mutliple rotation axes are linked together as well as how the DUT is rotated in space during a measurement. The different setups are well known and defined in the standards DIN5032–1, DIN EN13032–1, CIE70 or CIE121. These standards categorize the different types in classes ranging from 1, x. 2.x, 3.x up to type 4. Without explaining all of the different types in detail in this paper, let's have a closer look to three very common setups.

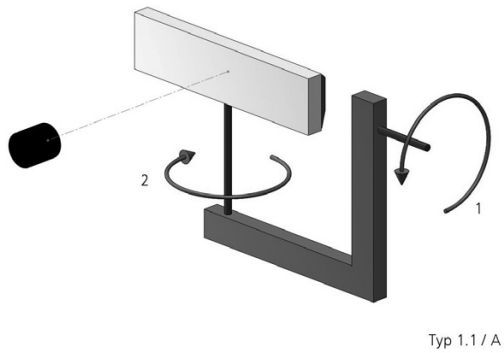

Fig. 1. Goniophotometer type 1.1

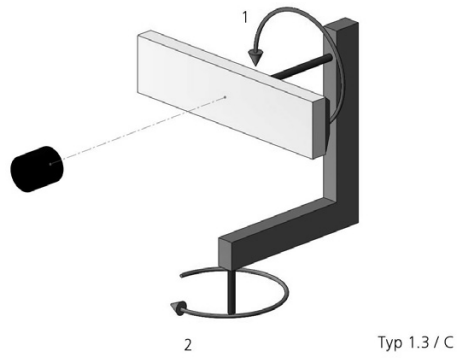

Fig.2. Goniophotometer type 1.3

Goniophotometer type 1.1, type A

This goniophotometer type uses a horizontal axis that is fixed in space (zenith axis with arrow 1) and a rotated "vertical" axis (azimuth axis with arrow 2). The detector/photometer is shown as a black cylinder. In a real setup measuring the far field distribution it is mounted at a much larger distance to the DUT than is shown in the Fig. 1.

The second axis is swivelling around the first axis and thus doesn't keep its vertical position.

This is, for example, the common way for the goniophotometric measurement of automotive head lamps. The resulting measurement coordinates and values are located around the equator of the corresponding polar coordinate system. The pole of this polar coordinate sytem points in the direction of axis 2.

Goniophotometer type 1.3, type C

This goniophotometer type (Fig. 2) uses a vertical axis that is fixed in space (zenith axis with arrow 2) and a rotated horizontal axis (azimuth axis with arrow 1). The detector is shown as a black cylinder again.

The second axis is swivelling around the first axis.

This is for example the common way for the goniophotometric measurement of general lighting luminaires. The resulting measurement coordinates and values are located around pole of the corresponding polar coordinate system. The pole of this polar coordinate sytem points in the direction of axis 1.

Goniophotometer type 3.1, type C

This goniophotometer type (Fig. 3) uses a mirror that rotates around a fixed horizontal axis (lower zenith axis 1 red arrow) and a second horizontal axis counterrotating with respect to the first axis. This second axis keeps the luminaire in the same operation position regarding the direction of gravity at all times. The first axis is co-linear with the optical axis of the photometer.

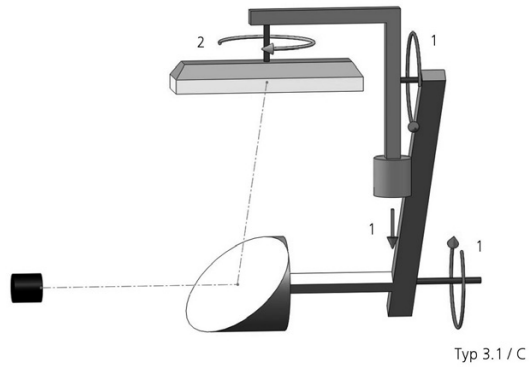

Fig. 3. Goniophotometer type 3.1

A third axis thus keeping its vertical position at all times too, rotates the DUT in different azimuthal positions (azimuth axis with arrow 2). The detector is shown as a black cylinder again.

This is again an example of a common way for the goniophotometric measurement of general lighting luminaires. The resulting measurement coordinates and values are located around pole of the corresponding polar coordinate system. The pole of this polar coordinate sytem points in the direction of axis 2.

The advantage of this approach is certainly that the DUT keeps its orientation with respect to the direction of gravity at all times during the measurement. However, a series of disadvantages like the fairly large mechanical structure, trouble with the mirror's flatness, spectral response and dustiness as well as very high system costs make this approach quite often unreasonable. Furthermore, the mirror method suffers from unpredictable and uncorrectable multi-interflexions of light between the luminaire and the mirror. Misreadings might occur.

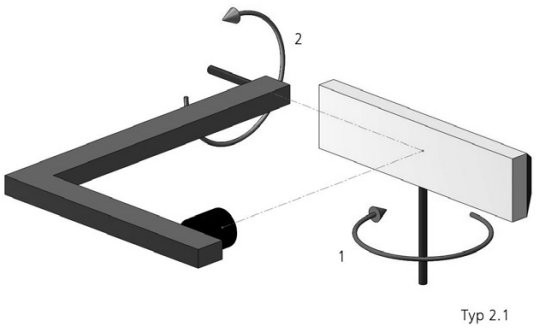

Fig. 4. Goniophotometer type 2.1

The mirror goniophotometer lost its importance even more because the influence to the photometric properties of the DUT due to an arbitrary rotation in space decreased tremendously with LED based lighting systems. Convential lighting systems, e.g. based on gas discharge sources, necessarily needed this kind of goniophotometer. LED based systems don't.

This trend is accomodated by recent standardization efforts, too. The fairly new European standard for the measurement of SSL driven systems, EN DIN13032–4, issued in 2013, explicitly states the arbitrary rotation of the SSL driven DUT during the goniophotometric measurement. Complex and expensive mirror systems are not needed anymore.

Near field vs. far field

Some decades ago a new application arose. So far, the different goniophotometer types mentioned before had been used almost solely in the far field. That means that the detector system (photometer) had been positioned in a reasonable distance to the DUT to reduce the geometrical error in the calculation of the luminous intensity in a range smaller than 1%. In the far field approach, the DUT itself is considered to be a point source without any extent.

The new goniophotometric method of measuring in the near field is motivated by two reasons:

- A demand for systems that are able to measure the luminous intensity distribution of even large DUTs in small space or small distance respectively, but still with a geometrical error small enough to receive reasonable results.
- A demand for much more detailed information about the DUTs. Not only the luminous intensity distribution coming from a virtual point in space, but also the space-resolved information about how and where the light is emitted from the DUT is of significant interest.

Fig. 5. Goniophotometer type "robogonio"

While the first application of near-field measurements generates the same information as the traditional far-field approach (the far-field luminous intensity distribution), the second reason is of larger importance.

By using the knowledge of the spatially-resolved emission all around a light source, detailed ray files can be derived for the use in optics design software packages to achieve close to reality simulation results. One typical setup for a near-field goniophotometer is the type 2.1 gonio (Fig. 4).

The DUT (light source or luminaire) is rotated about a vertical axis that is fixed in space (azimuth axis with arrow 1) and the detector is rotated about a fixed horizontal axis (zenith axis with arrow 2). Contrary to the two setups described before, the axes are not coupled in this goniophotometer type.

A very important fact is that a standard photometer is not suffiicient for the spatially-resolved measurement. An imaging detector like a luminance camera is needed. The amount of data obtained is much higher than with a traditional goniophotometer.

Traditional Goniophotometer summary

In the last sections we see that there are multiple geometric constructions to realize a goniophotometric solution for different applications (e.g. automotive vs. general lighting). Further we see that different kinematic constructions are needed and used for far field and near field measurements.

Fig. 6. Robogonio in type 1.1 mode

Fig.7. Robogonio in type 1.3 mode

NEXT GENERATION GONIOPHOTOMETRY

Thinking about the aforementioned traditional goniophotometer systems, we see that all of them possess, regardless of their individual type, 1.1, 1.3 or 2.1, five or more axes of movement in total.

- At least two rotation axes for the rotational positioning of the DUT and/or the detector;
- Three translation axes for the translational positioning of the DUT to the rotation center of the goniophotometer (typically used for the adjustment before the measurement only).

Furthermore, we see that for different applications different mechanical or kinematic constructions are used; 1.1 for automotive, 1.3 for general lighting. Or in other words, nowadays several different machines are used to perform the different applications.

The fundamental new way of realizing goniophotometric measurements is the use of an industry robot to perform the necessary movements and rotations. With a total number of six rotation axes, this machine called "robogonio" is able to realize the mentioned coordinate systems easily in one machine; for far-field and for near-field applications (Fig. 5).

Industry robots have been used since quite a bit in production environments. Why didn't we see the robogonio way of doing goniophotometry much earlier?

For one thing, due to the strongly rising need of robots in the production field, mainly in automotive production, the number of robots produced per year rose tremendously and thus the price of the robots came into a range where it became very interesting for goniophotometer applications. Another reason is that the precision of the robots improved in the last decade to a level comparable or even better than the angular accuracy of the traditional goniophotometers.

A number of significant advantages are coming with this new way of accomplishing goniophotometry:

- Arbitrary coordinate systems, eg. 1.1 or 1.3 or type A or type C goniometer respectively, can be realized with one single machine now.
- The mechanical structure of an industry robot is amazingly stable and rigid with a very high reliability in comparison to the the traditional go-

Fig. 8. Robogonio running similar to type 2.1 mode

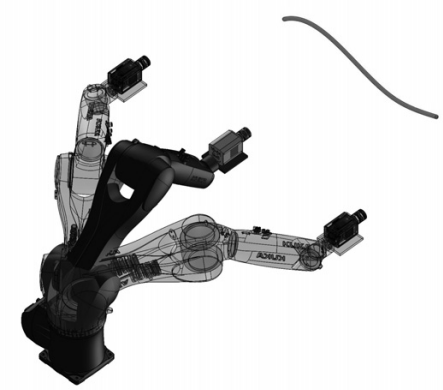

Fig. 9. Robogonio running in non-rotation mode

heating-up ready to measure measuring

Fig. 10. Robogonio's heating-up procedure

niophotometers produced in a comparably low volume only.

• Due to the flexibility of the robogonio axes, the center of rotation isn't fixed anymore and can be choosen arbitrarily in space.

• Multiple, even far distant pivot points can be realized easily in one measurement (e.g. different lighting functions of a complete car head lamp).

• The overall construction is much less restrictive for the measurement of large or long DUTs. As a result, the measurement of long luminaire structures can be preformed with the robogonio much easier (e.g. very wide CHMSLs).

• A large number of different robot sizes is available and thus robogonios starting at a payload of 6 kg up to a payload of more than 1000 kg are available.

• Quite fast measurements are possible. A complete 2 π LID with high resolution can be measured in about 2 minutes.

• The standard DIN EN13032–4 requests heating up the SSL lighting fixtures in standard working orientation (typically vertically downwards in most general lighting applications) for at least 15 min before measurement. After the heating-up period, the fixture is oriented to point to the detector (typically horizontally). The robogonio is able to realize the heating-up position and the measurement position automatically in one run due to its axial flexibility. A traditional general lighting 1.3 goniophotometer isn't able to fulfil this DIN EN13032–4 request.

Furthermore, one robogonio machine can be used for near-field and for far-field measurements in one installation. This enables the optics or lighting engineer to gather detailed properties of the tested light sources as a seed to perform the optics design process as well as to measure the luminous intensity distribution of the resulting lighting system with only one device, regardless if a 1.1 gonio (automotive) or a 1.3 gonio (general lighting) is required!

The following Figs. 6–10 show the different goniophotometer rotations in the different applications.

Robogonio running in type 1.1 Mode, (type a mode)

Running in 1.1 mode, the robogonio executes exactly the same rotations like a standard 1.1 goniophotometer.

Due to the almost unconstrained mechanical structure very large or very wide DUTs can be mounted and measured on the goniophotometer. Bi- or omni-directional fixtures or multi-functional lighting systems with several light exit windows can be measured easily.

Robogonio running in type 1.3 Mode, (type a mode)

The same machine, running in 1.3 mode now, executes exactly the same rotations like a standard 1.3 goniophotometer.

Apparently the lighting system to test can be quite long due to the open non-restrictive mechanics.

Robogonio running in type 2.1 Mode, (source imaging mode)

In the source imaging mode for the creation of ray sets similar solid angle sections are desired for the measurement. The path of the robogonio is kind of a spherical meander to efficiently gather a high number of luminance measurements on a virtual sphere around the source.

Non-rotation applications

An application a traditional goniophotometer isn't able to do at all is the motion along an arbitrary path in space. More and more we see elongated and

thin light pipes used for various lighting applications in different markets. The luminance of these structures have to be tested during development and even more during production control.

The robogonio together with a luminance camera can easily follow the light pipes's path in space to perform this measurement quickly with high spatial resolution. Due to the flexibility of the machine, the geometrical test sequence can be modified very easily for different geometries to be tested.

Heating-up according to DIN EN13032–4

The following figures display how the robogonio can position the lighting system in its standard burning/operating position for the heating-up period (downwards in this example). The changes in the photometric performance are monitored during the heating-up period with an auxiliary photometer.

After the heating-up period is finished, the robogonio directs the lighting system towards the photometer with its typical horizontal axis. Changes in the photometric performance due to the change of orientation are corrected by using the auxiliary photometer. Now the goniophotometric measurement with the heated-up DUT can run. Again, according 13032–4, an auxiliary photometer is monitoring for eventual changes in the photometric performance due to the arbitrary rotation of the DUT.

2.3. CONCLUSION

This paper introduces a fundamentally new way of performing goniophotometric measurements in a much more flexible way than before. The described technology can be used in various different lighting markets. A robot-based goniophotometer is a valuable device during the complete process from optics development up to the production control of lighting systems. The same machine gathers very detailed data of the sources at the beginning of the process and delivers accurate data of the designed lighting systems after production.

All these benefits come with a top of the line angular accuracy and a high end measurement speed to a very competitive price.

The next generation goniophotometer.

REFERENCES

1. R. Baer, D. Gall, "Grundlagen Beleuchtungstechnik", Huss-Medien GmbH, 2006.

2. DIN5032–1 Lichtmessung – Teil 1: Photometrische Verfahren, 1999.

3. DIN EN13032–1 Licht und Beleuchtung – Messung und Darstellung photometrischer Daten von Lampen und Leuchten – Teil 1: Messung und Datenformat, 2004.

4. CIE70 The measurement of absolute luminous intensity distributions, 1987.

5. CIE121 The photometry and goniophotometry of luminairs, 1996.

6. V. Schumacher, J. Weißhaar, F. Potekev, "Lichtquellenmodelierung für optische Simulation", Photonik 1/2001.

7. D. Hansen, "Messung und Simulation polychromatischer Strahlendaten", Automobiltechnische Zeitung 11, 868–873, 2012.

8. TÜV Fahrzeug – Lichttechnik GmbH, TÜV Rheinland, Technical Report No. 5356066, opsira robogonio, 2013.

9. DIN EN13032–4 – Licht und Beleuchtung – Messung und Darstellung photometrischer Daten von Lampen und Leuchten – Teil 4: LED-Lampen, – Module und -Leuchten; Deutsche Fassung prEN13032–4:2013.

Jürgen P. Weißhaar,
Dipl. – Ing., General Manager, opsira GmbH, 88250 Weingarten, Germany. In1993, graduation at the University of Applied Sciences, Ravensburg-Weingarten, final degree: Dipl. – Ing. (FH) Physical Science and Technology. In 1999 he founded the Opsira GmbH and has been General Manager since. His further qualifications: Technical Expert of Illumination acc. to BGG 917.
Official Expert and Consultant of lighting techniques and photometry. Visiting Lecturer for lighting and illumination engineering at the University of Applied Science, Isny/Germany since 2007. Visiting Lecturer for lighting engineering at the University of Applied Science, Ravensburg-Weingarten/Germany since 2008

Light & Engineering
Vol. 23, No. 4, pp. 81-87, 2015

Svetotekhnika
No. 6, 2015, pp. 17-20

EXPERIMENTAL RESEARCH ON THE PERFORMANCE OF OPTICAL MINISTICKS WITH A COMMON RECEIVER

Sergey A. Golubin[1,2], Alexei N. Lomanov[1], Vladimir S. Nikitin[1], and Valery M. Komarov[1]

[1]P.A. Solovyov Rybinsk State Aviation Technical University
[2]CEO&founder of Tenzosensor LLC
E-mails: 707gsa@mail.ru; lepss@yandex.ru; 505z@mail.ru; vs@rsatu.ru

ABSTRACTS

The paper proposes a design for a digital optical ministick on the basis of an elastodeformed polymeric element and a common receiver optical scheme. The paper describes the structure and principle of operation for an optical ministick and its advantages compared with traditional switching devices. Experimental research was carried out in order to determine the performance characteristics of the designed ministicks.

Keywords: digital ministick, elastic deformation, control system, photodiode, semiconductor laser, microcontroller

Various input devices are used to manipulate objects in aviation and robotics, portable electronic devices, 3D modelling and videogames: keyboards, mice, joysticks, trackballs, touch panels and touch screens. Ministicks are two-axis micro joysticks acting as input devices. The difference between ministicks and joysticks is that the former can be operated with fingers only. That allows the operator to use several ministicks to manipulate objects with many degrees of freedom.

Most of the existing ministicks are based on a resistive principle: deflection of a ministick's handle changes the resistance of sensing elements. Either potentiometers or resistive strips can serve as sen-

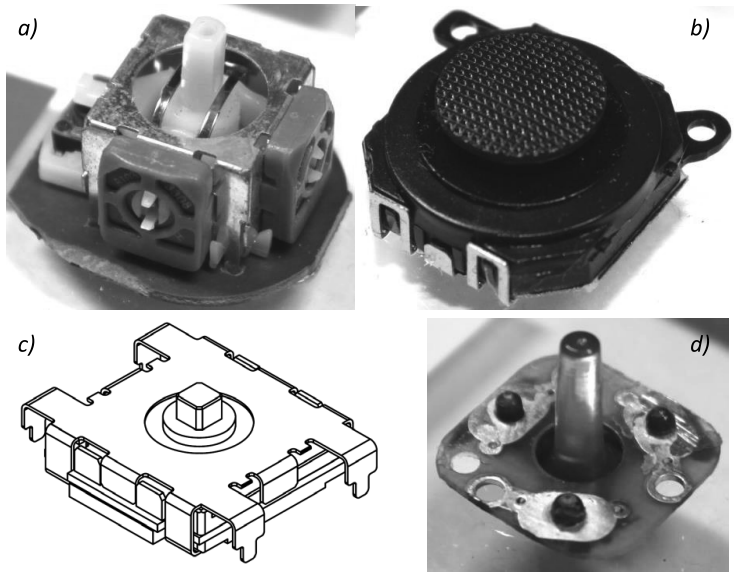

Fig.1. Ministicks: a) based on potentiometers, b) based on resistive strips, c) *EasyPoint EP*40–101, d) MD-14 based on polymer elastic deformation element

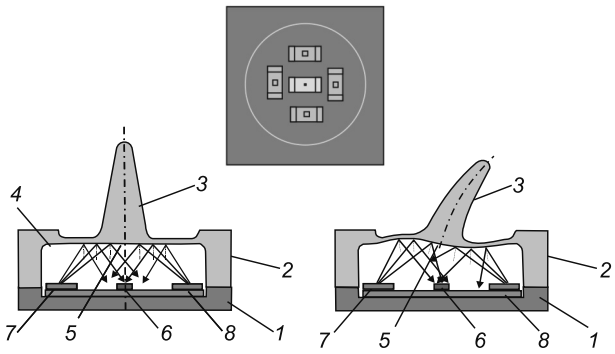

Fig.2. Schematic diagram of an optical ministick: 1 – circuit plate;
2 – body; 3 – handle; 4 – elastic deformation element,
5 – light-reflecting surface, 6 – photoelectric converter (photodiode, photoresistor); 7 – light source (light-emitting diode, laser)

sing elements. Such ministicks are difficult to produce as they consist of many parts (over 10). The performance of ministicks changes significantly as the resistive layer deteriorates.

Tenzosensor LLC developed the MD-14 resistive ministick based on polymer elastic deformation element with resisitve coating. This ministick consists of only a few parts. However, its endurance is not sufficiently high (200–300 thousand strokes).

There is also the *EasyPoint EP*40–101 ministick produced by *Austria Microsystems*, which is based on the Hall effect. The ministick has a highly linear performance and lasts for as many as 1 million deflections in each direction, but its high price prohibits the mass application of the device.

Fig. 1 shows the appearance of ministicks.

Tenzosensor LLC designed a digital optical ministick. Compared to existing ministicks, this device has the following advantages: simple design, mass production potential, high durability due to an absence of rubbing parts, low cost (< $1), low noise, fire and explosion safety, injury free operation, light weight, multi functionality (possible reprogramming).

Fig. 2 shows the schematic diagram of an optical ministick consisting of a body (2) positioned on a plate (1) and an elastic deformation element (4) integral with a handle (3). On the plate (1) under the elastic deformation element (4) there is a light receiver (photodiode, photoresistor) (6) and at least one light source (light-emitting diode, laser) (7) connected to a microprocessor. The elastic deformation element (4) in the form of a part made of elastic polymer material contains a light-reflecting and light-absorbing surface (5) positioned above the light source (7) and photoelectric converters (6). The elastic deformation element is made of elastic material in form of a plate with the handle (3) resting upon the elements of the body (2) of the optical ministick attached to the plate (1).

The optical ministick functions as follows: a light wave reflects from the light-reflecting surface of the polymer elastic deformation element, which is deformed by the handle depending on the pressed direction; light flux distribution is modulated from the light source to the light receivers.

In order to examine the dependence of the ministick's signals on the handle's linear deflection and the ministick's angular deflection (transfer function), an experimental device was created. Fig. 3 shows the flowchart of this device.

The ministick is positioned in the centre of a rotating platform that allows the rotation of the minis-

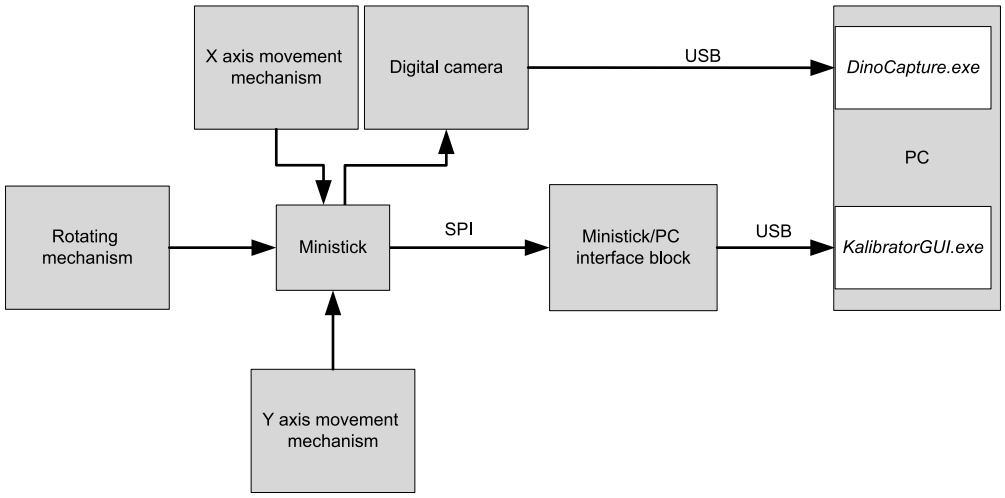

Fig.3. Experimental device flowchart

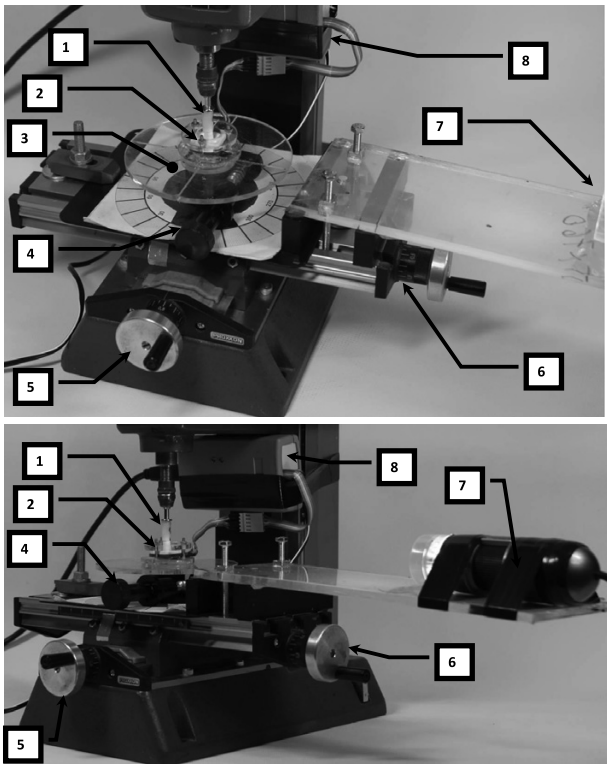

Fig.4. Photographs of the experimental device: 1 – ministick handle holding tool, 2 – ministick, 3 – rotating platform, 4 – rotating mechanism, 5 – X axis movement mechanism, 6 – Y axis movement mechanism, 7 – digital camera, 8 – ministick/PC interface block

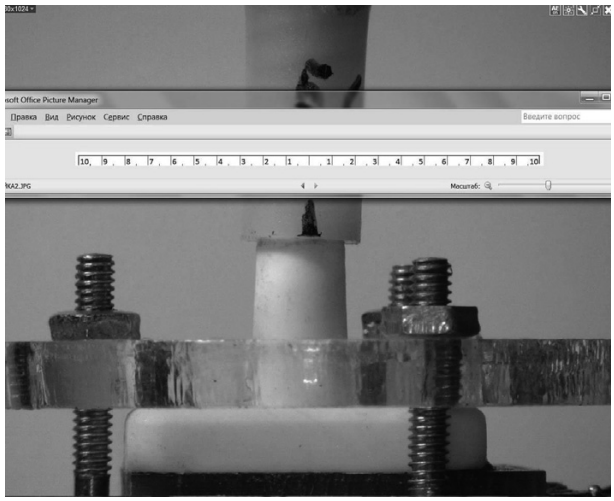

Fig.5. DinoCapture program

X axis deflection of the ministick's handle is monitored via a *Dino-LiteAD*413*TL–MA*1 digital camera, which transmits the image straight to a PC, and a *DinoCapture v*2.0 program. The camera follows the ministick's X axis movement. The deflection of the ministick's handle is measured visually using an on-screen ruler. See Fig.5 for the device program.

The ministick's readings are received via a *KalibratorGUI* program. The program allows for manual (Fig. 6) and automatic (Fig. 7) reading. In the manual mode, the program receives the ministick's readings when the user presses the button. The program issues a single or multiple requests (up to 10 iterations) at custom intervals – from 0.1 to 10 seconds. A reading request can be delayed for as long as 1 second – 5 minutes. The program can save read-

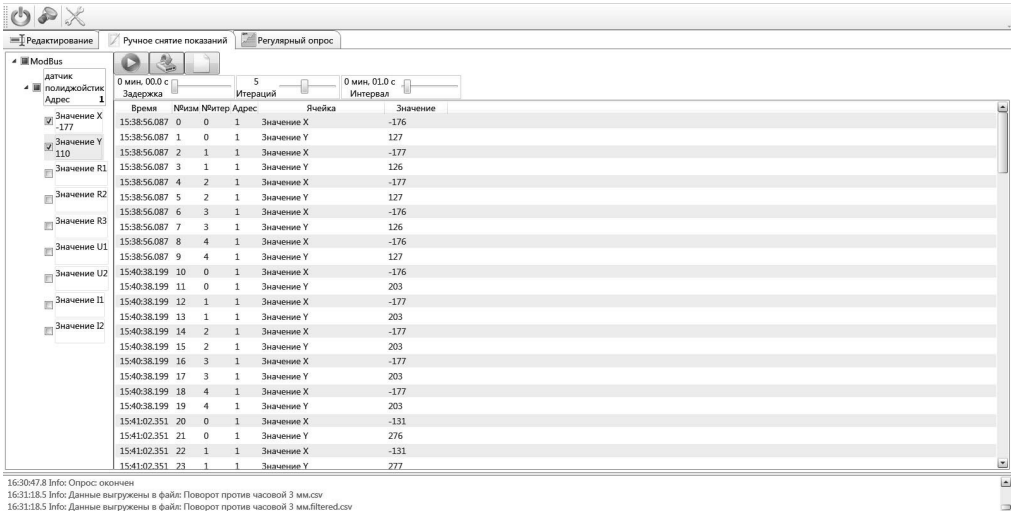

Fig.6. *KalibratorGUI* program in manual reading mode

tick against its centre. The ministick's handle has its loose end fixed in a holding tool. The platform has two mechanisms of movement: one for the X axis and the other for the Y axis, which deflect the handle of the ministick from the centre.

Fig. 4 shows the photographs of the experimental device.

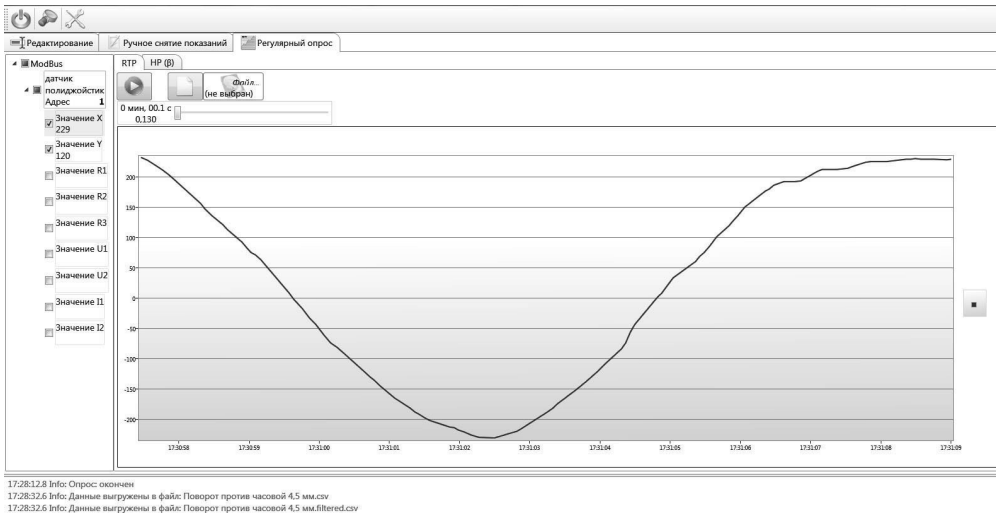

Fig.7. *KalibratorGUI* program in automatic reading mode

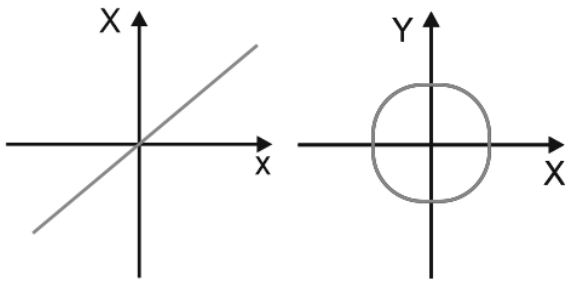

Fig.8. Ideal ministick dependence diagram: transfer function – X readings dependence on x handle deflection (left); radar chart of X and Y readings dependence on angular deflection (right)

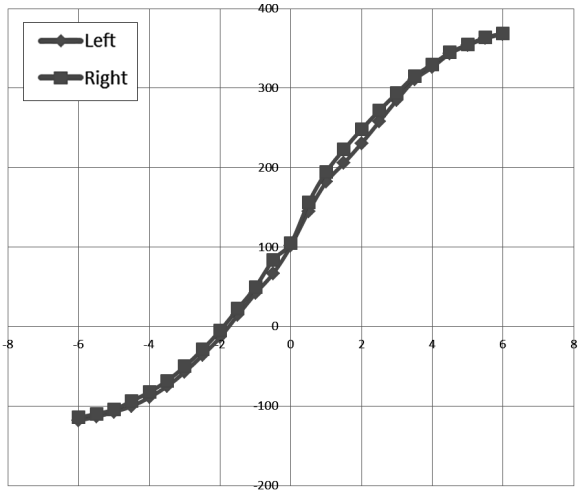

Fig.10. Measurement results for 90° angular deflection of the ministick (Y-coordinate)

ings as a **.csv* format file. In the automatic mode, the program regularly requests the ministick at 0.1–10 sec intervals. Readings can be saved automatically as a single file.

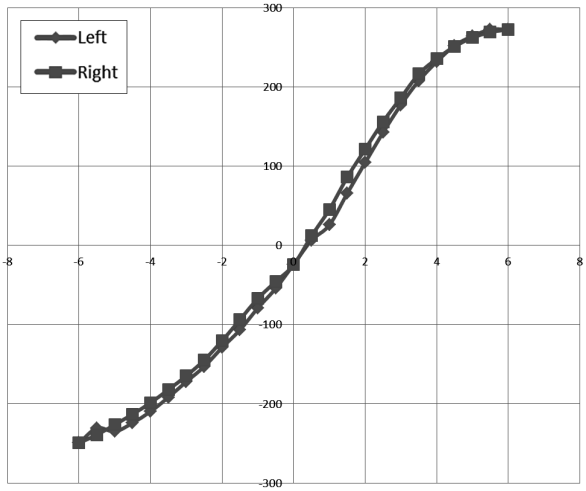

Fig.9. Measurement results for 0° angular deflection of the ministick (X-coordinate)

The goal of the experiment is to determine the dependence of the ministick's desired signal readings on the handle's linear deflection and the ministick's angular deflection.

Fig. 8 shows a theoretical dependence diagram for an ideal ministick. During the experiment, we determined how close the dependence of the desired signal of the ministick under investigation is to theoretical models.

The quality of the real ministick's desired signal is estimated by the following attributes:

a) precision – readings dispersion at certain handle deflection;

b) nonlinearity – curve deviation of the transfer function of the ministick under research from a straight line;

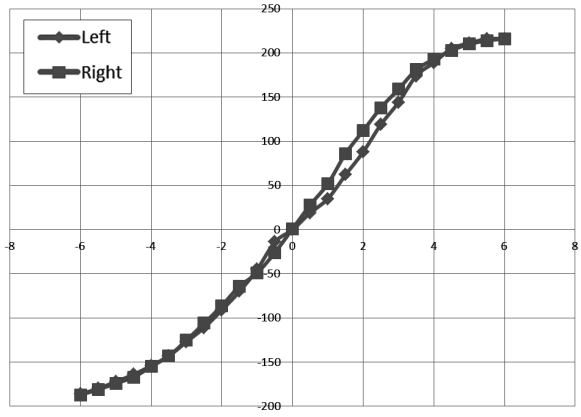

Fig.11. Measurement results for 45° angular deflection of the ministick (X-coordinate)

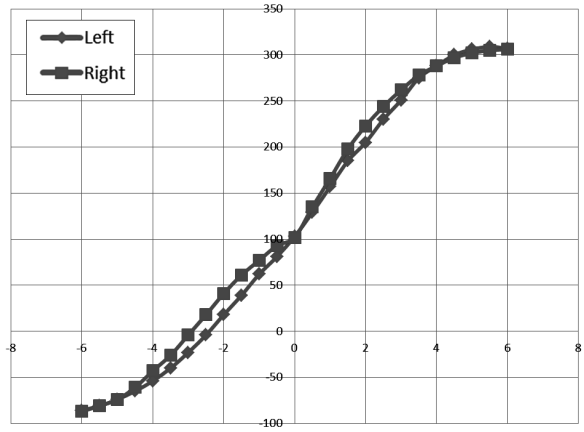

Fig.12. Measurement results for 45° angular deflection of the ministick (Y-coordinate)

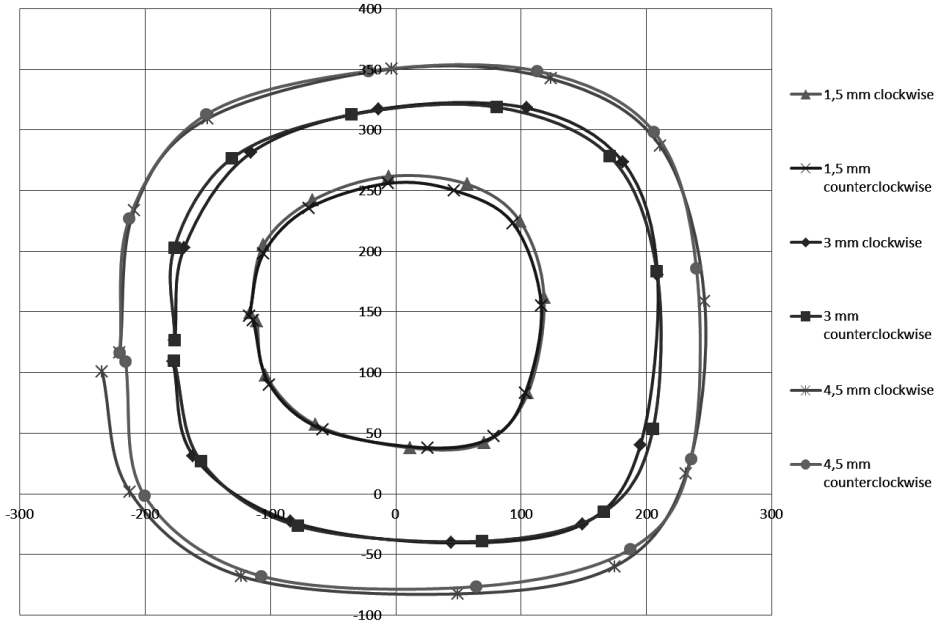

Fig.13. Readings measurement results with the ministick rotating at a constant handle deflection

c) hysteresis – output signal is different while handle deflection remains equal, but the direction changes.

During the experiment, the following *X* and *Y* readings of the ministick were measured:

a) readings at a constant angular deflection of the ministick and changing deflection of the handle;

b) readings at a constant deflection of the handle and changing angular deflection of the ministick;

Reading measurements at a constant angular deflection of the ministick and changeable deflection of the handle were performed under the following conditions:

a) maximum deflection of the ministick's handle from the centre: –6..+6 mm;

b) direction of the deflection: left (from +6 mm to –6 mm), right (from –6 mm to +6 mm);

c) angular deflection of the ministick: 0°, 45°, 90°;

d) number of readings measurement iterations: 3, with subsequent averaging of readings.

Fig. 9 shows measurement results for 0° angular deflection of the ministick, Fig. 10 – for 90° angular deflection, and Figs. 11 and 12 – for 45° angular deflection.

In order to evaluate the precision of readings, we used root-mean-square deviation (RMSD) value measured during reading iterations at a defined handle deflection. The relative value δ was calculated according to the formula

Table1. Parameters of the signal quality of the ministick under investigation

Attribute	0° angle, X-coordinate	90° angle, Y-coordinate	45° angle, X-coordinate	45° angle, Y-coordinate
Range of values	522	485	403	394
Max. deflection	35.36%	10.10%	141.42%	2.08%
Max. nonlinearity	9.52%	10.66%	9.64%	10.51%
Max. hysteresis	3.90%	3.65%	5.96%	5.84%

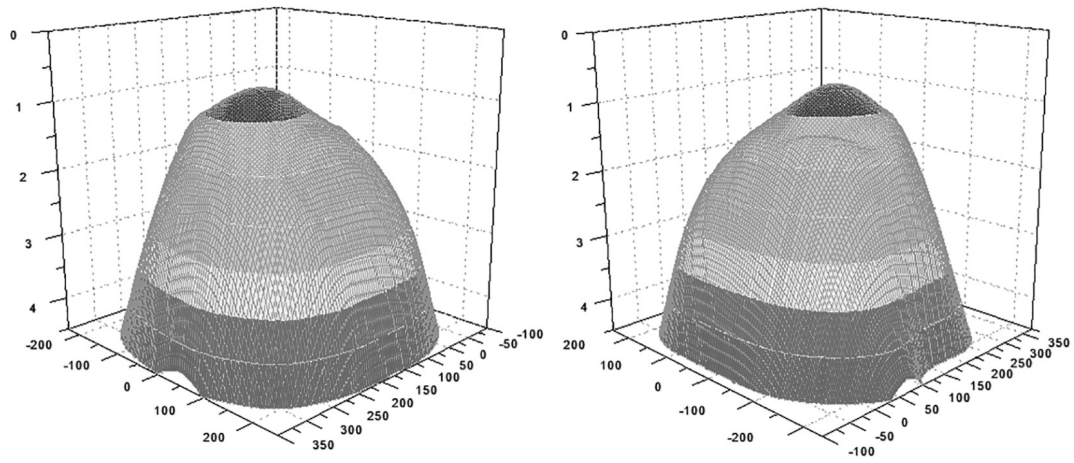

Fig.14. 3D surface plot of the dependence between the ministick's reading and the manipulator's deflection

$$\delta = |RMSD/Xav|, \quad (1)$$

where *Xav* is the average value at the defined point.

In order to evaluate nonlinearity using the least squares method (*MS Excel* LINEST() function), we built a straight line approximation function $X=kx+b$. N_L nonlinearity is then calculated according to the formula

$$N_L = |X - Xcalc|/\Delta X \quad (2)$$

where X is the real value of the coordinate at the defined point, Xcalc is calculated using an approximation function, ΔX is the range of transfer function values.

G hysteresis of the readings is evaluated according to the following formula:

$$G = |Xr - Xl|/Xav\ \Delta X, \quad (3)$$

where *Xr* is the parameter value at the defined point with the handle moving right, *Xl* is the parameter value at the defined point with the handle moving left, ΔX is the range of transfer function values.

Table 1 shows the calculation data.

Readings at a constant deflection of the handle and changing angular deflection of the ministick were measured in the following conditions:

a) angular deflection of the ministick: 0°..360° at a pitch of 30°;

b) rotation direction: clockwise (0°..360°), counterclockwise (360°..0°);

c) ministick's handle deflection from the centre: 1.5 mm; 3 mm; 4.5 mm;

d) number of readings measurement iterations: 5, with subsequent averaging of readings.

Fig. 13 shows measurement results in a radar chart. According to measurement results, a 3D surface plot was built that represents the dependence of *X* and *Y* readings on the handle's linear and angular deflection (see Fig. 14).

CONCLUSIONS:

1. The optical arrangement selected for a ministick based on elastic deformation element allows for functional and highly efficient devices.

2. Maximum deflection range for the ministick's handle is +/-6.0 mm, which suits the optimum amplitude range for fingers deflection (about 12–20 mm).

3. The transfer function of the ministick under investigation is linear and symmetric at the handle deflection range of –3..+3 mm. Readings curves become exponential at large deflections.

4. The ministick's dead zone does not exceed 0.5 mm across all coordinates.

5. Maximum hysteresis value is 5.96% of the range of transfer function values. Maximum hysteresis is observed at 45° angular deflection.

Thus, the transfer function of an optical ministick meets the requirements for complex robotics, manipulators and aircraft control tools. The ministick's design needs further refinement in order to improve precision, decrease nonlinearity and readings hysteresis.

Applied research and experimental development were conducted with financial support from the Ministry of Education and Science of the Russian Federation. Unique identifier of applied research and experimental development is RFMEFI57914X0087.

REFERENCES:

1. Golubin, S., Lomanov A., Nikitin V., Komarov V. Experimental research on the performance of optical ministicks with a common emitter. Wschodnie partnerstwo – 2015, 2015. Volume 4, pp. 41–51, DOI 10.17686/rusnauka_2015–200541.

2. Golubin, S., Lomanov A., Nikitin V. New optical ministicks to control robotic systems and aircrafts. Wschodnie partnerstwo – 2015, 2015. Volume 4, pp. 71–83, DOI 10.17686/rusnauka_2015–200543.

Sergey A. Golubin, post-graduate of Federal State-Financed Educational Institution of Higher Professional Education «P. A. Solovyov Rybinsk State Aviation Technical University» (RSATU). He is graduated from RSATU in 2013. At present, he is a systems engineer in Tenzosensor LLC

Aleksey N. Lomanov, Ph.D. and associate professor in Federal State-Financed Educational Institution of Higher Professional Education (RSATU). He is graduated from Rybinsk State Aviation Technological Academy (now RSATU) in 2003. He has much experience in electrical engineering, microcontroller systems, industrial control and thin-film technologies, works in RSATU since 2003. At present he is the dean of Faculty of radioelectronics and computer science

Vladimir S. Nikitin, Ph.D. and CEO&founder of Tenzosensor LLC. Inventor and idea man, leading expert in the field of R&D organization and performance, strategy development, organization of project team work. Miscellaneous expert in the field of Physics, Chemistry, Electronics, Material Sciences, highly qualified designer and programmer, possesses a great experience of working at executive positions. He has 24 patents, 5 certificates for PC software products, 100+ published works in scientific and popular editions; author of the book Technologies of the Future (Tekhnosfera publishing house, 2010)

Valery M. Komarov, Ph.D. and full professor of Federal State-Financed Educational Institution of Higher Professional Education «P. A. Solovyov Rybinsk State Aviation Technical University» (RSATU). Graduated from Rybinsk Aviation Technological Institute (now RSATU) in 1972, got an academic degree in 1980. He has more than 40 years' experience in designing microprocessor systems and technological control systems. Works in RSATU from 1977. He has 49 author's certificates, 60+ published works

Light & Engineering
Vol. 23, No. 4, pp. 88-90, 2015

Svetotekhnika
No. 1, 2016

APPLICATION OF ADDITIVE TECHNOLOGIES IN THE MANUFACTURE OF FIBER OPTIC SPLITTERS

Alexei N. Lomanov*, Vladimir S. Nikitin, Alexander V. Solostin[1],
Ernst I. Semyonov*, and Sergei V. Chayka

NTZ Introfizika LLC, Russia, Yroslavl Region, Rybinsk
[*]Rybinsk State Aviation Technical University (RSATU), Russia, Yaroslavl Region, Rybinsk
[1]E-mail: 21solo@mail.ru

ABSTRACT

Optical splitters are widely used in various lighting equipment, illumination and information systems, fiber-optic sensors, and multi-channel smart link connections. Traditionally, optical splitters are based on beam splitting cubes with precision coating and lenses, which determines their complexity and cost. NTZ Introfizika LLC developed a fiber optic splitter without the elements listed above, one that can be manufactured using additive technologies.

Keywords: optical splitter, light output, optical fiber, laser stereolithography, fused deposition modeling

INTRODUCTION

NTZ Introfizika LLC is currently developing multi-channel optical splitters utilizing 3D printing technology. The use of modern 3D prototyping technologies and polymer optical fibers as a filament for 3D printers allows the manufacture of high-quality optical details that do not require complex technological operations in terms of production and adjustment.

MULTI-CHANNEL OPTICAL SPLITTER

Fig. 1 shows a diagram of a multi-channel optical splitter (Application for an Invention No. 2015118753, May 19, 2015) [1].

A multi-channel optical splitter consists of several immediately adjacent plates formed by individual optical fibers printed using a 3D printer. Two types of plates are used to split the light output in two: plates of different shapes with rounded terminal ends are arranged alternately.

Alternating plates are connected on one side to form a common butt-end facing the junction with an optical bus or light source. The other sides form separate butt ends ending where the light output splits.

A multi-channel optical splitter functions in the following way: Light output coming on the A-A section is transmitted onto both packs of optical fibers, which split it in two sections as shown in the B-B

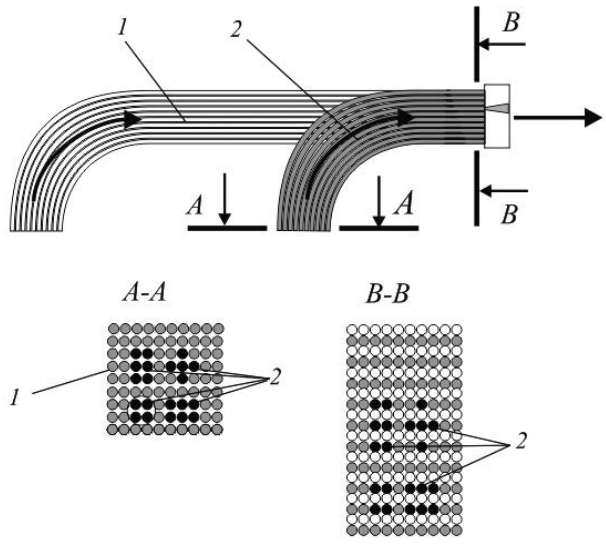

Fig. 1. Multi-channel optical splitter diagram

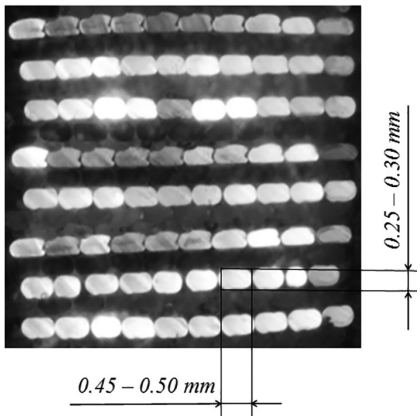

Fig. 2. Shape and size of optical fibers

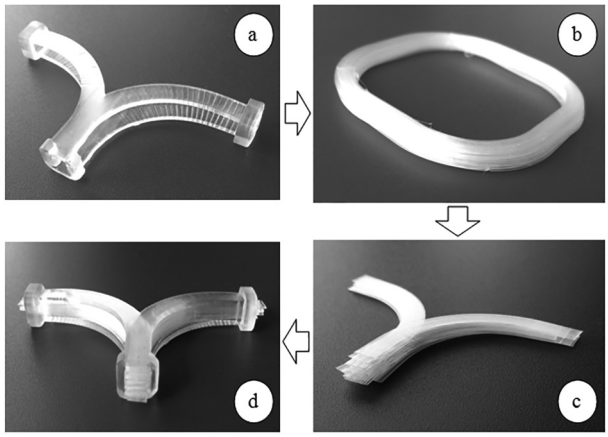

Fig. 3. Practical multi-channel splitter manufacturing

section. Thus, light output is split and gets through the splitters and optical bus.

Technologies for the manufacturing of multi-channel optical splitters were practically determined in the course of laboratory research.

It is advisable to manufacture the body of a splitter using digital light processing (DLP), which is a variety of stereolithography (SLA) [2]. An SLA-based Miicraft printer was used to manufacture a splitter body. The printer features printing resolution up to 5 microns, which is important as it allows the manufacturing of miniature high-quality details. Unlike laser 3D printers that scan the surface of the material with one or multiple laser heads, DLP 3D printers project the image of a whole layer until the polymer (resin) freezes completely. After that, a new layer of the material is applied and a new layer image is projected.

Despite the relative simplicity and low cost of the DLP technology, its application in the manufacturing of optical fiber plates has proved to be inefficient. It is virtually impossible to obtain an optical fiber thread with the required geometric properties and necessary surface undulation.

It has been empirically shown that fused deposition modelling (FDM) is a viable technology for the manufacturing of optical fiber plates from polymer fiber optic threads. An FDM-based Wanhao Duplicator 4X Black DH printer was used to manufacture optical fiber plates. The printer has two print heads (extruders) allowing it to print two-colour products. The Wanhao printer forms the product layer-by-layer, pouring a thread of melted material onto the working plate. The printer moves the extruder in accordance with the model, so the printed object is an exact match to its virtual prototype. The process of 3D printing commences at the bottom layer. Polymer 1.4 mm optical fibers were delivered in the print head as a filament. Melted optical fiber quickly cools and freezes on the working plate. Under specific conditions of the manufacturing process, the structure of the polymer optical fiber remains intact when it is extruded through the nozzle of the print head. However, optical fibers are deformed, changing their shape from cylindrical to oval or even rectangular with rounded corners (Fig.2).

Still, such deformed optical fibers fully retain the ability to transmit light output.

Fig. 3 shows the practical manufacturing process for a multi-channel optical splitter.

Fig. 3a shows a body of an optical splitter printed with a Miicraft printer. Fig. 3b shows printed workpieces from optical fiber in the form of flat fiber optic buses (optical fiber packs). The core of the optical fibers consists of methylmethacrylate (MMA) and methylacrylate (MA) inhibited with nitroxide radical 2,2,6,6-tetramethyl-2-oxopiperidine-1-oxyl. The reflective coating of optical fibers is made of poly-2,2,3,3-tetrafluorpropyl methacrylate (p-MN-1) and poly-2,2,3,3-tetrafluorpropyl-α-acryl fluoride (p-FN-1). After the required number of optical fiber packs were printed, they were cut and assembled into a block group (see Fig. 3c).

Fig. 3d shows an assembled multi-channel optical splitter: a block of the required number of optical fiber packs is mounted inside a splitter body using a polymer adhesive.

CONCLUSION

The first completely polymer fiber optic splitter without lenses or beam splitting cubes was developed and manufactured using additive technologies.

The simplicity and low cost of such a splitters allows for application in a wide range of devices: from basic light output splitters to multi-channel self-restorable smart link connections.

The research is conducted as a part of a scientific project regulated by the Agreement with the Ministry of Education and Science of the Russian Federation dated November 24, 2014 No. 14.579.21.0067 (unique project identifier RFMEFI57914X0067).

REFERENCES

1. Nikitin V. S., Solostin A. V. 3D printing of multi-channel signal splitters // Proceedings of the XI International Research and Practice Conference "Nauchny Potenzial Mira – 2015" [World Science Potential – 2015]. (In Russian). Sofia, Bulgaria: Byal GRAD-BG. 2015. VOL. 5. PAGE33–42. Available at: http://doi.org/10.17686/rusnauka_2015–200529.

2. Digital light processing (DLP). Available at: http://3dtoday.ru/wiki/ DLP_print/ (accessed 9.09.2015).

3. MiiCraft+, SLA-based DLP pico 3D printer. Available at: http://www.miicraft.com/product/ (accessed 9.09.2015).

4. Fused Deposition Modeling (FDM). Available at: http://manufacturing.materialise.com/fdm (accessed 9.09.2015).

5. Wanhao Duplicator 4X Black DH. Available at: http://www.wanhao3dprinter.com/Unboxin/ShowArticle.asp? ArticleID=28 (accessed 9.09.2015).

Aleksey N. Lomanov,
Ph.D. and associate professor in Federal State-Financed Educational Institution of Higher Professional Education (RSATU). He is graduated from Rybinsk State Aviation Technological Academy (now RSATU) in 2003. He has much experience in electrical engineering, microcontroller systems, industrial control and thin-film technologies, works in RSATU since 2003. At present he is the dean of Faculty of radioelectronics and computer science

Vladimir S. Nikitin,
Ph.D. and CEO&founder of Tenzosensor LLC. Inventor and idea man, leading expert in the field of R&D organization and performance, strategy development, organization of project team work. Miscellaneous expert in the field of Physics, Chemistry, Electronics, Material Sciences, highly qualified designer and programmer, possesses a great experience of working at executive positions. He has 24 patents, 5 certificates for PC software products, 100+ published works in scientific and popular editions; author of the book Technologies of the Future (Tekhnosfera publishing house, 2010)

Alexander V. Solostin,
graduated from Mikhailovskaya Artillery Academy in 1998 with a degree in Mathematical Methods and Operations Research, Deputy Director of NTZ Introfizika LLC (Rybinsk, Yaroslavl Region). Area of expertise: research and development in natural and engineering sciences, 3D modelling

Ernst I. Semyonov,
Ph.D., Prof., graduated from Rybinsk Evening Aviation Technological Institute (RSATU) with a degree in Radio Engineering. Area of expertise: light film manufacturing process control, automatics, radio electronics, microelectronics, computer engineering

Sergei V. Chayka,
graduated from RSATU with a degree in Program Engineering in 2009, programmer at NTZ Introfizika LLC. Area of expertise: data transfer systems, complex systems modelling

CONTENTS

VOLUME 23 **NUMBER 1** **2015**

LIGHT & ENGINEERING
(SVETOTEKHNIKA)

CONTENTS

VOLUME 23 **NUMBER 2** **2015**

LIGHT & ENGINEERING
(SVETOTEKHNIKA)

CONTENTS

VOLUME 23 NUMBER 3 2015

LIGHT & ENGINEERING
(SVETOTEKHNIKA)

PARTNERS OF LIGHT & ENGINEERING JOURNAL

Editorial Board with big gratitude would like to inform international lighting community about the Journal Partners Institute establishment. The list with our partners and their Logo see below. The description of partner's collaboration you can found at journal site *www.sveto-tekhnika.ru*

GENERAL PARTNER

BL Group — Холдинг BL GROUP

ITMO UNIVERSITY

BRILLIANT PARTNERS

LED ИНТЕР РАО СВЕТОДИОДНЫЕ СИСТЕМЫ

СВЕТЛАНА-ОПТОЭЛЕКТРОНИКА

SVETLED

SvetaLED

PLATINUM PARTNERS

LIGHTING SOLUTIONS

enercom СОЗДАЕМ ВОЗМОЖНОСТИ

ЛИСМА LISMA там, где рождается свет

PHAROS-ALEF

ГЛОБАЛ ЛАЙТИНГ

GOLD PARTNERS

MOCCBET

ГСТЗ г. Гагарин

ZUMTOBEL

Instrument Systems light measurement

SILVER PARTNERS

alanod

ВНИСИ

Светотехнический завод ВЛАДАСВЕТ

НИИ

BRONZE PARTNERS

ВНИИОФИ

TS TENZOSENSOR

СВЕТОВЫЕ СИСТЕМЫ

НИИИС

ЦФ

СОЛАР МАГИЧЕСКИЙ СВЕТ